New Methods in Polymer Brush Synthesis: Non-Vinyl-Based Semiflexible and Rigid-Rod Polymer Brushes

Caleb J. Reese & Stephen G. Boyes

Affiliations

Department of Chemistry, The George Washington University, Washington, DC USA 20052

Abstract

Non-vinyl-based 'grafted from' polymer brushes have generated much interest and growth in the past decade due to the potential for stiffer backbones, long-range order, and new backbone functional groups, compared to the traditional vinyl-based polymer brushes. This area of polymer brushes has been spurred on by the recent advancements in the development of new polymerization techniques, such as chain-growth condensation polymerization, that allow for the conversion of traditional step-growth polymers into the required chain-growth polymers to form polymer brushes via the 'grafting from' technique.[1] This exciting new category of polymer brushes forms semi-flexible or rigid-rod structures that have potential in a variety of applications including organic photovoltaics, organic light emitting diodes, tribological coatings, membranes for water purification and desalination, membranes for fuel cells, high performance coatings, and biosensing due to aromatic groups in the backbone, secondary bonding forces connecting chains, or conjugated backbones.[[2],[3]] This review will focus on the synthesis and characterization of non-vinyl-based polymer brushes, primarily prepared via the 'grafting from' technique, while also including an overview of potential applications of these systems and highlighting prospective areas for future developments.

Keywords

Surface Modification; Polymer Brushes; Semiflexible Brushes; Rigid-rod Brushes; Chain Growth Condensation Polymerization; Catalyst transfer Chain Growth Condensation Polymerization; Substituent effect Chain Growth Condensation Polymerization; Ring opening Polymerization

Contents

Abbreviations

ADC, azelaoyl dichloride; AFM, atomic force microscopy; AIBN, azobisisobutyronitrile; AROP, anionic ring opening polymerization; ATRP, atom transfer radical polymerization; BEMA, 2-bromoethyl methacrylate; CGC, chain-growth condensation; CROP, cationic ring opening polymerization; DAH, 1,7-diamineoheptane; DCM, dichloromethane; DMSO, dimethyl sulfoxide; DP, degree of polymerization; dppe, 1,2-bis(diphenylphosphino)ethane; dppp, 1,3-bis(diphenylphosphino)propane; DSC, differential scanning calorimetry; FTIR, Fourier-transform infrared spectroscopy; GPC, gel permeation chromatography; H_b, thickness of the brush film; HCl, hydrochloric acid; HF, hydrofluoric acid; H_m, thickness of the mushroom film; IR, infrared; XPS, X-ray photoelectron spectroscopy; ITO, indium tin oxide; MLD, molecular layer deposition; M_n number average molecular weight; M_w, weight average molecular weight; MWCNs-COOH, carboxylic acid functionalized multiwalled carbon nanotubes; MWD, molecular weight distribution; N_A, Avogadro's Number; NCA, N-carboxyanhydride; $Ni(bipy)Cl_2$, [2,2'-bipyridine]dichloronickel(II); $Ni(COD)(PPh_3)_2$, (cyclooctadiene)-bis(triphenylphosphine)nickel(0); $Ni(COD)_2$, bis(cyclooctadiene)nickel(0); $Ni(COD)_2$/bpy, bis(cyclooctadiene)nickel(0)/2,2'-bipyridine; $Ni(dppp)Cl_2$, [1,3-bis(diphenylphosphino)propane]dichloronickel(II); $Ni(PPh_3)_4$, tetrakis(triphenylphosphine)-nickel(0); NMP, nitroxide-mediated polymerization; OLED, organic light emitting diode; OPV, organic photovoltaic; PANI; polyaniline; PDI, polydispersity index; PEG, poly(ethylene glycol); PLA, poly(lactic acid); PPE, poly(phenylene ethynylene); PPO, poly(phenylene oxide); PPy,

polypyrrole; PVDF, poly(vinylidene fluoride); RAFT, reverse addition-fragmentation chain transfer; R_g, radius of gyration; rms, root mean square; ROMP, ring opening metathesis polymerization; ROP, ring opening polymerization; RT, room temperature; SCF, self-consistent field; SEM, scanning electron microscopy; SI-ROP, surface-initiated ring opening polymerization; SWCN, single walled carbon nanotubes; TDI; toluene 2,4-diisocyanate; TEM, transmission electron microscope; T_g, glass transition temperature; TGA, thermal gravimetric analysis; THF, tetrahydrofuran; UV-Vis, ultraviolet–visible; VDP, vapor deposition polymerization;

1. Introduction

The modification of surfaces with polymers is a field that has fascinated chemists and physicists for over half a century due to the unique ability of polymers to control interfacial properties.[4] Surface modification using polymers has been directly responsible for both the expansion and improvement of existing technologies and the development of new technologies.[5] This is nowhere more evident than in the establishment of technologies focused on nanometer scale phenomena.[6] The development of cutting-edge nanotechnology relies not only on the synthesis of materials of controlled size, shape, and structure but also on the development of techniques to allow these nanomaterials to be integrated into advanced devices containing superior function and properties.[[7],[8],[9],[10],[11],[12]] The development and use of new surface modification techniques will enable the application of nanomaterials in the next generation of electronic, photonic, and sensing devices, biological imaging and delivery systems, and functional nanocomposites.[13] One of the most promising approaches for the rational assembly and application of nanomaterials is modification of the surface of these materials by attachment of polymer chains.[14] Of the many different surface modification techniques available, polymer

brushes have received considerable attention and have been used in applications ranging from sensors to smart coatings.[15]

Polymer brushes are composed of polymers that are attached to a surface or interface by either covalent attachment or through physical absorption from one end of the polymer and possess a high enough grafting density that the polymer chains start compressing one another causing them to stretch away from the surface.[[16],[17]] Over the past three decades, polymer brushes have gone from a fundamental concept to being utilized for many different applications due to the inherent flexibility in creating highly customized thin films in which thickness, chemical composition, architecture, and overall function can be easily controlled.[[18],[19]] Some of the applications of polymer brushes include control over wetting, lubrication, corrosion and colloidal stability, 'smart' optical systems, microelectromechanical systems, textiles, biomedical surfaces, patterned surfaces, protective coatings, hybrid solar cells, and surface electronic properties.[[2],[16]] Despite the tremendous interest in polymer brushes, research and applications have been primarily limited to polymers prepared via chain-growth polymerization techniques involving, predominantly, vinyl-based monomers.[[14],[16],[19]] This is in part due to the requirement that to prepare well-defined polymer brushes, a polymerization technique that provides controlled polymer growth, narrow molecular weight distributions (MWDs), and that can be effectively initiated from the desired substrate, is required.[20]

One emerging area of research in the field of polymer brushes is the use of non-vinyl-based monomers. This research has been driven by the need to develop polymer brushes based on the desire for polymer backbones with different functionalities and on the development of conjugated and/or aromatic polymers for various applications, including organic photovoltaics (OPVs), organic light emitting diodes (OLEDs), tribological coatings, membranes for water purification

and desalination, membranes for fuel cells, high performance coatings, and biosensing.[[2],[3]] Some of the unique properties that separate these polymers from the traditional vinyl-based polymers include conjugation in the polymer backbone, biocompatibility, high tensile strength and modulus, improved thermal integrity, enhanced chemical stability, biodegradability, secondary bonding forces, and a high degree of alignment.[[21],[22],[23]] This review will serve as a summary of the recent work in the area of polymer brushes synthesized from non-vinyl-monomers, primarily using the 'grafting from' technique.

2. Polymer Brushes

2.1 Surface Modification Using Polymers

While polymers can be used to modify a variety of different surfaces, there are two general types of surface modification techniques: physisorption or covalent attachment. Of these techniques, covalent attachment is generally preferred as it overcomes many of the disadvantages of physisorption, which include thermal and solvolytic instabilities, and lower grafting densities.[17] Because of these disadvantages and the difficulty in producing brush structures using physisorption, the covalent attachment method will be the primary focus of this

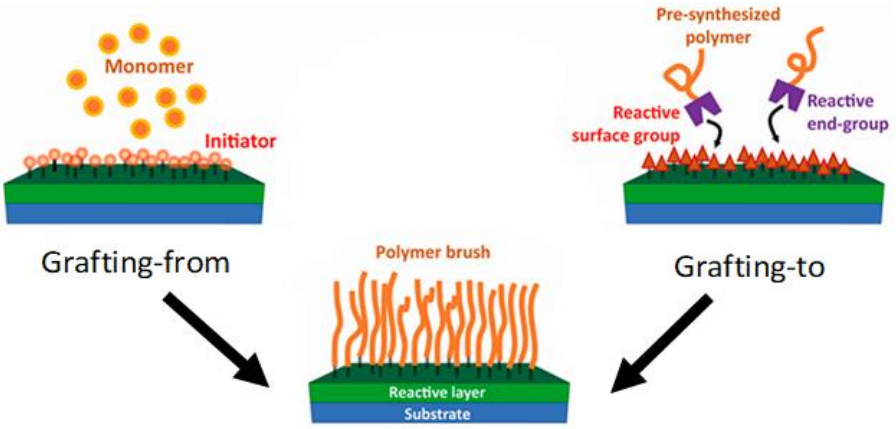

Figure 1. Illustration comparing of the 'grafting from' and 'grafting to' techniques for the preparation of polymer brushes. [24], Adapted with permission. Open Access distributed under the terms of the Creative Commons Attribution License CC BY 4.0.

review. There are two main methods for covalent attachment of a polymer chain to a surface or substrate: the 'grafting to' method and the 'grafting from' method (**Figure 1**).[24] The 'grafting to' method involves a pre-synthesized polymer chain that is bound to the surface by reacting a functional group on the polymer chain to a surface binding site. This method is extremely versatile due to the wide range of polymers and surfaces that can be utilized. The main requirement is that a reactive group must be present on the polymer chain, commonly as an end-group, to allow for attachment to the substrate. Another advantage of the 'grafting to' method is that the polymer chains can be fully characterized before they are attached to the surface. This is extremely important when knowledge of the molecular weight, MWD, or functionality of the polymer is critical to the application of the polymer-modified surface. The main disadvantage of the 'grafting to' method is that it typically results in a lower grafting density.[25] The lower grafting density comes from the fact that as polymers start binding to the surface they can sterically block reactive sites. This steric hindrance makes it difficult for new polymers to reach the surface and can inhibit the grafting density from reaching the values required for brush formation. Where the 'grafting to' technique works the best is with lower molecular weight polymers or surface applications that do not depend on grafting density or require a polymer brush structure. Typically, lower molecular weight polymers will result in a higher grafting density when using the 'grafting to' technique. This relationship between molecular weight and grafting density is shown in **Equation 1** where grafting density (σ, chains/nm^2) decreases with increasing number average molecular weight (M_n) at a fixed surface coverage (Γ, g/nm^2). Surface coverage is given by **Equation 2** where h is the thickness of the polymer film and ρ is the density of the polymer being used.[26]

$$\sigma = \frac{\Gamma N_A \times 10^{-23}}{M_n} \quad (1)$$

$$\Gamma = h\rho \quad (2)$$

To overcome the limitation of lower grafting densities, the 'grafting from' method can be used. The 'grafting from' method typically focuses on the use of living chain-growth polymerization techniques to grow the polymer directly from the substrate. This is achieved by surface-immobilizing an initiator on the substrate then polymerizing the desired monomer(s) from that initiator. The use of surface-immobilized initiators and the 'grafting from' technique typically allows for the preparation of polymer-modified surfaces with high grafting densities and has generally become accepted as the most attractive way to prepare thick, covalently tethered polymer brushes.[27] Because of this, polymer-modified surfaces prepared via the 'grafting from' method will be the focus of this review. The downside to the 'grafting from' method is that, traditionally, only polymerization techniques that involve a living chain-growth process can be employed to grow thick, controlled polymer brushes. This has, for the most part, limited the types of polymers that can be grown to those primarily from vinyl-based monomers.

2.2 Conformation of Surface-Immobilized Polymers

From the above discussion, it is clear that the conformation polymers adopt on surfaces is critical in defining the type of polymer-modified surface produced. Surface-immobilized polymers adopt different conformations depending on the type of polymer used, the grafting density, and any

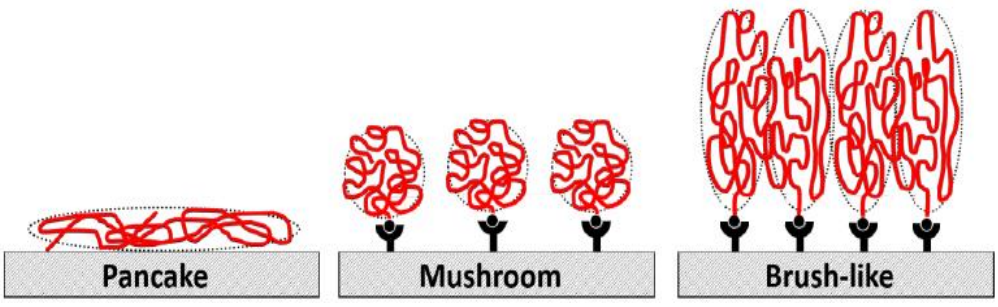

Figure 2. Scheme depicting the different conformations polymers can adopt when attached to a surface.

intra- or inter-molecular forces between the polymer chains and the surface (**Figure 2**). As mentioned previously, polymer brushes are composed of polymer chains present at a high enough grafting density to force the chains to compress each other and extend away from the surface. When this regime is achieved, new or improved properties can be obtained, such as ultralow friction surfaces and auto-phobic behavior.[17] The conformation most commonly associated with a polymer brush is a compressed random coil (**Figure 2**).[19] This conformation is conventionally obtained by using polymers synthesized from vinyl-based monomers. The backbone of these polymers is typically composed of single carbon-carbon bonds, which enhance the flexibility of the polymer chains and result in the polymer chains adopting a random coil shape.

There are three main conformations that these random coils can adopt when attached to a surface, all of which depend on the grafting density (**Figure 2**). In order to find the grafting density of a surface-initiated polymer **Equation 3** can be used where h is the film thickness, ρ is the density of the polymer, M_n is the number average molecular weight, and N_A is Avogadro's number.[28]

$$\sigma = \frac{number\ of\ chains}{unit\ area} = \frac{h\rho N_A}{M_n} \tag{3}$$

$$\Sigma = \sigma\pi\ R_g^2 \tag{4}$$

Another important parameter that is often used for comparing surface-initiated polymer brushes is the reduced tethered density (Σ). Σ is described by the number of polymer chains that could fit the same space that an uncompressed polymer chain would possess under the same conditions.[29] This is calculated from **Equation 4** where R_g is the radius of gyration of a tethered chain under the specific experimental conditions of solvent and temperature.[19] In an ideal system, polymer brushes would be formed starting at Σ = 1 but in reality this occurs at a higher value for random coil brushes (**Figure 3**). If Σ is lower than 5, meaning the distance between

attachment sites is greater than the size of the polymer coil, then either a pancake conformation or a mushroom conformation

will result.[29] When the polymer has minimal interactions with the surface, a mushroom conformation is observed. Whereas, when the interactions with the surface are high, a pancake conformation where the polymer lays flat results. Due to the typically lower grafting density of polymer films prepared using the 'grafting to' technique, either a pancake or mushroom conformation is often formed. When Σ is greater than 5, meaning the distance between attachment sites is less than the size of the polymer coil, a brush conformation is observed. When this occurs, the polymer chains try to avoid overlap by pushing away from the surface, resulting in a compressed random coil polymer brush.

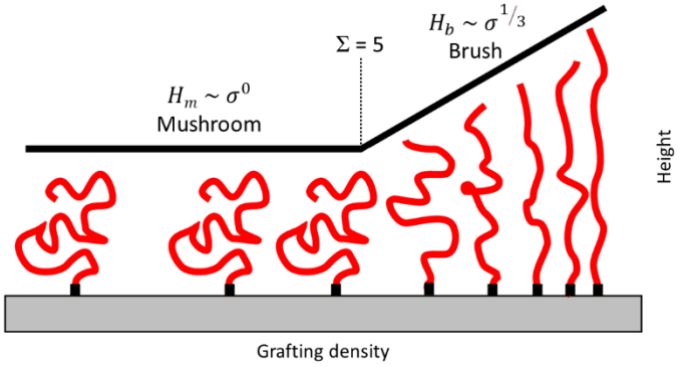

Figure 3. Schematic of grafting density versus brush height in the transition from the mushroom regime to the brush regime.

To find the scaling relationship of polymers in the brush and mushroom conformations, **Equations 5** and **6** can be used, where polymer chains consist of N statistical segments of diameter a, H_m is the thickness of the mushroom film, and H_b is the thickness of the brush film.[28]

$$H_m \sim a\left(\frac{N}{6}\right)^{1/2} \sim N\,\sigma^0 \tag{5}$$

$$H_b \sim N\sigma^{1/3} \tag{6}$$

In **Equation 5,** the film thickness of polymers in the mushroom conformation can be seen to increase with grafting density to the power of zero meaning the thickness is independent of grafting

density. Whereas, in **Equation 6,** the thickness of films in the brush conformation can be seen to scale with grafting density to a power of one third (**Figure 3)**. This occurs due to chain and/or steric interactions forcing the film thickness to increase with increasing grafting density in a brush. It should be noted that the vast majority of brush conformation studies, both experimental and theoretical, have been based off random coil polymers due to the fact that the majority of polymer brushes have been prepared from polymers that adopt random coil structures.

A new area of interest within polymer brush research is incorporating polymers with stiffer, more rigid backbones, such as polymers with aromatic groups in the backbone, conjugated backbones, or backbones with different linking functionalities. These polymers make what are called semi-flexible or rigid-rod polymer brushes and are believed to possess more long-range order than compressed random coil brushes.[30] Despite the interest in these newer types of polymer brushes, there have been few studies on their conformation. One study suggests a lower Σ, ~0.4, is needed to enter the brush regime for polypeptides when compared to brushes produced from vinyl-based monomers.[31] As discussed earlier because of the predictions of stiffer backbones and higher ordering, there is the potential for many new applications ~~have been predicted for rigid-rod polymer brushes, including OPVs, OLEDs, tribological coatings, membranes for water purification and desalination, membranes for fuel cells, high performance coatings, and biosensing~~.[[2],[3]] Before delving into the different types of non-vinyl-based polymer brushes that have been developed, the traditional methods to prepare conventional polymer brushes will be briefly discussed.

2.3 Synthesis of Polymer Brushes

In order to obtain well-defined polymer brushes using the ‘grafting from’ technique, a living chain-growth polymerization technique is most commonly used. Similar to conventional

chain-growth polymerization, living chain-growth polymerizations are defined by the sequential addition of monomers to the end of a propagating polymer chain. However, in a living system, termination reactions are minimized to allow for the continued growth of the polymer chains. In addition, if initiation is fast relative to propagation, the molecular weight will increase linearly with conversion producing polymers with a low polydispersity index (PDI). This process is critical in producing uniform, well-defined polymer brushes, because fast initiation relative to propagation ensures that all chains are initiated at the same time and linear evolution of molecular weight results in all the polymer chains growing at the same rate. The need for these properties has traditionally excluded the step-growth polymerization techniques for the synthesis of polymer brushes, as these techniques involve the random addition of monomer and/or oligomers, and the slow evolution of molecular weight. In a step-growth polymerization, the polymer chains begin by growing slowly with increasing conversion as dimers, trimers, etc. are formed. Once larger chains start reacting with each other, the molecular weight grows rapidly at high conversion. The random reaction of functional groups in step-growth polymerizations leads to molecular weights that are commonly lower than those achieved via many of the chain-growth polymerizations and higher PDIs, approaching 2.0 in an ideal system.[32] Because of this, the use of step-growth polymerization to prepare polymer brushes is best suited for a 'grafting to' process, which typically results in lower grafting densities and non-uniform films. Regardless of the polymerization technique used, the formation of polymer brushes via the 'grafting from' technique requires the immobilization of initiators on the surface to be modified, followed by surface-initiated polymerization. The following discussion will briefly discuss these processes, as a more detailed discussion of these topics can be found in recent review papers.[[24],[33],[34],[35],[36]]

2.4 Surface-Immobilization of Initiators

Chemical attachment of suitable initiators to the surface of interest is critical to the preparation of polymer brushes using the 'grafting from' technique. This has been shown to occur from a wide variety of substrates, ranging from organic to inorganic materials.[[33],[27]] One of the most widely used methods for surface immobilization of initiators is the use of silanes.[34] Silanes have been shown to attach to a wide variety of surfaces, with a focus on oxide-containing ceramic materials, such as silica, and can contain a large range of different functional groups. When oxide substrates are not available, another popular method is the use of thiol groups to attach polymers to noble metals, such as gold. Polymer substrates have been used to make polymer brushes, but have had issues due to the substrate dissolving, swelling, or breaking down.[37] One way to avoid these issues is to produce a cross-linked curable polymer substrate. This limits the polymer dissolving or breaking down and reduces swelling.[24] While other processes have been used to attach initiators to surfaces, due to the prevalence of the use of silanes, these will be the focus of discussion.

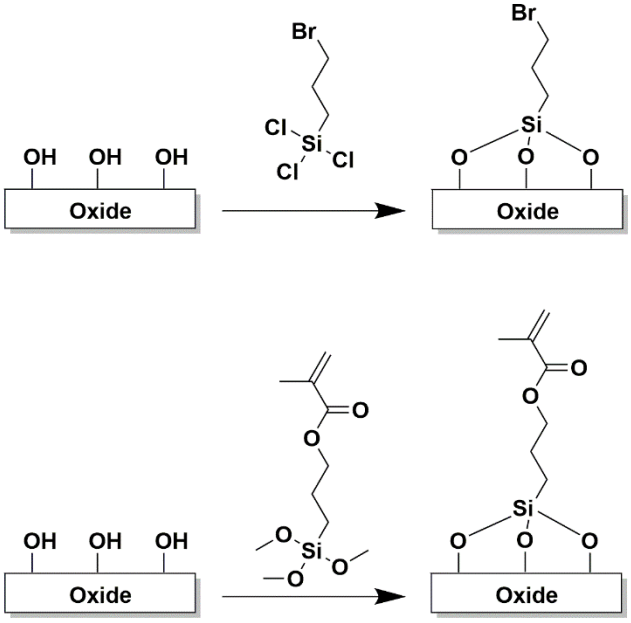

Figure 4. Hydroxylated surface reactions with example silane initiators used for 'grafting-from' surface initiated polymerization. [[24],[37]]

The attachment strategy for immobilization of silanes typically involves hydrolyzing alkoxylsilanes or chlorosilanes with the oxide of interest. These oxide substrates are routinely activated using acidic-based cleaning to increase the amount of hydroxyl groups on the surface. This helps produce a more uniform coverage of the surface with the silane coupling agent. Silane

coupling agents are comprised of two main functional groups. One functional group will initiate the polymerization, while the other functional group is composed of a silicon atom that has hydrolysable groups, such as alkoxy groups or chlorides, that can be used to attach the coupling agent to a substrate. When the silane coupling agent gets near the substrate, the hydroxyl groups on the surface act as nucleophiles, attacking the silicon atom to eliminate the alkoxy or chloride leaving group (**Figure 4**). Comparing the different side products of this reaction, the alcohol from the alkoxide makes for a more stable and/or typically less reactive leaving group compared to the hydrochloric acid generated from chlorosilanes.[38] Another variable is how many hydrolysable groups are available on the coupling agent. This can vary between one to three groups and the number of groups has been shown to play a critical role in surface morphology.[39] These coupling agents have been shown to form a siloxane bonds between silane coupling molecules linking them together. The use of more hydrolysable groups increases the reactivity of the coupling reagent with the surface but also results in the formation of aggregates on the surface. To negate this, it has been shown that using less hydrolysable groups decreases aggregation.[40]

2.5 Living Radical Polymerization for Synthesizing Polymer Brushes

As mentioned previously, by far the majority of polymer brushes synthesized via the 'grafting from' technique have utilized vinyl-based monomers. These monomers have been extensively studied due to the existence of multiple living chain-growth polymerization techniques that utilize them and produce well-defined polymers, which is essential for growing polymer brushes.[[16],[19],[24]] While a number of different living polymerization techniques have been used for the synthesis of polymer brushes based on vinyl monomers, the majority have focused on the use of living radical polymerization techniques, which include atom transfer radical polymerization (ATRP), reversible addition-fragmentation chain transfer (RAFT) polymerization, and nitroxide-mediated polymerization (NMP) (**Figure 5**). All of these techniques utilize an activation/deactivation mechanism, to minimize termination reactions, and promote fast initiation relative to propagation to ensure the preparation of living polymers with defined molecular weights and narrow MWDs.

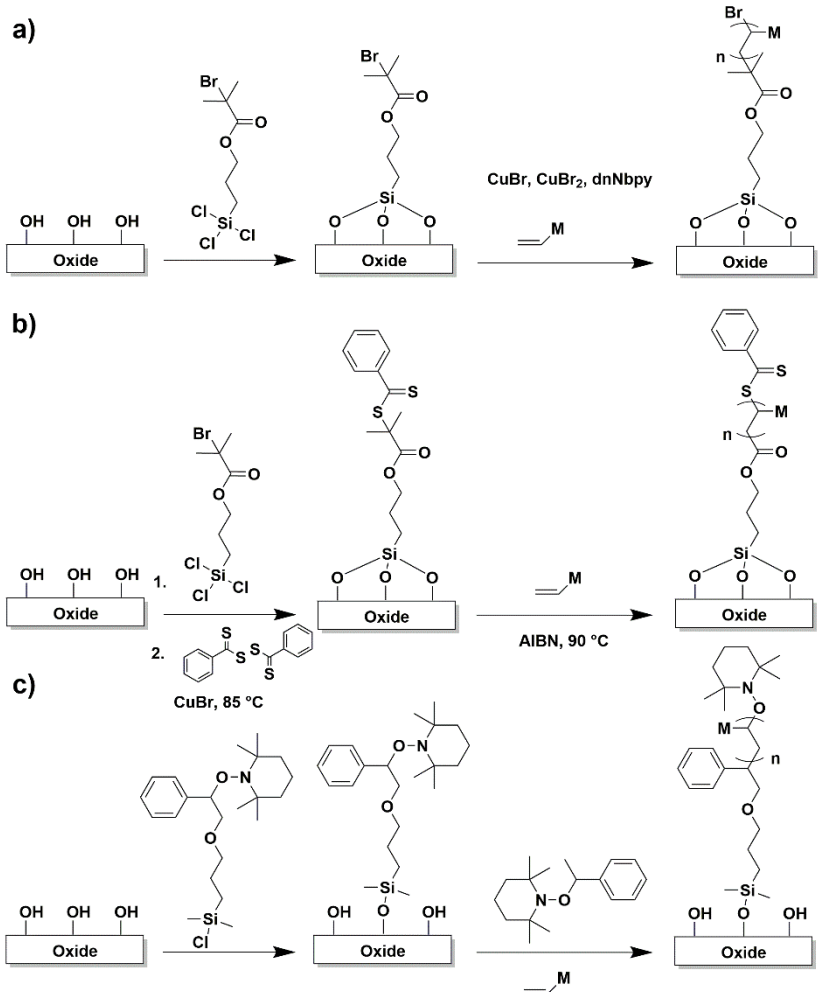

Figure 5. Reaction schemes for commonly used radical surface-initiated polymer brush synthesis. a) SI-ATRP, b) SI-RAFT, c) SI-NMP. [19]

Polymer brushes prepared from vinyl-based monomers have been studied for application in numerous areas, including control of wetting properties, prevention of nonspecific binding of biomolecules, bio-adhesion, colloidal stabilization, resistance to fouling, polymer compatibilizers, new adhesive materials, chromatographic devices, etch barriers, and many others.[[19],[16],[24]] However, despite the large amount of work already performed utilizing these polymer brushes, they continue to be investigated as researchers look to develop new structures, functionality, architecture, and applications. Due to the wide spread use of these systems in polymer brush synthesis, this review will not include a detailed background of the living radical polymerization systems and the reader is directed to recent reviews of this topic for more information.[[19],[16],[24],[27],[39],[25],[41],[42]]

3. New Polymerization Methods for the Synthesis of Polymer Brushes

As mentioned above, in order to obtain well-defined polymer brushes via the 'grafting from' technique, a living chain-growth polymerization should be utilized. This requirement has traditionally limited the types of polymer brushes that could be synthesized to those coming primarily from vinyl-based monomers. In an effort to expand the field of polymer brushes prepared via the 'grafting from' technique, there has been a search for new polymerization methods that either follow a living chain-growth process or can be modified to do so. One of the most interesting polymerization methods in this regard is chain-growth condensation (CGC) polymerization. Yokozawa et al was the first to report CGC via substituent effect with polyamides, polyesters, and polyethers.[[43],[44],[45]] A few years later, Yokozowa et al. and McCullough et al. separately demonstrated catalyst transfer CGC of polythiophenes ~~some of the first work reporting new techniques to convert polymers traditionally synthesized via a step-growth process compared to a chain-growth mechanism~~.[[46],[47],[48]] ~~Their seminal work demonstrated that polymers, such~~

~~as~~ Because of this seminal work, polyamides, polyesters, polyethers, and many different conjugated polymers, which were almost exclusively prepared via step-growth polymerization, could be transformed into well-defined polymers with narrow MWDs using a chain-growth process. The conversion of traditional step-growth polymerizations into living chain-growth polymerizations has the potential to significantly increase the application for these traditional step-growth polymers due to the control of molecular weight, lower PDIs, and the new architectures that can be prepared. This is particularly evident in the field of polymer brushes.

The underlying principle of the CGC polymerization technique centers on controlling the polymerization so that monomer preferentially reacts with an initiator or propagating chain end instead of other monomers. The two main CGC polymerization techniques are: catalyst transfer polymerization and substituent effect chain-growth polymerization. The following discussion will provide a brief overview of each of these techniques. For a more in-depth explanation of CGC polymerization methods, there are a number of recent reviews.[[1],[49],[50],[51],[52],[53],[54]]

3.1 Catalyst Transfer Polymerization

Catalyst transfer polymerization, as the name suggests, utilizes a catalyst that stays on the end of a propagating polymer chain to promote monomer insertion, converting a traditional step-growth polymerization to a living chain-growth polymerization. Many new polymerization techniques have been developed that utilize catalyst transfer polymerizations.[1] One of the most popular methods is the use of Grignard monomers with nickel catalysts. This process has been used to enable the chain-growth polymerization of many different monomers including thiophenes, selenophenes, pyrroles, phenylenes, fluorenes, cyclopentadithiophenes, dithiosiloes, bithienylmethylene, pyridines, benzotriazoles, thiazoles, and diaryl monomers.[3] Other types of polymerizations that have been developed include Pd-catalyzed Suzuki-Miyaura coupling

polymerization of acid ester monomers, Pd-catalyzed Mizoroki-Heck polymerization of p-iodostyrene, transition metal-free polymerization of pentafluorophenyl, Negishi coupling polymerization using zinc monomers with a Pd catalyst, among many others and have been reviewed extensively.[[1],[49],[50],[51],[52],[53],[54]

The earliest work in this area was published by McCullough and co-workers when they reported the metal catalyzed polymerization of 2-halo-3-alkylthiophenes transformed into a head to tail polythiophene using Kumada coupling.[[55],[56],[57],[58]] This work was followed by Yokozawa et al. who used a bromothiophene Grignard-type monomer with a nickel catalyst and lowered the PDI of the resultant polythiophene.[46] In order to obtain a low PDI, monomer was purified and the feed ratio of monomer to nickel catalyst was used to control molecular weight. This polymerization type was given the name Kumada catalyst-transfer polycondensation (KCTP) and has been widely used for developing a variety of conjugated and aromatic polymers. One of the unique aspects of Yokozawa's discovery was control over the chain end group functionality. Using this controlled functionality, block copolymers have been synthesized using ATRP, RAFT, and NMP in conjunction with most types of catalyst transfer polymerizations.[1] An example of this was shown by Ogino et al. who made a poly(3-hexylthiophene)-b-polystyrene block copolymer using a Suzuki coupling reaction between the two presynthesized polymers, which were

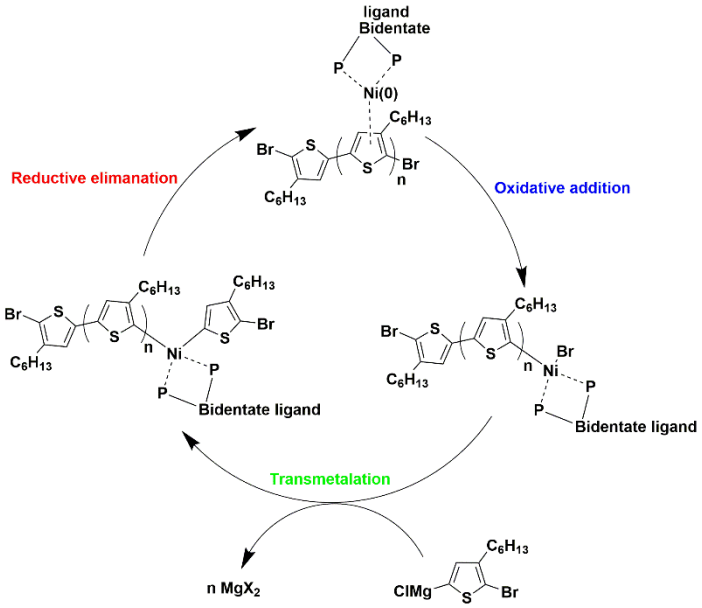

Figure 6. Reaction scheme showing a proposed mechanism for nickel catalyst "ring-walking" across the aromatic backbone of polythiophene. [53]

polymerized using Grignard metathesis polymerization and ATRP, respectively, for use in OPV applications.[59]

The mechanism of catalyst transfer polymerization has been theorized to work by the catalyst 'ring-walking' across the aromatic backbone to the end of the propagating chain (**Figure 6**).[53] When this occurs three steps take place: reductive elimination, oxidative addition, and transmetalation. Computational work has demonstrated that these steps are more favorable continually occurring on one chain end, rather than the catalyst complex leaving the chain end altogether and reacting with a monomer in solution.[60] This 'ring-walking' step is predicted to be favored by polarization of the pi-conjugated system from the electron withdrawing halide atom. Computational studies by Zenkina et al. have shown a 2-3 kcal/mol stabilization as the nickel-catalyst complex 'walks' towards the electron withdrawing bromide.[60] This 'ring-walking' differs from step-growth polymerization using these types of catalysts, in that the catalyst can dissociate from the reactive site instead of staying on that propagating chain. The development and application of the 'ring-walking' mechanism is responsible for converting step-growth polymerizations into living CGC reactions, which has in turn made many new polymer brushes possible.

3.2 Chain Growth Condensation Polymerization via Substituent Effects

CGC polymerization via substituent effects uses activation and deactivation, via induction or resonance effects, to selectively activate the propagating polymer chain end to monomer addition, after an initiation process, rather than the random reaction of monomer with monomer. While different methods can be used to achieve this, typically control is obtained by removal of a proton, via a strong non-nucleophilic base, from a functional group on one side of an aromatic ring. This results in a strong electron donating group, with the increased electron density

distributed through the ring via an inductive or resonance effect to stabilize or reduce the reactivity of an electrophilic site attached to the aromatic ring. Typically, groups that are para and ortho to each other use a resonance effect and groups that are meta to each other use an inductive effect. Once monomer adds to the propagating chain end, the resultant functional group is weakly electron donating, which increases the reactivity of the chain end, relative to monomer, and results in selective reaction of the monomer with the propagating chain rather than between monomers.

CGC polymerization via substituent effects was first observed with para-substituted monomers, such as 4-halothiophenols, 4-halo-2,6-dimethylphenols, the potassium salt of 4-fluoro-4′-hydroxybenzophenone, sodium 4-fluorobenzenesulfinate, methylphenyldichlorosilene with alkali metals, and condensation polymerization of dibromomethane with bisphenol A (**Figure 7**).[[61],[62],[63],[64],[65],[66]] These polymerizations proved difficult due to the low solubility of the polymer and the presence of step-growth polymerization side reactions. In an ideal CGC polymerization reaction monomer would only react with propagating chain end. This occurs because after a monomer reacts with an initiator or propagating chain the reactivity of the end group increases due to the substituent effect. In most cases, the new functional group formed is significantly less

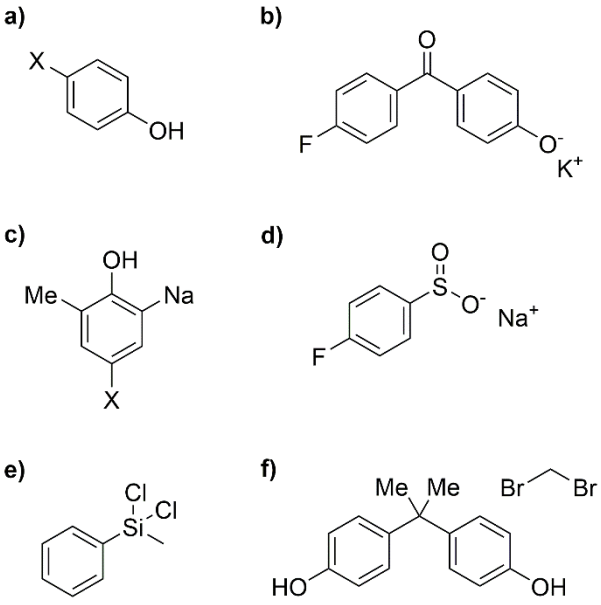

Figure 7. Some of the first monomers used when CGC polymerization was observed. a) 4-halothiophenols b) 4-halo-2,6-dimethylphenols c) 4-fluoro-4′-hydroxybenzophenone d) sodium 4-fluorobenzenesulfinate e) methylphenyldichlorosilene f) dibromomethane with bisphenol A. [49]

electron donating than the previous negative charge on the monomer, which encourages monomer reacting with propagating chains instead of monomer reacting with monomer.

Following on from this initial work, the activation/deactivation method has been developed further, resulting in modern living CGC polymerizations that provide higher levels of control over monomer reactivity and well-defined polymers. In addition to controlling monomer reactivity, living CGC polymerizations require the addition of an initiator to provide fast initiation relative to propagation and to effectively define the number of growing chains in the polymerization system. The addition of an initiator is also important as it has been demonstrated that CGC monomers can react with each other without an initiator, which results in a broadening of the MWD.[49] However, as this reaction is slow relative to reaction with an effective initiator or the propagating chain end, well defined polymers with a narrow MWD distribution can be achieved using a variety of different monomers.

Well-defined aromatic polyamides, polyesters, and polyethers have all been produced using CGC polymerization via substituent effects.[1] Polyamides have been formed using an ester group that is either para, ortho, or meta to an amine group on an aromatic ring. Because the amide bond is more stable than an ester bond, the amine makes for a good nucleophile and the ester carbonyl acts as a good electrophile in the nucleophilic acyl substitution reaction to form the polyamide. The use of

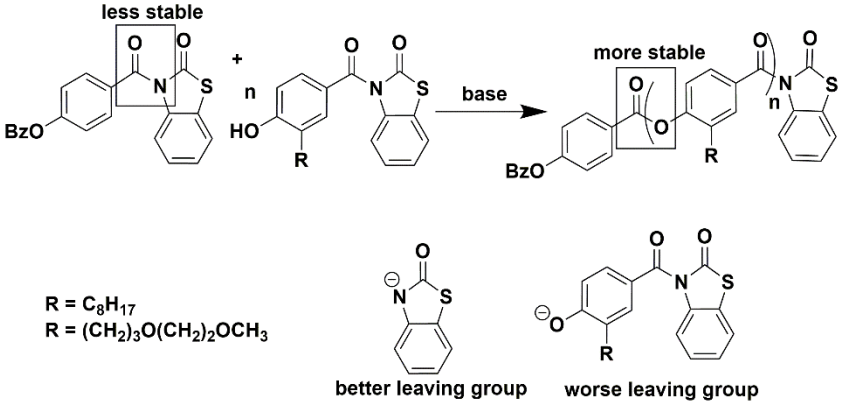

Figure 8. Reaction scheme depicts CGC polyester formation comparing 3-acyl-2-benzothiazolone as a stable leaving group to the transesterification product as a less stable leaving group. [67]

CGC polymerization via substituent effects for the preparation of polyesters is more complicated due to ester bonds being more prone towards reaction with nucleophiles, resulting in transesterification reactions during the polymer synthesis.[67] When a backbone ester bond is broken this cleaves the polymer, lowering the molecular weight, and broadens the MWD. To avoid this, a high concentration of initiator is often used, which limits the process to low molecular weight polymers, and the reaction is carried out at lower temperatures.[49] The leaving group from the nucleophilic acyl substitution reaction forming the polyester is also important and must be very stable compared to a normal ester hydrolysis alcohol leaving group (**Figure 8**). For example, a 3-acyl-2-benzothiazolone leaving group resulted in a low PDI polyester due to the 3-acyl-2-benzothiazolone substituted carbonyl group possessing higher reactivity and a more stable by-product compared to typical ester leaving groups. Unlike polyamides and polyesters, polyethers have been formed using nucleophilic aromatic substitution between a phenoxide and an aryl halide. These reactions are performed at high temperature and have been shown to produce polymers with narrow MWDs.[50]

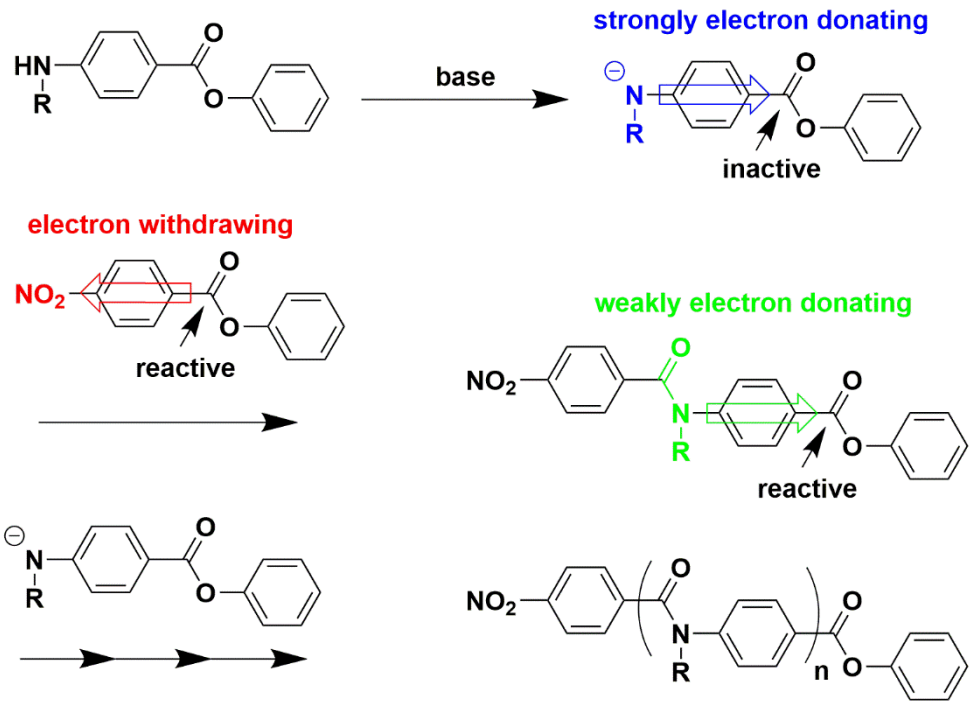

Figure 9. Hypothesized mechanism for the synthesis of polyamides via CGC polymerization using substituent effects depicting inactive monomer, highly reactive initiator, and reactive propagation chain end. [54]

While a number of different polymers have been produced using CGC polymerization via substituent effects, the majority of research by Yokozawa et al. has focused on producing aromatic polyamides.[52] The synthesis of polyamides using CGC via substituent effects has three main aspects to the proposed mechanism (**Figure 9**). First, a monomer with a secondary aromatic amine, either para, ortho, or meta, to an ester group on an aromatic ring is used. A strong, non-nucleophilic base is then used to deprotonate the amine, giving it a negative charge. Yokozawa theorized that this charge deactivates the ester towards nucleophilic acyl substitution, through a resonance or inductive effect, by making the carbonyl carbon less electrophilic. Once all monomers have been deprotonated, an initiator with an electron withdrawing group, typically para to an ester group, is introduced. The electron withdrawing group on the initiator pulls electron density away from the ester carbonyl, via resonance, making it more electrophilic and, thus, more reactive towards nucleophilic acyl substitution. The deactivated monomers readily react with the initiator, rather than with each other, starting a propagating chain. The amide bond formed via addition of monomer to the propagating chain is weakly electron donating, making the ester bond at the chain end less electrophilic than the initiator but more electrophilic than the deactivated monomer. This overall process allows for fast initiation compared to propagation, which produces a low PDI, and selective reaction with the chain end, providing controlled molecular weights.

Research by Yokozawa et al. has attributed the success of CGC polymerization via substituent effects in producing well-defined polymers of low PDI on the electrophilicity of the ester carbonyl, which is modified by either a resonance or induction effect to alter its reactivity towards nucleophilic acyl substitution.[1] Recent work done by our group has shown that the basicity of the leaving group on the ester plays an equally important role in this process.[68] By varying the basicity of the leaving group, the propagation rate constant of the monomer was shown

to change by up to four orders of magnitude while maintaining a low PDI in the resultant aromatic polyamide. The change in propagation rate constant was attributed to altering the activation energy for elimination of the leaving group from the tetrahedral intermediate formed as part of the nucleophilic acyl substitution mechanism. Decreasing the basicity of the leaving group lowers the activation energy for the elimination process and, thus, increases the propagation rate constant. It was also shown, using theoretical calculations, that these large changes in reactivity occurred with minimal changes in the electrophilicity of the ester group carbonyl carbon. In fact, the most reactive monomer, trifluromethylphenyl 4-(octylamino) benzoate, had the least electrophilic ester carbonyl carbon when compared to the other monomers used in the study. From this work it is apparent that the mechanism for CGC polymerization via substituent effects relies on a balance between the reactivity of the ester carbonyl group and the basicity of the ester leaving group.

3.3 Ring Opening Polymerization

Before discussing different non-vinyl-based polymer brushes a brief overview of ring opening polymerization (ROP) will be included as this technique has been extensively used to form these types of polymer brushes. However, since the technique has been the topic of many review papers, the reader is directed to these reviews for a more extensive discussion on the topic.[[69],[70],[71]] Although ROP was used as early as 1907 to form polypeptides it has seen significant growth in recent years.[72] There are four major mechanism to synthesize polymers using ROP; radical ROP (RROP), cationic ROP (CROP), anionic ROP (AROP) and ring-opening metathesis polymerization (ROMP).[71] ROPs have become very useful polymerization techniques, in that, they have become widely used in both research and industry. For example, a significant portion of engineering plastics are prepared from ROPs due to the many different backbones that can be formed. Applications for ROP-based polymers range from industrial

engineering plastics to biomedical uses.[70] Unlike condensation polymerizations or vinyl-based radical polymerizations, the main driving force for ROP normally revolves around releasing ring strain of cyclic monomers.[73] Most ROP monomers consist of heterocyclic compounds, which gives them a high degree of polarization. This allows these rings to undergo heterolysis of a functional group. This exact process depends on which type of ROP mechanism is being used (**Figure 10**). For ionic ROP this typically involves a nucleophile or electrophile reacting with a functional group to start the ionic polymerization. ROMP utilize unsaturated alicyclic monomers which are polymerized using transition metal catalysts. RROP differs from the previous mechanisms by being able to undergo 'homolytic' dissociation instead of using a requiring a functional group and, in some cases, can be used with vinyl-based monomers.[70]

There are several reasons why ROP, specifically living ROP, makes for a good synthetic route to make polymer brushes via the 'grafting from' technique. Arguably, the primary reason is that the ROP synthetic routes typically provide good control over molecular weight and polymers with a narrow MWD, two factors critical in forming polymer brushes. In addition to this, many ROP polymerizations are known for their ease of use as they are commonly stable towards moisture and oxidation, which drastically simplifies reactions compared to other air-sensitive polymerizations.[70] Another reason ROP is useful for surface modification

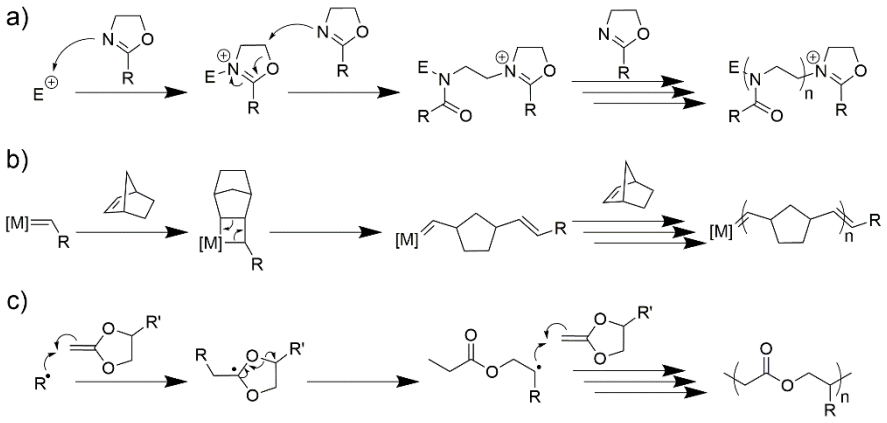

Figure 10. Reaction scheme showing general ring opening mechanism including a) cationic ring opening polymerization of oxazoline monomer b) ring opening metathesis polymerization of of a norbornene monomer c) radical ring opening polymerization of a 2-methylene-1,3-dioxolane monomer. [70]

is that, due to the ring opening nature of these polymerizations, polymer chain backbones with a variety of different functional groups can be prepared compared to conventional vinyl-based polymerizations. This significantly expands possible structures to those including polypeptides, polyesters, polyamides, and polycarbonates, which are not possible with vinyl-based polymerizations. As such, ROP can easily be used to form 'grafting from' polymer brushes with unique backbone functionality, especially compared to living radical polymerization techniques that commonly require stringent air free conditions and are limited to carbon-carbon backbones.[74]

4. Non-Vinyl-Based Polymer Brushes

Many reviews have been written on polymer brushes that focus on polymers produced from vinyl-based monomers so this review will focus non-vinyl-based brushes.[[16],[24],[19],[41],[39]] ~~To the best of our knowledge, a comprehensive review discussing the use of the 'grafting from' technique for the formation of non-vinyl-based brushes does not exist and, as such, is the focus of this review.~~ Many types of non-vinyl-based polymer brushes have been synthesized, including polynorbornenes, polypeptides, polyesters, polyoxazoline, polyaniline, polythiophenes, polyfluorenes, polyphenylenes, poly(phenylene ethynlene), polypyrrole, polyisocyanate, polyisocyanide, poly(phenylene oxide)s, and polyamides.[[2],[21],[75],[76],[77],[78],[79],[80],[81],[82],[83],[84],[85],[86]] The following section of this review provides an overview of these systems, in addition to a discussion on theoretical studies focused on semi-flexible or rigid rod polymer brushes.

4.1 Semi-flexible Polymer Brush Theory

Before polymer brushes were prepared experimentally they were studied extensively via theoretical studies.[87] While the vast majority of theoretical work examining polymer brushes has focused on flexible polymers, typically prepared from vinyl-based monomers, recently there has been an increasing number of studies looking at semi-flexible or semi-rigid polymer brushes.[[23],[30],[88],[89]] Semi-flexible polymer brushes are predicted to have had many unique and improved characteristics over existing brush architectures including tribological properties, long-range order, and liquid crystallinity.[[23],[30],[90],[91]] As such, before discussing the different types of non-vinyl-based polymer brushes that have been synthesized, an overview of some of the predictions based on computational studies will be examined.

In 1994 Fleer et al. devised a self-consistent field (SCF) lattice model for polymer brushes that incorporated chain stiffness and introduced neighboring bond correlation.[88] The polymer brushes were viewed using Kuhn segments, which treat the polymers more on a course grain level rather than an atomistic view. Chain stiffness was introduced by forbidding back folding of the chain segments and introducing an energy difference between forward and perpendicular conformations. From this, an increase in chain height was predicted when chain stiffness was increased, which was directly proportional to the change in the Kuhn segments in the polymer chains. An increase in brush density was also predicted from the introduced neighboring bond correlation, which decreased the polymer brush height. When both the chain stiffness and neighboring bond correlation were introduced together and compared to a normal freely jointed chain polymer brush, with the same polymer end to end distance, very similar brush thicknesses were observed due to these two parameters balancing each other out.

The same year, Fredrickson et al. examined the potential differences in semi-flexible polymer brushes compared to flexible brushes.[23] For flexible polymer brushes, it has been

demonstrated that a Gaussian model describes the flexibility of the backbone of the polymer chains accurately.[87] However, this model does not effectively describe the rigidity seen in conjugated, highly crystalline, or sterically affected semi-flexible polymer brushes. To account for this, Fredrickson utilized a wormlike chain model instead of a Gaussian model. This proved to describe these semi-flexible brushes in a way that accounted for stiffness of the backbone and allowed this stiffness parameter to be changed. From this work Fredrickson was able to predict that introducing a large amount rigidity or stiffness into a polymer brush gives very different properties from a traditional flexible polymer brush model, such as strong orientation order, weak interpenetration, and a strong interfacial tension.

In 1998 Pryamitsyn et al. studied compression and subsequent extension of two main chain liquid crystalline polymer brushes facing towards one another.[90] The polymers brushes were examined using a SCF approximation. When compressed the brushes showed interpenetration with each other, forming one structure. Once the chains underwent extension the polymers stayed "glued" together, remaining in the same structure as the compressed brushes. This behavior is typical of liquid crystalline polymers where interactions between neighboring chains is very high, which is one of the major factors in obtaining a high degree of strength.[92]

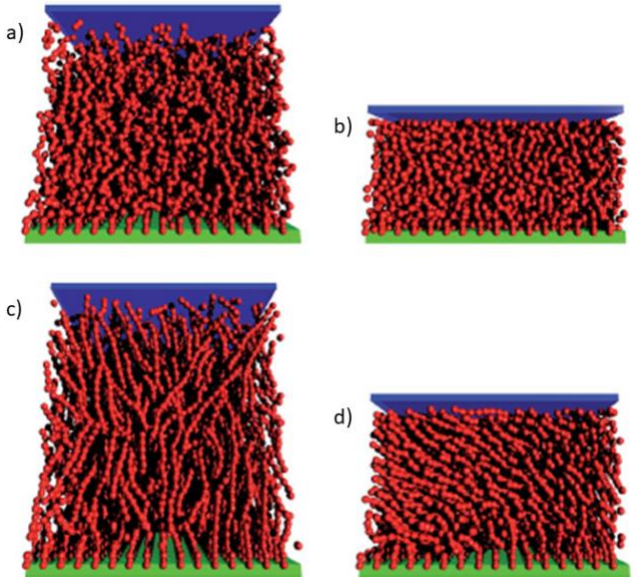

Figure 11. Illustration shows molecular simulation of flexible vs semi-flexible polymer brushes under pressure. a) flexible brush, b) flexible brush under compression, c) semiflexible brush, d) semiflexible brush under compression. [30], Copyright 2014. Reproduced with permission from Royal Society of Chemistry.

The work of the Binder group has contributed significantly to the computational

chemistry of semi-flexible polymer brushes in recent years. Through his work, Binder has discovered some unique findings, while also helping to cement other results.[[87],[30],[89]] One of the unexpected discoveries was that when compressing both flexible and semi-flexible brushes, of the same grafting density, the pressure needed to maintain the brush at a given degree of compression for the flexible brushes was greater compared to the semi-flexible brushes (**Figure 11**).[30] This was attributed to the semi-flexible chains all moving together, or collectively tilting in a common orientation, unlike the flexible chains, which moved closer towards one another with no long range order. The added stiffness of the chains in the semi-flexible polymer brush makes this motion possible compared to flexible chains that do not possess enough long-range order to maintain a common tilt. This has implications for tribological polymer surfaces composed of semi-flexible brushes, due to the low amount of force needed to maintain this degree of compression. Another important discovery by Binder was that increasing polymer backbone stiffness drastically increases the size of the random coil observed for a given polymer length, which lowers the mushroom to brush crossover compared to flexible brushes.[89] Because of this higher stiffness, weaker excluded volume interactions were observed allowing for some chain overlap, without significant chain stretching, which added an 'in-between brush' regime. To establish the differences in brushes, a semi-flexible random coil and a flexible random coil were both modelled and the grafting density of each was slowly increased. This resulted in different regimes being observed. It was shown that the semi-flexible random coils were much larger for a given molecular weight compared to the flexible random coils. Once the grafting density was increased, these semi-flexible random coils converted into the brush regime far before the flexible random coils did, resulting in smaller grafting densities required for brush formation for semi-flexible brushes

compared to flexible brushes. This importantly demonstrated that the grafting density needed to make a polymer brush-like structure is decreased as chain stiffness increases.

These discoveries, based on theory, were an important step in pushing for the synthesis of new types of non-vinyl-based polymer brushes. Without this groundbreaking work, semi-flexible brushes may not have sparked the interest of the synthetic polymer brush community, as they have today. The next sections will outline many of the advances that have been made making new types of non-vinyl-based polymer brushes a reality. The following table summarizes the polymer structures of the brushes that will be covered in the subsequent discussion and how they were synthesized. (**Table 1.)**

Surface Initiated Polymers	**Structure**	**Technique**
Polynorbornenes		
Poly(bicyclo[2.2.1]hept-5-en-2-yltrichlorosilane)	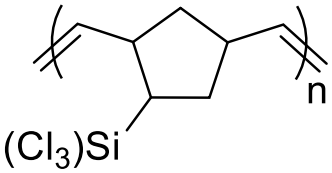	ROMP – 2nd gen. Grubbs catalyst [77]
Poly(bicyclo[2.2.1]hept-5-en-2-yltriethoxysilane)	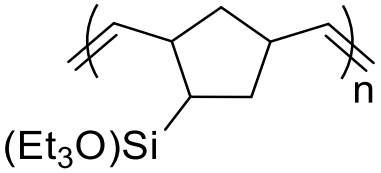	ROMP – 2nd gen. Grubbs catalyst [77]
Poly(2-methyl-3a,4,7,7a-tetrahydro-1H-4,7-epoxyisoindole-1,3(2H)-dione)	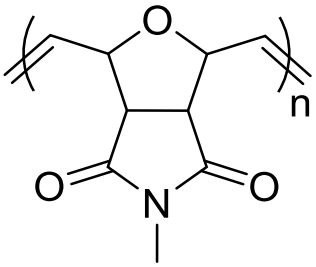	ROMP – 2nd gen. Grubbs catalyst [77]
Poly(bicyclo[2.2.1]hept-2-ene	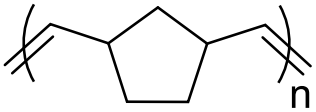	ROMP – 2nd gen. Grubbs catalyst [93] ROMP – 1st gen. Grubbs catalyst [94]

Poly(bicyclo[2.2.1]hept-5-ene-2,3-dicarbonyl dichloride)	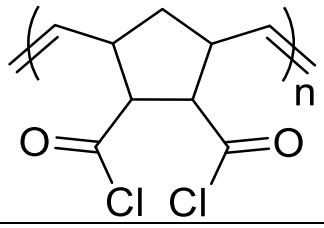	ROMP – 3rd gen. Grubbs catalyst [95]
Polypeptides		
Base Polypeptide unit	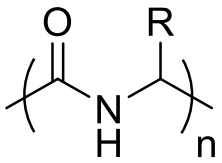	Primary amine-initiated polymerization organonickel catalyst-mediated polymerization [[96],[97],[98]]
Polyesters		
Poly(ε-caprolactone)	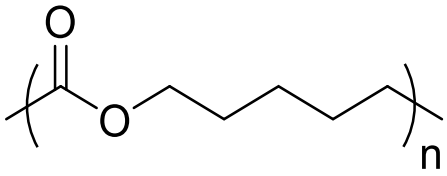	ROP – Organometallic catalyst [75] – Enzyme catalyst [99]
Poly(L-lactide)	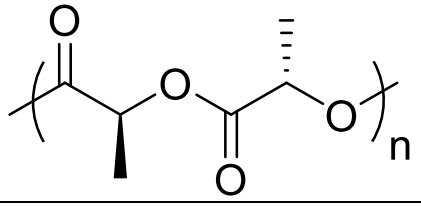	ROP – Organometallic catalyst [100]
Poly(p-dioxanone)	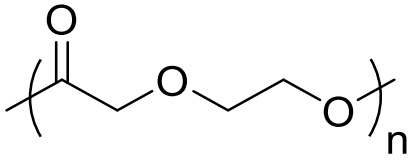	ROP - Enzyme catalyst [99]
Polyoxazolines		
Poly(2-ethyl-2-oxazoline)	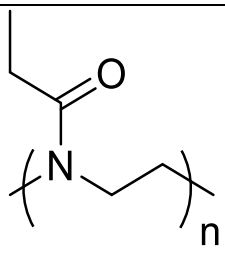	CROP – [[76], [101]]
Poly(2-methyl-2-oxazoline)	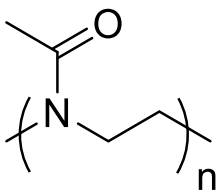	CROP – [[102], [103]]
Nylons		

Polycaprolactam	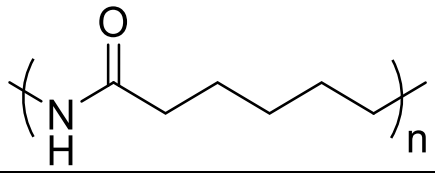	AROP – [[104], [105], [106]]
1,7-diaminoheptane and azelaoyl dichloride	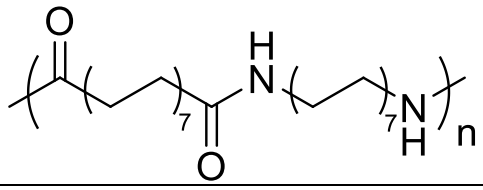	MLD – [107]
Polyurea		
1,4-diisocyanatobutane and ethylenediamine	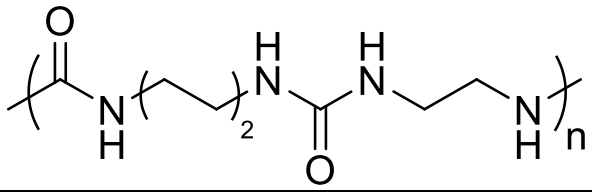	MLD – [108]
Polythiophenes		
Poly(3-hexylthiophene)	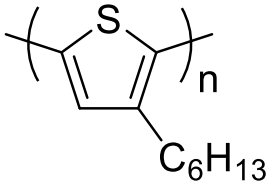	Catalyst transfer CGC polymerization – [[80], [109]]
Polythiophene	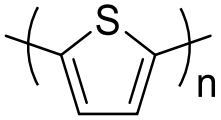	Catalyst transfer CGC polymerization – [86]
Poly(3-methylthiophene)	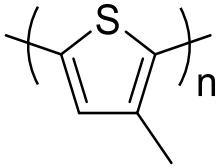	Catalyst transfer CGC polymerization – [[110], [[111], [112], [113]]
Poly(3-bromohexylthiophene)	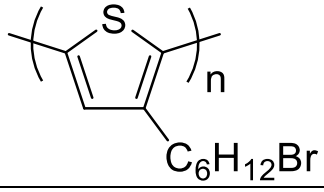	Catalyst transfer CGC polymerization – [114]
Polyfluorenes		
Poly(9,9-di(heptan-3-yl)-9H-fluorene)	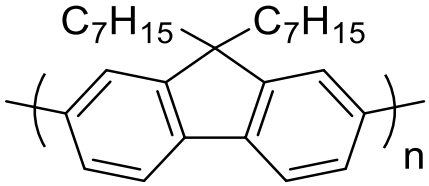	Catalyst transfer CGC polymerization – [81]
Polyphenylene		

Polyphenylene		Catalyst transfer CGC polymerization – [86]
Poly(phenylene ethynylene)		
Poly(1,4-bis((2-ethylhexyl)oxy)-2-ethynylbenzene)	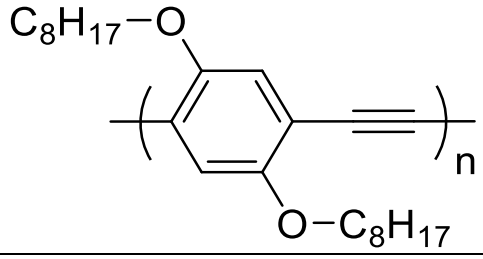	Catalyst transfer CGC polymerization – [78]
Polyisocyanates		
Poly(n-hexyl isocyanate)	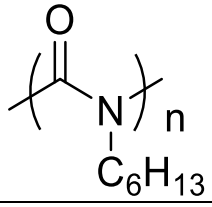	Organometallic catalyst – [83]
Polyisocyanides		
Poly(L-isocyanoalanyl-L-alanine methyl ester)	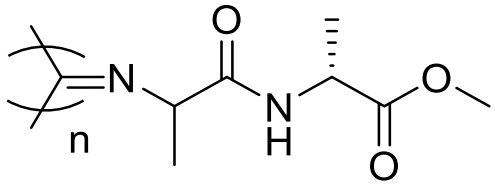	Organometallic catalyst – [84]
Poly(L-isocyanoalanine 2-(9H-carbazole-9-yl) ethyl amide)	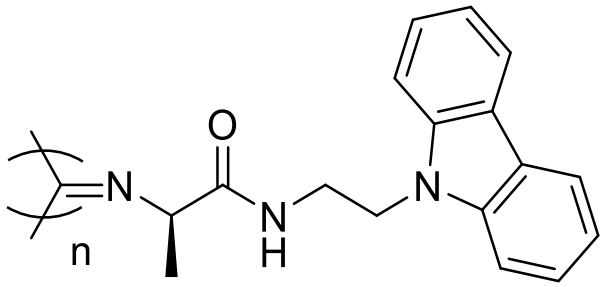	Organometallic catalyst – [115]
Poly(phenylene oxide)s		
Poly(3-(trifluoromethyl)phenylene oxide)	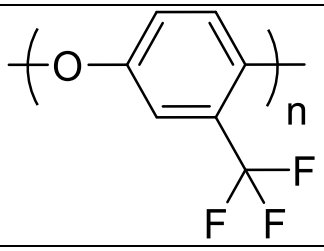	Substituent effect CGC polymerization – [85]
Aromatic Polyamides		
Poly(methyl 4-(octylamino)benzoate)	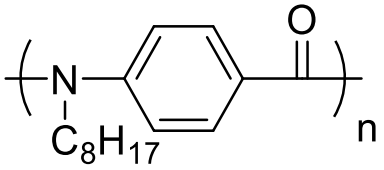	Substituent effect CGC polymerization – [2]

Polyaniline		
Polyaniline	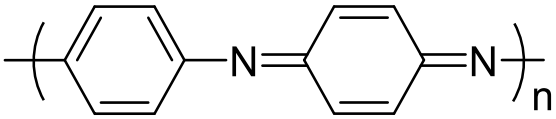	Oxidative polymerization – [[79], [116], [117], [118]]
Polypyrrole		
Polypyrrole	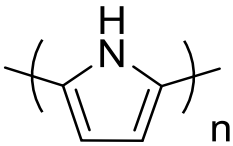	Oxidizing agent catalyzed polymerization – [[82], [119], [120]] Radical polymerization – [101]
Polycarbonates		
Poly(propylene carbonate)	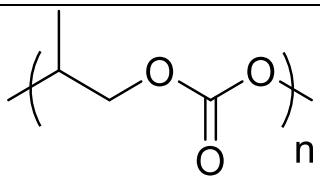	Immortal polymerization – [121]
Poly(trimethylene carbonate)	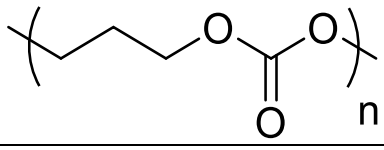	ROP Organocatalyst – [122]

Table 1. Non-vinyl-based polymer brush structures discussed in this review with corresponding polymerization methods used.

4.2 Molecular Layer Deposition

The first synthetic examples of non-vinyl-based polymer brushes via the 'grafting from' technique were prepared via molecular layer deposition (MLD). This technique has the advantage of overcoming the need for a living chain-growth polymerization to form a 'grafted

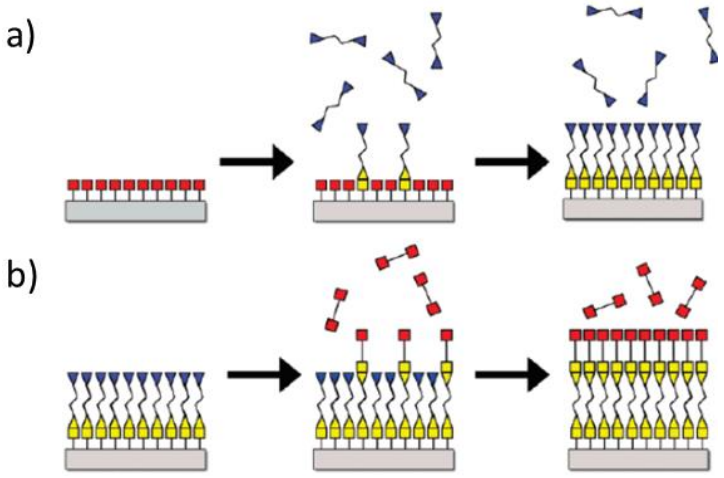

Figure 12. Schematic showing molecular layer deposition (MLD) method. In both the a) and b) schemes show bifunctional molecules reacting to the surface via a surface terminated reactive end group. [125], Copyright 2008. Reproduced with permission from American Chemical Society.

from' polymer brush but the exceedingly large time required to make polymer brushes of reasonable thickness is a major disadvantage. The MLD process involves using bifunctional molecules that do not react with themselves but can react with specific sites on the surface. One layer of molecules is deposited on the surface at a time then repeated with the next molecule (**Figure 12**).[[123],[124],[125]] This process continues until the desired thickness is achieved. The most common way to prepare polymer brushes via MLD is by using vapor deposition. This involves using a heated chamber that allows a substrate to be saturated with one of the bifunctional molecules.[126] Once this molecule has fully reacted there is a purge period to remove the first molecule then the next molecule is allowed to saturate the substrate. This is then repeated until the desired number of repeat units has been added. Many different polymers brushes have been prepared using the MLD process including polyamides, polyimides, polyureas, polyurethanes, polythioureas, polyesters, and polyimines.[[123],[127],[128],[129],[130],[131],[132]]

One of the earliest examples of successfully growing a polyamide film via MLD was performed by Okui et al. in 1996.[107] In order to form the polymer film, 1,7-diamineoheptane (DAH) and azelaoyl dichloride (ADC) monomers were used to form a nylon 7,9 polymer film. A vapor deposition reaction was utilized using an alternating condensation reaction of an acid chloride with an amine and vice versa. Each monomer was evaporated separately, 25 °C for DAH and 40 °C for ADC, and introduced into the chamber at different times. The vacuum chamber was evacuated at $1x10^{-5}$ Torr before each deposition. A quartz crystal plate with amine groups on the surface was used as the substrate. Each monomer was allowed to react for 850 seconds before the next monomer was introduced. Using this method polyamide films of up to 40 nm were produced. The films were monitored using transmission and reflective adsorption spectra from infrared (IR) spectroscopy, which showed the polymers characteristic peaks. However, it is important to note

that no grafting density was reported, and no other characterization was performed on the polymer films. As such, it is difficult to conclude that a polymer brush regime for this structure was obtained.

More recently Bent et al. made cross-linked polyurea films using MLD and demonstrated improved strength compared to non-cross-linked polyurea films.[108] In order to make these films silicon wafers were first treated with piranha solution followed by addition of 3-aminopropyltriethoxysilane to add an initiator the surface. After this process, the monomers were deposited in different chambers. 1,4-diisocynateobutane, diethylenetriamine, ethylenediamine were kept at room temperature (RT) while triethylenetetramine and tris(2-aminoethyl)amine were warmed in an oil bath to 40 °C. Cycles for the addition of monomer started with reacting the isocyanate monomer followed by purging with nitrogen then reacting the surface with one of the amine monomers. Each monomer cycle was given enough time to fully saturate the surface before purging with nitrogen between cycles. Using this method, film thicknesses approached 50 nm while showing characteristic IR peaks for the desired polymer, along with stoichiometric compositions of cross-linked films, as determined using X-ray photoelectron spectroscopy (XPS). In addition, X-ray reflectivity was used to show that the overall density of the polymer film was increased by up to 50% as a result of cross-linking. Lastly, using vacuum annealing, the decomposition temperature of the films was demonstrated to also increase by approximately 30 °C after cross-linking. This example highlights the potential non-vinyl-based polymer films possess in being able to not only increase polymer density but also increase the thermal stability of the resulting films.

The development of MLD was an important step forward in achieving new types of polymer brushes based on non-vinyl monomers. Despite this advance, the MLD method presents

many difficulties in producing well-defined polymer brushes, including variability in growth rate, long overall reaction times, and self-limiting growth.[[125],[133]] Based on these restraints, by itself, MLD has a limited use. One of the major uses that MLD does have is using it in conjunction with atomic layer deposition to form organic and inorganic hybrid films.[126] This has many applications but falls out of the scope of this review. Because of the issues with MLD, new techniques have been explored to make similar types of polymer brushes while overcoming the above issues.

4.3 Ring Opening Polymerizations

4.3.1 Polynorbornene

Polynorbornene brushes have many unique applications due to ease of synthesis, an inherent flexibility in modifying the side chain off of the main monomer unit, the high degree of film thickness possible, a heat resistance above 300 °C, and a relatively high glass transition temperature (T_g), ranging from 134–325 °C, of the polymers that have been produced.[134] In particular, modification of the base norbornene monomer side chain has been shown to tailor properties for applications including electrochemical sensors, tribological films, patterned films, antimicrobial surfaces, and metal insulator semiconductor devices.[[77],[93],[135],[136],[137]] By far the most common technique used to synthesize polynorbornene brushes is ROMP, typically with a ruthenium Grubbs catalyst.

One of the first examples using ROMP to make polymer brushes via the ‘grafting from’ technique was successfully demonstrated by Laibinis et al. in 2000.[77] In this work, a silane initiator with a norbornene group was attached to a silica wafer followed by addition of a Grubbs catalyst to react with the cyclic alkene group on the surface and activate the initiator towards

polymerization (**Figure 13**). Using this method, polymer brushes were synthesized up to 90 nm in thickness utilizing a variety of different monomers. The versatility of this method was also demonstrated by patterning of a surface using micro contact printing. This resulted in polymer brushes with a high degree of uniformity in the brush thickness and high resolution along the edges of the patterned structures. Scanning electron microscopy (SEM), Fourier-transform infrared (FTIR) spectroscopy, ellipsometry, atomic force microscopy (AFM), and XPS were used to characterize the surface and show characteristic chemical compositions, production of desired patterns, defined film thickness, and low surface roughness. However, no grafting densities were reported for the polymer films and the polymers were not degrafted to characterize the molecular weight of the surface attached polymers. The absence of both of these results, make it difficult to establish if the polymer film was actually in the brush regime, however, this work was an excellent first step in demonstrating the ability to produce non-vinyl-based polymer films via surface initiation of norbornene monomers.

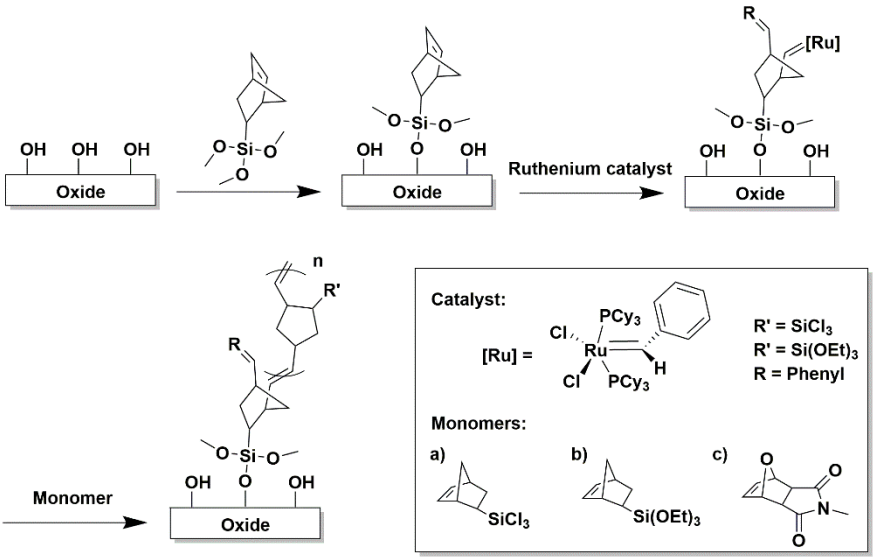

Figure 13. Reaction scheme shows the use of ROMP to grow polynorbornene brushes with different monomers that have successfully polymerized by Laibinis et al. starting with initiation of the surface and activation using a ruthenium catalyst. [77]

In 2001, Lewis et al. reported the growth of polynorbornene brushes up to 5500 nm thick, which represents one of the thickest polymer brushes published to date.[93] This was achieved by varying the concentration of the norbornene monomer, bicyclo[2.2.1]hept-2-ene, from 0.01 to

2.44 M and using a unique initiator-modified surface, which started directly from the silica surface. The polymerization process was very similar to the Liabinis et al. surface-initiated polymerization process but involved a different initiator. The surface-immobilized initiator was prepared by first etching the silica (111) wafer with 49% hydrofluoric acid (HF) for 30 minutes then aqueous 40% NH_4F for 15 minutes. Once the silica surface was protonated to give silanol groups, a substitution reaction with phosphorus pentachloride took place with trace amounts of benzoyl peroxide, to act as a radical initiator, resulting in chlorine in place of the hydroxyl groups. The chlorinated surface was then exposed to allylmagnesium chloride and then reacted with the ruthenium catalyst, $(cyclohexyl_3P)_2Cl_2Ru{=}CHPh$, to attach it to the surface. The surface was subsequently cleaned thoroughly and different concentrations of norbornene monomers were used to synthesize the polymer brushes. The polymer brushes were grafted directly onto the silica (111) in order to obtain more control over insulation properties for use in electrical device construction. SEM and ellipsometry both confirmed the 5500 nm thickness while XPS confirmed the atomic composition for each step of the synthesis. Again, no grafting density was obtained nor was polymer degrafted for molecular weight characterization, however, this extremely thick surface-initiated film was a novel step forward in the polymer brush field.

In 2018 Berron et al. showed that by cross-linking a polynorbornene brush it could withstand solvent degradation much better than without cross-linking.[94] While surface-initiated polynorbornene films have shown to be of value for a variety of applications, they have the inherent weakness of being prone to solvent degradation. For example, in one study a polynorbornene brush was shown to decrease in thickness by up to 93% when washing with dichloromethane (DCM) at ambient conditions.[138] This degradation is hypothesized to be due to the polymers allylic hydrogens being readily liable to oxidative degradation and cleaving from

the surface. To overcome this, cross-linked polynorbornene brushes were prepared on a 200 nm chromium layer, as an adhesion layer, and an 800 nm gold layer sputtered on a silica wafer. The gold covered silica wafers were annealed at 220 °C, then placed in a solution of ethanol with 11-mercapto-1-undecanol to form a SAM, and finally placed in DCM with 5 mM solution of trans-3,6-endomethylene-1,2,3,6-tetrahydropthaloyl chloride to give a norbornene functionalized surface. The initiated wafer was then activated with a 5 mM solution of a 1st generation Grubbs catalyst in DCM, followed by washing with DCM to remove any unreacted initiator. The polymerization was conducted with 0.5 mM of norbornene monomer and either 0.25 mol%, 0.5 mol% or 1 mol% of a dinorbornene cross-linker with reaction times ranging from seconds to up to 2 hours (**Figure 14**). The cross-linker used was two norbornene molecules with ester groups directly attached to the norbornene molecules and 34 poly(ethylene glycol) (PEG) repeat units between the ester groups. By adding the cross-linking molecule, the films decreased thickness drastically compared to non-cross-linked norbornenes, approximately 30 nm compared to 1 μm, respectively. Due to this decrease, the lower 0.25 mol% solution of cross-linker was prioritized, as it resulted in the thickest cross-linked polymer films of those prepared. No grafting density or

molecular weight characterization was performed but, based off a previous study, an approximate grafting density of approximately 10^{12} molecules per cm^2 (which equates to 0.01 molecules per nm^2) of Grubbs catalyst was estimated.[139] Although this is a good number to report, this does not directly correlated to polymer brush grafting density, which is normally lower than the density of initiating sites. When cleaning the cross-linked polynorbornene wafers compared to the un-cross-linked polynorbornene wafers a decrease in thickness of only 28% after 10 rinses, compared to the original 73% decreased, was observed. While the PEG cross-linker demonstrated a decrease in thickness, future studies using a more compatible cross-linker or a more tolerant catalyst were predicted to increase the brush thickness.[94] This study does show proof of concept but in order to solve some of the fundamental polynorbornene brush issues, such as film stability, the cross-linker compatibility needs to be resolved along with better understanding of why the thickness decreases in the first place.

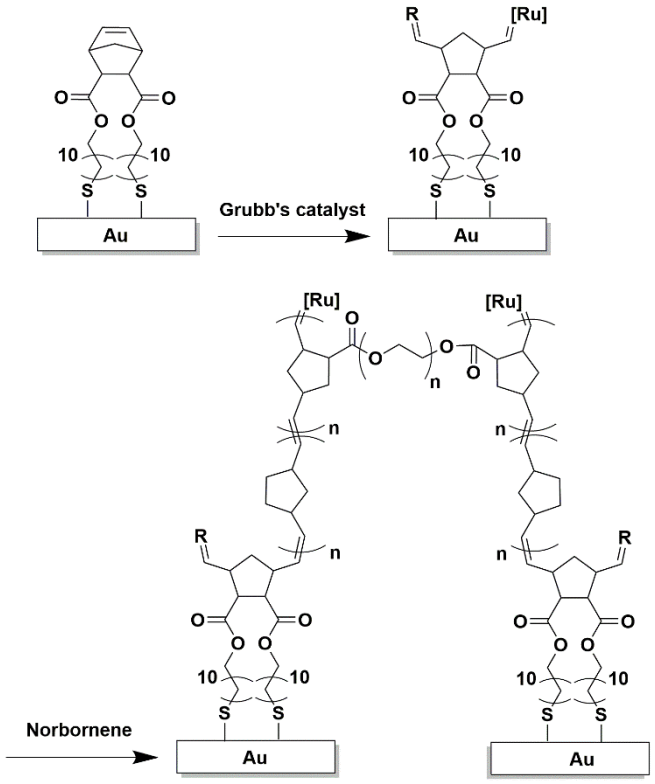

Figure 14. Reaction scheme shows the synthesis of a random polynorbornene brush with crosslinked PEG chain to help prevent solvent degradation performed by Berron et al. [94]

In 2019 Jennings et al. made polynorbornene brushes with acid halide side groups that could be easily modified post polymerization for a variety of applications.[95] This polymer functionality has the advantage that it can easily react with water, alcohols, and amines to form

carboxylic acids, esters, and amides, respectively, after polymerization is complete to tailor the side chain properties. The films were prepared by adding a 100 Å chromium layer and a 1250 Å gold layer on silicon wafers. The gold layer was then modified with a hydroxy-terminated SAM layer using 4-mercapto-1-butanol. The hydroxy-terminated gold wafer was then exposed to the trans-3,6-endo-methylene-1,2,3,6-tetrahydrophthaloyl chloride monomer in DCM to attach the norbornene monomer to the surface. Finally, the wafer was exposed to a third generation Grubb's catalyst in DCM. To start the polymerization, a 65 °C chamber with pure liquid monomer was preheated and the initiated wafer was placed inside and reacted with the vapor phase monomer. After the polymerization was completed the wafer was cleaned with DCM to remove excess monomer and the surface was immediately reacted with different molecules such as an amine, water, or an alcohol. Polymerization reaction times ranged from 1-10 minutes and gave a max thickness of 370 nm, as determined by profilometry. Modification of the acid chloride functional group using water, ethanol, and ethylamine was confirmed using FTIR spectroscopy. In addition to these molecules, the polymer brushes were exposed to more complex molecules, such as aniline and 2-dimethyl-aminoethanol. Each molecule was shown to undergo complete reaction with acid chloride the side groups using FTIR spectroscopy. Although this work demonstrated the ability to prepare and modify functional polynorbornene polymer films, no molecular weight characterization or thermal gravimetric analysis (TGA) was performed, so no grafting density was reported to definitively show these films were polymer brushes.

4.3.2 Polypeptide

Polypeptide brushes are among earliest examples of brushes synthesized using non-vinyl-based monomers via the 'grafting from' technique. These brushes utilize a surface-initiated ring opening polymerization (SI-ROP) method from N-carboxyanhydride (NCA) monomers. Multiple

comprehensive reviews have been written covering the leading research on this topic so this review will only discuss the highlights.[[21],[96],[97],[98]] Polypeptide brushes have many exciting properties that can be utilized in a variety of applications, including drug-delivery vectors, artificial cells, biomaterials, micro-electronic devices, stimuli-responsive surfaces, energy capture/storage, membrane technology, separation technologies, non-biofouling surfaces, antibacterial coating, protein binding, immobilization, piezoelectric effects, and liquid crystal displays.[[21],[96],[97]] These applications come from the unique properties of amino acids, such as biocompatibility and the long range order of alpha helices and beta sheets that can be formed from polypeptides. Almost all naturally existing and synthetic amino acids have been reported in making polymer brushes.[21]

Multiple 'grafting from' routes have been used to produce polypeptide brushes, including solution polymerization, vapor deposition polymerization (VDP), and melt polymerization. Solution polymerization is the most widely used technique and the simplest to perform. This technique involves placing an initiator-modified substrate into a solution of monomer and directly polymerizing from the surface. This technique has proven to be successful with a variety of substrates and has been shown to be capable of producing polymers of difference architectures, including block copolymers.[97] One of the major challenges of the solution polymerization technique is the extremely high ratio of monomer concentration in solution to the concentration of initiator on the surface. Because of this high ratio reproducibility of the technique can be a problem, due to the sensitivity of the polymerization to impurities in the monomer and moisture in the solvent, both of which limit the thickness of the grafted polymer film.[21] In addition to this, self-initiated free polymer, formed in solution, can block surface sites by aggregating on the surface. In contrast to solution polymerization, melt polymerization spin casts a monomer solution onto an initiated substrate and subsequently removes the solvent used to spin cast the monomer. Next, the

substrate and monomer are heated past the monomers melting point and the polymerization is carried out in a bulk polymerization. This improves on solution polymerization by removing the need for a solvent and reducing the moisture that can limit solution polymerizations. However, this technique typically results in a large amount of thermally induced ~~thermal induced self-initiated non-grafted~~ polymers produced in the bulk, which can block initiation sites from continued growth, resulting in premature termination of the surface-initiated polymerization and reducing the thickness and grafting density of the polymer film. VDP works by placing an initiated substrate in a heated and depressurized chamber. Monomer is then allowed to vaporize and react with the surface. This technique removes the moisture and monomer sensitivity that melt and solution polymerizations experience. VDP has been used to prepare polypeptide brushes as thick as 187 nm.[21] The main drawback to VDP is that not all amino acids can be used. The amino acids that have been reported to work the best are the amino acids that form alpha helices and parallel beta sheets. Antiparallel and random coil conformations have been reported to not be as successful.[21]

There are currently two main polymerization mechanisms for SI-ROP to produced polypeptide polymer brushes: 1) primary amine-initiated NCA polymerization; and 2)

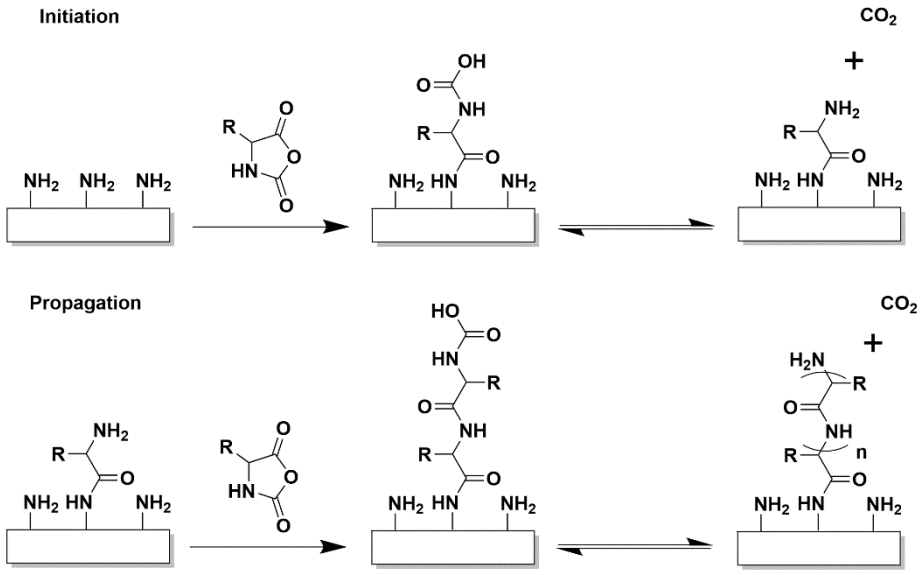

Figure 15. Reaction scheme shows initiation and propagation of SI-ROP utilizing a primary amine-initiated surface and an NCA monomer. [21]

organonickel catalyst-mediated NCA polymerization. Primary amine-initiated SI-ROP of NCAs works by first attaching a primary amine to the desired surface (**Figure 15**). This primary amine then acts as a nucleophile and reacts with an NCA forming a carbamic acid, thus starting a propagating chain. The carbamic acid is not very stable and undergoes decarboxylation to generate another primary amine, which continues the reaction.[21] The initiator's primary amine is more nucleophilic than the NCAs primary amine, causing a faster rate of initiation compared to propagation, and results in a living chain-growth polymerization and polymers with a low PDI. This polymerization is very accessible due to the ease of initiating a variety of surfaces but comes with its challenges due to it being very sensitive to water and impurities. These can lead to side reactions such as chain transfer, self-cyclization, and premature termination of the propagating chain. Organonickel catalyst-mediated NCA polymerization has proven to work well in solution polymerization and has been studied extensively.[21] However, utilizing this technique on surfaces has proven more problematic due to difficulty in attaching the nickel catalyst onto the surface. Two main methods for attachment of the catalyst have been developed (**Figure 16**). The first method is called the "block copolymerization approach" and reacts a surface bound NCA with

excess nickel initiator complex. The second method is called the "alloc-amide approach" and works by attaching an alloc-amide to the surface then reacting this surface bound alloc-amide with $Ni(COD)_2$ and phenantroline. The "alloc-amide approach" is reported to produce a larger amount of grafted polymer and less free polymer, in addition to being a more straightforward synthetic route.[140] However, neither of these methods work as well as the primary amine-initiated SI-ROP and have only reported brushes up to 10 nm thick.[21]

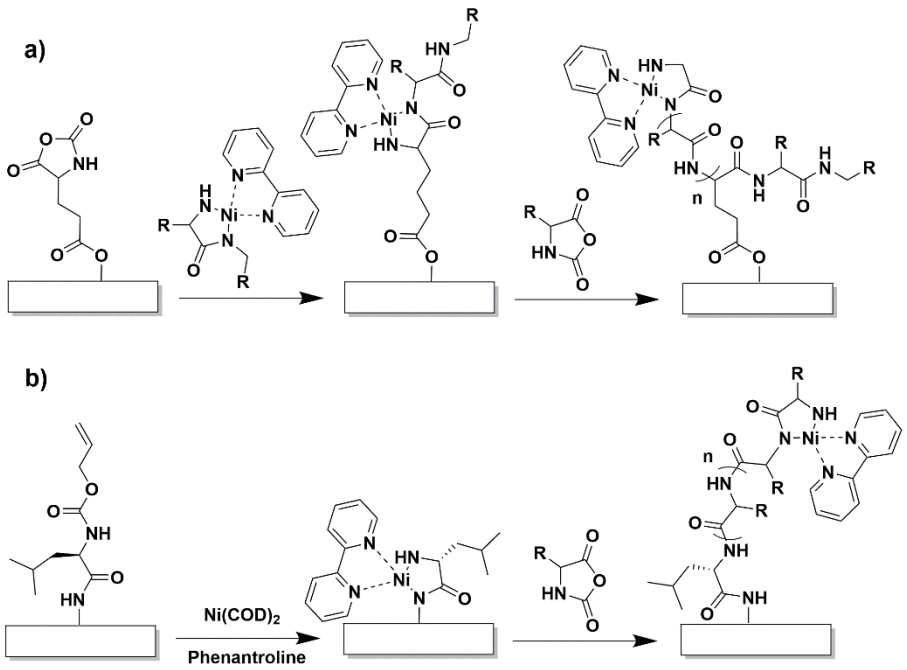

Figure 16. Reaction pathways using SI-ROP organonickel catalyst mediated NCA polymerization using a) "block copolymerization approach"; and b) "alloc-amide approach". [21]

4.3.3 Polyester (Polylactides, Polycaprolactones, and Polydioxanones)

Polyester brushes synthesized from lactides, caprolactones, and dioxanone are unique in that they are easily biodegradable, have biocompatibility, and can be synthesized in a variety of ways. Most of the applications of these polymer brushes arise from these characteristics and include passivation of prosthetic devices and implants, coatings for drug delivery devices, surgical sutures, and scaffolds for tissue engineering.[[141],[142]] These types of polymer brushes have been shown to be synthesized using metal catalysts, enzymatic catalysts, and organic catalysts, which has helped in expanding the applications further.[[75],[99],[143]]

The first example of polyester brushes formed was from Abbot et al. in 1999.[75] In this study ε-caprolactone was grown from a primary alcohol on the surface of a gold-covered glass slide using triethylaluminium as an organometallic catalyst. In order to gain more control over the polymerization and increase the brush height a free initiator was used in conjunction with the surface initiator. To make the brushes, a thiol-based initiator with a primary alcohol was reacted to a glass slide covered with 200 nm gold layer. To prepare for the polymerization, the diethyl aluminum alkoxide initiators were prepared in inert atmosphere by first reacting the triethylaluminium with benzyl alcohol in toluene then adding the initiator coated gold-covered slide. After the triethylaluminium had reacted with the surface-attached alcohol, the toluene was removed under vacuum. Dry toluene, ε-caprolactone, and solution initiator were then added to the initiated slides and reacted for 3 hours at 25–30 °C followed by quenching with acetic acid (**Figure 17**). The glass slides were washed with DCM, toluene, tetrahydrofuran (THF), and ethanol to remove free polymer. The solution polymer was then precipitated from solution using methanol to allow for further characterization. The thickness of the polymer brushes was compared to the degree of polymerization (DP) of the free polymer and showed a linear correlation of DP with film thickness. Uniform brushes up to 70 nm were achieved with this technique but no grafting density

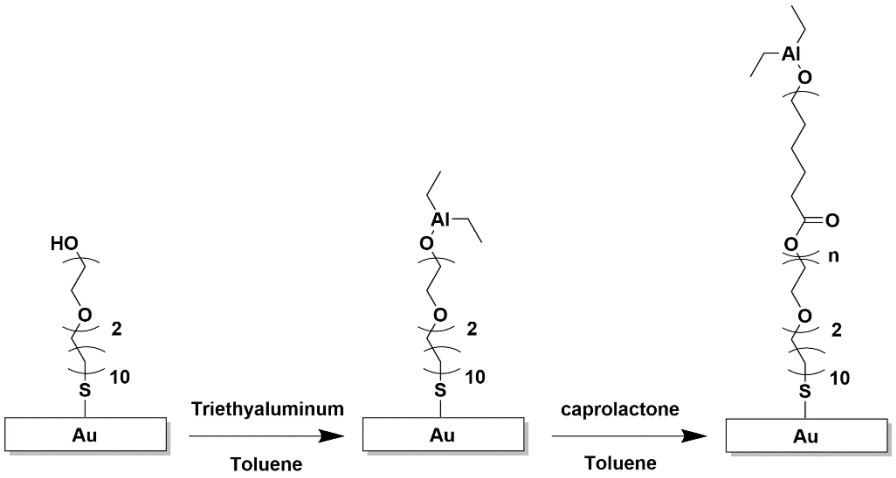

Figure 17. Reaction scheme shows the first example of SI polycaprolactone polymer brush synthesized by Abbot et al. starting from surface alcohol group to activation with catalyst then propagation by addition of caprolactone monomer. [75]

or grafted polymer molecular weight was reported to confirm a true polymer brush structure was obtained. Because solution initiators were needed for control over the polymerization and increased brush height, this technique is not ideal for easily growing polymer brushes due to the need for extensive washing to remove physical absorbed polymer.

In 2001 Choi and Langer showed the first example of growing poly(lactic acid) (PLA) brushes.[100] PLA brush growth was demonstrated from both gold and silica substrates. Similar to Abbot, a primary alcohol was used as an initiator for the gold substrates, whereas a primary amine initiator was used for silica substrates. The polymer brushes were grown by adding the initiated wafers to a THF solution of $Sn(Oct)_2$ and L-lactide, followed by heating to the desired temperature. PLA is conventionally synthesized in this manner at 80 °C but due to thiol instability on the gold substrates above 60 °C this reaction was carried out at 40 °C for 3 days. For the silica substrates a reaction temperature of 80 °C was used and reactions were also carried out for 3 days. Once the reaction times were completed the wafers were cleaned with DCM, ethanol, and water and dried with nitrogen gas. Due to the lower reaction temperatures for the gold substrates a film thickness of only 12 nm was reported, whereas, a thickness of up to 70 nm was reported for the higher reaction temperature used for the silica substrates. No grafting density or molecular weight characterization were reported for either substrate although, based off of AFM, the films visually lacked uniformity, potentially suggesting a lower grafting density.[19] The root mean square (rms) roughness of the 70 nm thick films was 38 nm and was hypothesized to be high due to PLA possessing high levels of crystallinity, which could form aggregates instead of having a uniform surface. As PLA has a T_g of 60 °C and a melting point of 190 °C, the brushes were annealed at 180 °C for 5 minutes followed by 130 °C for 2 hours to investigate the presence of aggregates. After annealing, the rms roughness increased further to 52 nm and circular shapes were noticed in

the AFM topography. This was presumed to be due to elongation structures of the PLA, which can form lamella like structures. This demonstrated that by annealing the polymer brush, different surface morphologies could be obtained.

In 2003 Choi et al. reported the first example of growing polyester brushes using an enzyme catalyst.[99] The poly(ε-caprolactone) and poly(p-dioxanone) brushes were grown off gold substrates with a primary alcohol initiator. To synthesize the brushes the enzyme, lipase B, along with the initiator-coated wafers were dried under vacuum at 55 °C to remove water from the lipase B. The lipase B enzyme has been proposed to form an activated monomer complex that possesses a highly reactive ester group, which can either be hydrolyzed by water or by a hydroxyl containing molecule (**Figure 18**). After drying, anhydrous toluene and monomer were sequentially added via a syringe pump and the reaction took place at 55 °C for 24 hours. The substrates were then sonicated for 5 minutes in solvent to remove any physically absorbed polymer. The solvents used were DCM for poly(ε-caprolactone) and 1,1,1,3,3,3-hexafluoro-2-propanol for poly(p-dioxanone). The thickness of the poly(ε-caprolactone) film was determined by ellipsometry and reported to be 93 nm with a rms roughness of 1 nm and the film showed the characteristic IR peaks for poly(ε-caprolactone). Although no grafting density or molecular weight characterization was performed

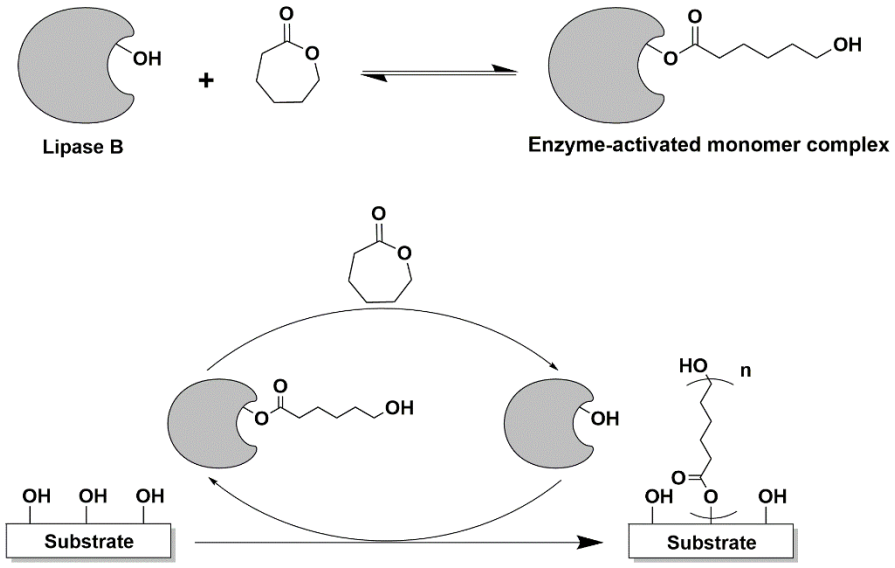

Figure 18. Proposed mechanism by Choi et al. for enzyme surface-initiated polymerization to form a polyester. [99]

on the films, solution polymer was prepared using the same reaction conditions to obtain an approximation of the molecular weight and PDI. From this solution polymerization, a weight average molecular weight (M_w) of 33,600 and a PDI of 1.93 was obtained using gel permeation chromatography (GPC). Due to the higher PDI value, the uniform film coverage, as suggested by the very low rms roughness, is unexpected but the authors note that this could be due to the polymer brushes collapsing on the surface to give the appearance of uniform coverage.

4.3.4 Polyoxazoline

Similar to the polyesters reviewed above, polyoxazolines have become prevalent in biomedical and pharmaceutical applications, including polymer−drug and polymer−protein conjugates, self-assembled carriers for drug delivery, solid dispersions, hydrogels, antibiofouling and antimicrobial surfaces, wound healing, and fluorescent imaging.[[144],[145]] Not only are these polymers biocompatible but their properties are highly tunable depending on the synthesis technique and the use of any post polymerization modifications. This allows polyoxazolines to possess properties that range from amorphous polymers to semi-crystalline polymers with a T_g ranging from below 0 °C to over 230 °C and melting points ranging from below 90 °C to over 300 °C, depending on the side chain that is used. In addition to this, polyoxazolines have highly tunable hydrophilicity allowing for the preparation of a range of hydrophobic to hydrophilic polymers.[76] Based on these properties, polyoxazoline brushes are promising due to the high levels of tunability in being able to coat nanoparticles or substrates.[102]

Yoshinaga and Hidaka were the first to attempt to make polyoxazoline brushes in 1994.[146] Although the polymerization was difficult, they managed to grow octamers and nonamers from silica nanoparticles covered with a polystyrene layer. One of the primary issues encountered in this system was the polystyrene layer dissolving from the particles, as this layer

was not cross-linked. In addition, it was believed that early termination resulted from water left inside of the particles, which caused the formation of the observed low molecular weight oligomers on the particles.

In 1998 Jordan and Ulman demonstrated the first example of a surface-initiated polyoxazoline using a living cationic polymerization.[76] The polymer films were grown from gold substrates using a thiol anchor to attach a primary alcohol layer to the substrate. The alcohol initiator was then activated with a trifluoromethanesulfonic anhydride vapor to form a triflate functional group. The reaction vessel was subsequently purged with nitrogen followed by addition of dry chloroform and the 2-ethyl-2-oxazoline monomer being added at 0 °C. The reaction was heated to reflux and reacted for 7 days after which time the reaction was terminated by addition of N,N-dioctadecylamine (**Figure 19**). Using this technique, polymer films up to 10 nm were grown, which showed all the characteristic IR peaks and had a similar contact angle when compared to spin coated films of the same polymer. No molecular weight or grafting densities were directly reported but the films were compared to films of the same polymer prepared via the 'grafting to' technique using FTIR spectroscopy. The amide band on the surface-initiated film had a higher integral adsorption compared to the 'grafting to' film of similar thickness, which was hypothesized to be due to a higher grafting density. To estimate the molecular weight, a minimum DP of 26-28 was calculated using the distance of a fully

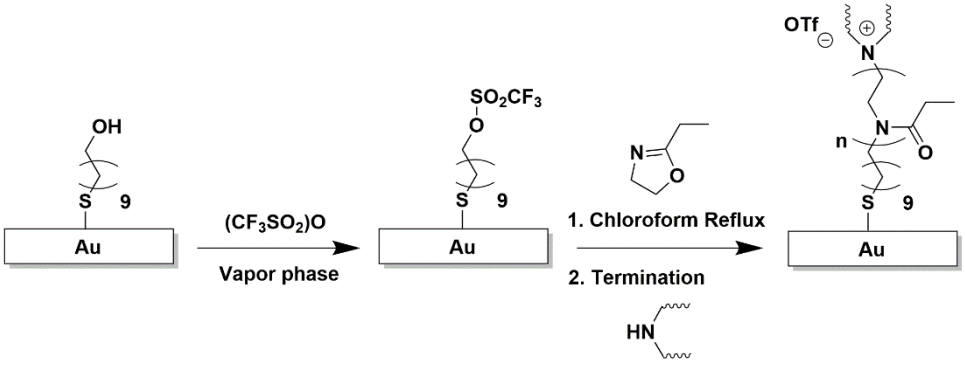

Figure 19. Reaction scheme shows the first example of surface-initiated polymerization of polyoxazoline by Jordon and Ulman starting with a surface alcohol, activating the alcohol with triflate functional group, and, finally, the addition of monomer. [76]

stretched poly(2-ethyl-2-oxazoline) chain and the polymer brush thickness. Although both calculations were approximations, they suggest that this technique produces polymer films with a higher grafting density compared to the corresponding 'grafting to' films, which increased the probability that the polymer films were in the brush regime.

In 2010 Bicak et al. used 2-bromoethyl methacrylate (BEMA) cross-linked particles to grow poly(2-methyl-2-oxazoline) surface-initiated polymer brushes.[147] In this study the bromine present on the surface of the cross-linked particles was used to initiate the 2-methyl-2-oxazoline. This was achieved by starting with well-defined and cleaned BEMA particles of 210–420 μm in size. The polymerization was carried out by adding BEMA particles, 2-methyl-2-oxazoline, and acetonitrile to a reaction flask, which was then purged with nitrogen before being heated to 110 °C for 24 hours. The reaction was then poured into water and the particles filtered off. The particles were cleaned with water and ethanol and dried at 50 °C for 24 hours. The particles were also modified after cleaning by adding the poly(2-methyl-2-oxazoline)-coated BEMA particles to a solution of hydrochloric acid (HCl) and refluxed for 48 hours to reduce the backbone amide to an amine. After the polymerization the particle weight increased by 62%, while also showing the characteristic amide IR peaks associated with poly(2-methyl-2-oxazoline). Kinetic studies showed first order kinetics suggesting that this polymerization has the characteristics of a living chain-growth polymerization. Following amide cleavage of the original brushes, the FTIR showed characteristic amine stretching and bending vibrations while the amide peaks disappeared. Although no grafting density or molecular weight characterization was performed, SEM images of the BEMA poly(2-methyl-2-oxazoline) covered particles were taken and showed uniform coverage, which suggested that these brushes have a reasonably high grafting density.

In 2016 the first polyoxazolines grown on silica nanoparticles using the 'grafting from' technique were reported by Bissadi and Weberskirch.[102] Similar to Bicak et al., the initiator for the polymerization was a halide, in this case a chloride, and surface-initiated CROP was used. The initiator used was ((chloromethyl)phenylethyl) trimethoxysilane, which was attached to the surface of the approximately 53 nm silica nanoparticles. The polymerization was performed by adding the initiator-modified silica nanoparticles and potassium iodide into anhydrous acetonitrile and sonicating for an hour to exchange the chloride with the iodide ion on the initiator. Once complete, the monomer, 2-methyl-2-oxazoline, was added to the acetonitrile solution and the reaction was conducted at 120 °C while stirring, for varying amounts of time (**Figure 20**). Once the polymerization was complete and cooled to RT, piperidine was added to terminate the reaction and it was stirred overnight. The solvent and excess piperidine were then removed by reduced pressure. Chloroform was used to dilute the mixture and it was then precipitated by ethyl ether and collected via centrifugation. Using FTIR spectroscopy all the characteristic peaks for the polyoxazoline were observed. Transmission electron microscope (TEM) was used to show a uniform coating, of up to 3 nm in thickness, of the polymer brush around the nanoparticles. Unlike previous studies, grafting density and molecular weight characterization was performed. In order to find the grafting density and molecular weight of the polymer brushes, TGA was used to find the percent weight loss for the polymer coating. NaOH was used to cleave the polymer from the nanoparticles, which was isolated and then characterized using GPC, allowing for calculation of the grafting density. GPC showed increasing molecular weight with reaction time and the degrafted polymer that had low PDI values, suggesting that this system shows characteristics of a living chain-growth polymerization. From these studies, polymer brushes with a maximum M_n of

6,473 g/mol, and a PDI of 1.24, were prepared. Grafting densities of up to 1.49 chains/nm^2 were observed for this 'grafting from' based technique, which exceeds those obtained for similar polymer films prepared via 'grafting to' methods that range from 0.18 to 0.45 chains/nm^2.[103] To make these polyoxazolines more diverse, an amine-functionalized terminating agent was used to allow for post polymerization modification. The brushes were modified with either fluorescein isothiocyanate or folate, which are used as a fluorescent imaging molecule and cancer targeting ligand, respectively. Because of the living chain-growth polymerization technique employed, adding end capping agents like these are easily possible and can help expand the applications of these systems.

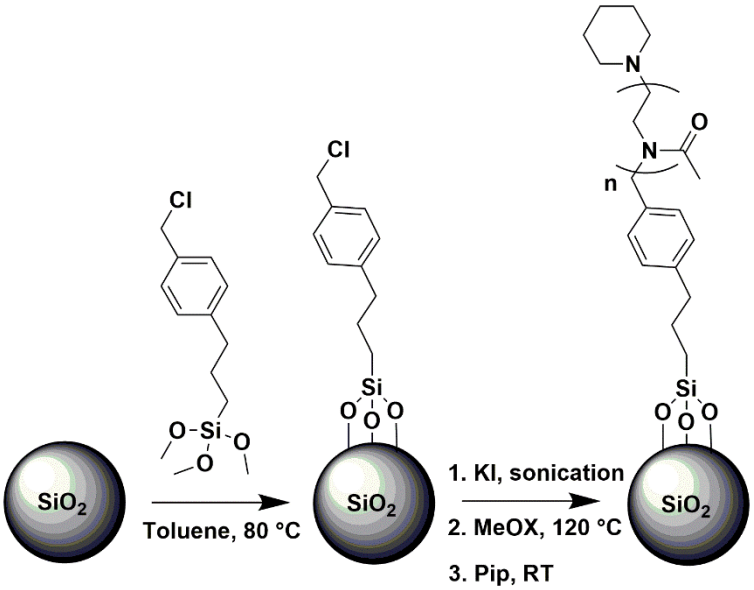

Figure 20. Reaction scheme shows surface initiated polyoxazolines grown from silica nanoparticles including initiation step and polymerization steps as synthesized by Bissadi and Weberskirch. [102]

In 2019, Wei et al. grew polyoxazoline off fluorescent hydroxyapatite nanoparticles to use for biological imaging.[101] In this case, hydroxyapatite nanoparticles were modified using tosyl chloride, as an initiator, in toluene and triethylamine. The initiator-modified hydroxyapatite nanoparticles and 2-ethyl-2-oxazoline monomer were added to a Schlenk flask and underwent three freeze-pump-thaw cycles. Acetonitrile was then added, and the mixture was stirred at 120 °C for 8 hours to carry out the surface-initiated CROP. The solution was then quenched using a methanol/NaOH solution. To remove excess monomer and any physically absorbed polymer, the

solution was dialyzed in a methanol/NaOH solution and centrifuged. Using NMR spectroscopy, FTIR spectroscopy, and XPS, characteristic peaks and corresponding atomic percentages of polyoxazoline were observed, confirming the presence of a polymer layer on the hydroxyapatite particles. TEM images take before and after polyoxazoline modification showed little change in the particle size, suggesting that the polymer formed was of low molecular weight. TGA was also used and showed a 33.9% weight loss of polymer in the 300-450 °C range. Based off this weight loss, the authors estimated a molecular weight of 5,850 g/mol and a DP of 59. The polyoxazoline modified particles were shown to disperse well in water, which is crucial for their biological application, unlike the tosyl chloride-initiated hydroxyapatite particles. Cell studies were also performed and showed excellent biocompatibility. This study, although missing grafting density and direct molecular weight characterization, showed the first example of these polymers being surface initiated from hydroxyapatite particles, which is promising for a variety of biological applications.

4.3.5 Nylon

Nylons have long been known for their high degree of strength and applications that take advantage of this property.[148] Because of their high strength, nylons typically possess resistance to wear and abrasion, a low coefficient of friction, good resilience, and high impact strength, and have long been used for applications in thermal protective clothing and firefighter suits, among many other industrial applications.[149] Recently, using nylon in conjunction with other materials to form composites has been of increasing interest.[150] As a result of this, research groups have investigated using surface-initiated polymerization for the modification of carbon nanotubes, silica nanoparticles, and carbon nanofibers with nylons.[[104],[105],[106]]

In 2005, Sun et al. successfully utilize surface-initiated polymerization to modify carbon nanotubes with nylon using surface-initiated AROP of caprolactam.[104] This was performed by first activating the surface of the carbon nanotubes with caprolactams via reacting the single walled carbon nanotubes (SWCN) with thionyl chloride at 70 °C to introduce acid chloride functional groups. Once completed, the modified SWCNs were reacted with caprolactam at 110 °C for 24 hours. The particles were separated by filtration with polyvinylidene fluoride (PVDF) membranes and extensively washed, to remove excess caprolactam, using Soxhlet extraction with chloroform. The polymerization was then carried out with the cleaned SWCN-caprolactam activated material using caprolactam as the monomer and sodium to initiate the polymerization under a nitrogen atmosphere for 24 hours. To clean the composite particles, the SWCN-nylon particles were dissolved in formic acid, precipitated in water, and filtered through PVDF membranes to remove sodium, unreacted caprolactam, and any unattached polymers. Using NMR spectroscopy, the SWCN-nylon particles were compared to commercially available 10,000 g/mol nylon 6 and showed matching peak overlap. The particles were also examined using TGA and demonstrated that 40 wt.% of the material was the SWCNs, indicating a high ratio of nylon to SWCN. SEM analysis examined the particles before and after removal of nylon using TGA, however, it proved difficult to see the SWCNs due to the large amount of modified nylon present until after the removal process. AFM provided better characterization of the SWCN-nylon particles, as the individual SWCNs were able to be observed. No grafting density or molecular weight data was obtained for the grafted nylon, however, an approximate grafting density of activated caprolactam initiator was reported at 1 caprolactam per 125 nanotube carbon atoms from the 7% weight loss of the caprolactam obtained from TGA.

In 2007, Li et al. demonstrated the grafting of nylon from silica nanoparticles.[105] This was performed by first modifying 20 nm silica particles via reaction with toluene 2,4-diisocyanate (TDI) at 80 °C in a nitrogen atmosphere for 72 hours. The particles were then cleaned, using centrifugation, and washed several times with toluene to remove excess TDI. To activate the particles, caprolactam was reacted, under nitrogen, with the surface immobilized isocyanate group in toluene at reflux for 5 hours. The remaining caprolactam was removed using a chloroform wash. The polymerization was then carried out by adding caprolactam-initiated silica particles, caprolactam monomer, and sodium in a nitrogen atmosphere and sonicating at 80 °C for 30 minutes to disperse particles. The flask was then transferred to an oil bath and heated at 170 °C for 6 hours (**Figure 21**). Similar to Sun et al., following polymerization the particles were dissolved in formic acid, precipitated in water and, subsequently, filtered. The particles were then washed with methanol and dried. FTIR spectroscopy of the particles showed both the characteristic peaks of nylon but also of the SiO_2 particles. TGA analysis performed at each stage of the synthesis showed that approximately one third of the silanol groups reacted with the TDI initiator and almost 100% of the TDI initiator

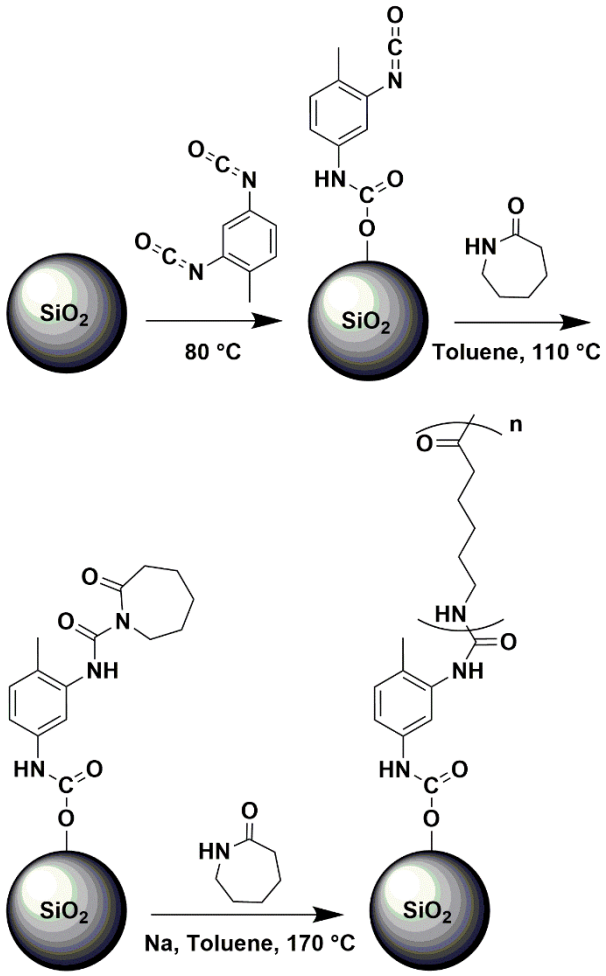

Figure 21. Reaction scheme shows surface-initiated nylon 6 from silica nanoparticles synthesized by Li et al. [105]

reacted with the caprolactam activator. TGA showed the nylon polymer burned off from 400-500 °C and composed up to 98 wt.% of the modified particles, depending on the concentration of monomer used. Differential scanning calorimetry (DSC) was performed on both the free polymer and the grafted polymer and showed that both the T_g and crystallization temperature increased by 8 °C and 6 °C, respectively, for the grafted polymer. This was hypothesized to be due to the chains possessing restricted movement because of one end being attached to the surface. To obtain the molecular weight of the grafted polymers, they were degrafted from the particles using HF and then characterized using viscometer measurements to find the viscosity average molecular weight. The molecular weight analysis demonstrated a linear evolution of polymer molecular weight with time, which is characteristic of a living chain-growth polymerization. Using this technique, surface-initiated polymers with up to approximately 12,000 g/mol were grown. Although molecular weight and TGA studies were performed, no grafting density for the modified particles was reported.

More recently, Lu et al. used stacked cup carbon nanofibers to make hybrid polymer-modified fibers to enhance the bulk properties of nylon 6.[106] The modified nanofibers were produced by using nitric acid to add carboxylic acid groups to the surface of the nanofibers, followed by reaction of the carboxylic acid groups with a difunctional isocyanate, and finally reacting the exposed isocyanate group with caprolactam to activate the surface. Using both a solution initiator and the initiator-modified carbon nanofibers in the polymerization allowed for dispersed particles to be formed in bulk nylon and also allowed for the wt.% of carbon nanofibers in the bulk polymer to be changed based off of the ratio solution initiator to initiator-modified carbon nanofibers. FTIR spectroscopy, TGA, and TEM were used to confirm that the nanofibers were modified with initiator but only mechanical tests were performed on the final nylon 6

modified nanofiber composites. Because of this, it is difficult to determine the effectiveness of this synthesis in producing well-defined polymer brushes. However, mechanical tests showed that the stiffness was enhanced, in addition to a slight improvement in the degree of toughness. Separate synthesis and testing of the modified nanofibers from the bulk nylon would be beneficial in determining the characteristics of the polymer grown from the surface and how changing the molecular weight of the attached polymer influences mechanical properties.

4.4 Catalyst Transfer Polymerizations

4.4.1 Polythiophene

Polythiophene, one of the most widely synthesized conjugated polymers, has shown a lot of promise for conductive thin films and has potential for use in many applications, including OLEDs for flat panel displays and lighting, field-effect transistors for display backplanes and disposable electronics, photodetectors, OPVs, gas sensors, pH sensors, and lithium batteries.[[151],[152]] There are many stand out characteristics that have made polythiophenes popular for these applications, including tunable optical properties, tunable band gap, and improved stability when compared to many other conjugated polymers.[153] The promise of these polymer films is hypothesized to come from their potential for making low cost devices due to polymer film flexibility, along with the low density, conformability, and versatility of these films. Covalent attachment of conjugated polymers is thought to be a very important aspect of their application due to the improved mechanical stability, efficiency of conductivity, and ease of attachment to both organic and inorganic substrates.[111] Much of the early work in this field was performed using the ‘grafting to’ technique, however, this work experienced the previously discussed issues of low grafting densities and non-uniform films.[151] The ‘grafting from’ technique was later introduced, due to developments in catalyst transfer polymerization, and

resulted in improvements by producing polymers with narrow MWDs and films with higher grafting densities.[154] Many reviews on conjugated polymers, including polythiophene, have been published. As such this review will specifically focus on the critical advances of using the 'grafting from' technique to produced conjugated polymer brushes.[[3],[151],[154],[155],[156],[157],[158]]

The first example of a polythiophene polymer brush prepared using the 'grafting from' technique was performed by Kiriy et al in 2007.[80] This work was able to use the early work of McCullough et al. and Yokozawa et al.[1] on solution polymerization using Kumada catalyst transfer and directly translate it to the surface of silica wafers and glass slides. In order to obtain a nickel catalyst on the surface as the initiation site, a 2 nm layer of poly(glycidyl methacrylate) was deposited on the surface to be modified, followed by a 30 nm layer of poly(4-bromostyrene). The bromine functional group was then reacted with a tetrakis(triphenylphosphine)-nickel(0) ($Ni(PPh_3)_4$) complex to produce the surface immobilized initiator (**Figure 22**). The $Ni(PPh_3)_4$ complex represented a compromise between reactivity and selectivity due to the alternative [1,3-bis(diphenylphosphino)propane]dichloronickel(II) ($Ni(dppp)Cl_2$) catalyst not being sufficiently reactive toward the non-active initiator's aryl halide. Following immobilization of the catalyst on the surface, the monomer 2-bromo-5-chloromagnesio-

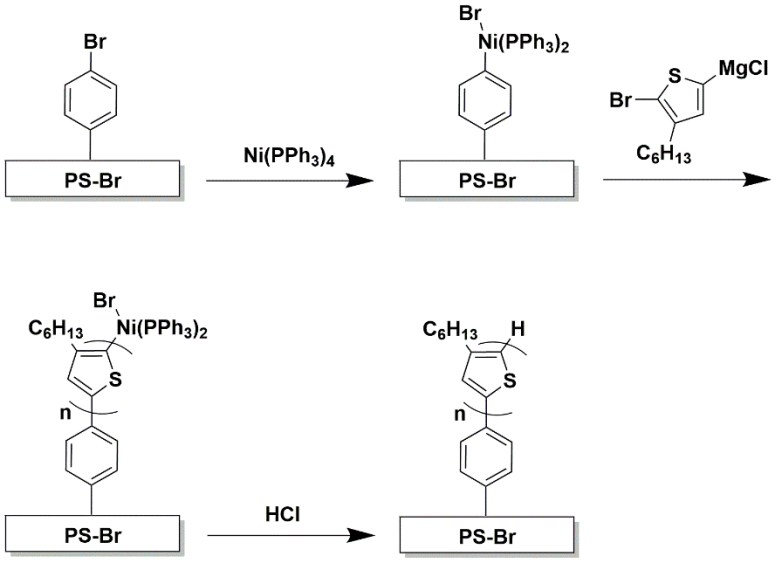

Figure 22. Reaction scheme of the first surface-initiated polythiophene brush synthesis demonstrated by Kiriy et al. [80]

3-hexylthiophene was introduced and the polymerization proceeded. Brushes ranging from 40 to 70 nm in thickness were achieved using this technique. NMR spectroscopy and GPC were used to identify the optimum reaction temperature, by characterizing the MWD of the produced polymers, but the grafting density and molecular weight of grafted chains were not reported. This work represented an excellent proof of concept and led the way in many regards to synthesizing future polythiophene brushes.

In 2009 Locklin et al. was able to make a thiol-based initiator that directly attached to a gold substrate for the synthesis of polythiophene brushes.[86] Instead of using a $Ni(PPh_3)_4$ complex like Kiriy, this work used a more reactive (cyclooctadiene)-bis(triphenylphosphine)nickel(0) ($Ni(COD)(PPh_3)_2$) complex, due to the $Ni(PPh_3)_4$ complex having insufficient reactivity when used with the thiol initiator. In order to prepare the surface for the nickel complex, a glass slide was used as the base with a 10 nm chromium layer and a 100 nm gold layer. Once the gold was cleaned, a thiol with an aryl bromide group was attached to the gold substrate. The thiol-based initiator was prepared by reacting the aryl bromide with a solution of bis(cyclooctadiene)nickel(0) ($Ni(COD)_2$) and then reacting the complex with four equivalences of triphenylphosphine to form the $Ni(COD)(PPh_3)_4$ complex. With this new initiator system, brushes up to 36 nm thick were synthesized. Free polymer was also observed in solution, which was believed to be due to the nickel catalyst undergoing chain transfer off the surface and into solution. Once again, no grafting density or molecular weight characterization was obtained for the polymers. AFM showed a surface with a rms roughness of 3.9 nm, which is lower than the gold substrate used that had a rms roughness of 11.9 nm. However, the surface did show a globular morphology, which was potentially due to a low grafting density or incomplete surface coverage.[19] While it is difficult to determine if polymer brushes were formed in this system, it

was the first example of an electroactive conjugated polymer grafted directly from a monolayer, which was important in the advancement of the applications of these conductive brushes.

Further work by Kiriy et al., making hybrid polythiophene particles to use with solar cells, demonstrated that reacting [2,2'-bipyridine]dichloronickel(II) ($Ni(bipy)Cl_2$) with an aryl halide, then switching the ligand with the better performing 1,3-bis(diphenylphosphino)propane (dppp) or 1,2-bis(diphenylphosphino)ethane (dppe) ligands, worked significantly better than the previously used $Ni(PPh_3)_4$ complex.[109] This was achieved by first reacting aryl halides attached to 460 nm Stöber silica particles with the $Ni(bipy)Cl_2$ complex. Once the bipy ligand was replaced by the phosphorous ligands of dppp or dppe, extensive washes were performed to remove any excess nickel complex and ligand. Polymerizations were then conducted using a technique similar to previous studies.[80] Of particular interest in this study was that it was the first example of degrafting the poly(3-hexylthiophene) polymer chains and characterization of the grafting density and molecular weight properties. With this new ligand exchange system, a grafting density of 0.28 chains/nm^2 was reported with a Σ value of 148, showing that these chains were in the polymer brush regime. To find this value, HF was used to degraft the polymers from the silica particles. The degrafted polymer chains were then analyzed by GPC to find a M_n of 43,000 g/mol and a PDI of 2.6. Using SEM, a thickness of 20 nm was found for these brushes. In this work Kiriy et al. also demonstrated that these hybrid polythiophene particles exhibited strongly altered optical properties, including a red shift in absorption and fluorescence spectra, compared to physical absorbed polythiophene-modified particles. This was hypothesized to occur due to stronger chain interactions resulting from a high grafting density polymer film.

In order for polythiophene brushes to demonstrate their full potential in electronic devices, control over thickness and a greater understanding of the effect of film thicknesses on the

properties of the system must be attained. In 2012 Luscombe et al. used a modified indium tin oxide (ITO) substrate to grow poly(3-methylthiophene) brushes of varying thickness.[110] This was achieved by using a surface-immobilized phosphoric acid initiator with a Ni(COD)/$(PPh_3)_2$ complex. A ligand exchange with dppp was then carried out for improved polymerization results, similar to the process used by Kiriy.[109] Once cleaned thoroughly, different concentrations of the monomer 2-bromo-5-chloromagnesio-3-methylthiophene were added and polymerized (**Figure 23**). Polymer film thicknesses of 30 - 265 nm were reported by changing the monomer concentration from 0.03 M to 0.18 M. Instead of using ellipsometry to determine the film thickness, AFM was used due to difficulties in using ellipsometry on ITO substrates. In addition, AFM demonstrated that this procedure produced rough films, with a rms roughness of 20 – 21 nm, which was attributed to a low grafting density and the potential collapsed mushroom configuration of the attached polymer chains. While this work was effective in showing that the thickness of the polymer films could be controlled, no grafting density or molecular weight information was reported. However,

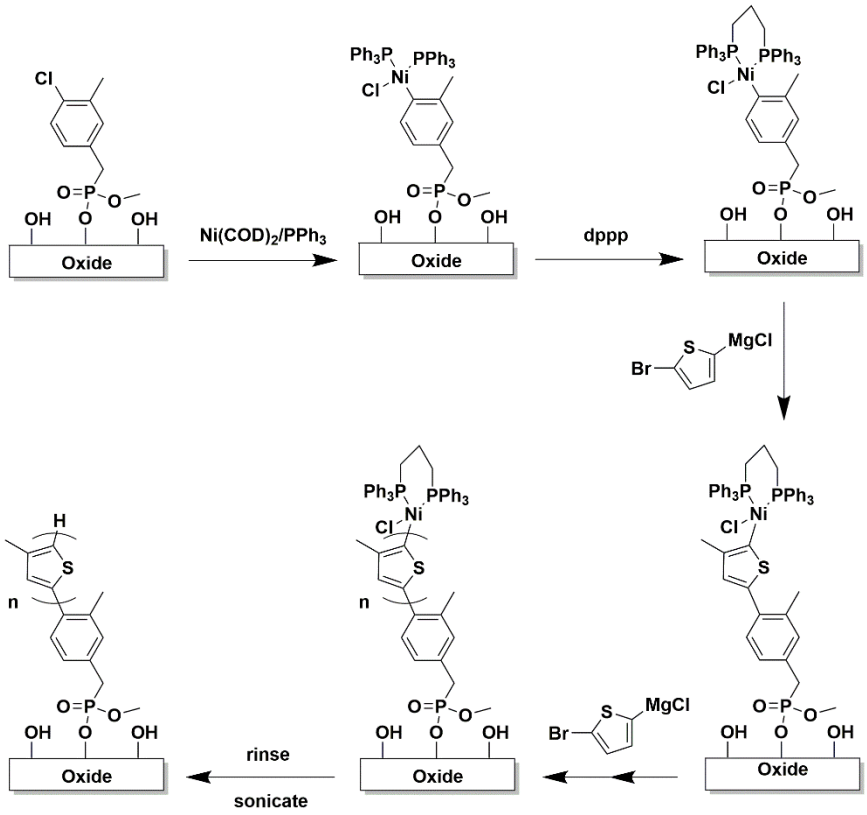

Figure 23. Reaction scheme showing surface-initiated polythiophene surface initiation, initiator activation and switching of the nickel ligands for better reactivity. Synthesis performed by Luscombe et al. [110]

importantly Luscombe also demonstrated that the electrochemical properties of the brushes were stable and robust and that with varying thickness, control over work function was obtained, which leads to numerous potential applications in electronic devices.

The same year as Luscombe's work, Locklin et al. explored changing the normally used nickel catalyst to a palladium catalyst in order to improve grafting density and film thickness.[111] Palladium was first used in Kumada catalyst transfer polycondensation in solution by Yokozawa and showed a reduced propensity towards disproportionation compared to nickel catalysts.[159] This was proposed to be due to palladium having a weaker d-electron donating ability and a more stable zerovalent oxidation state. In order to grow poly(3-methylthiophene) brushes, Locklin et al. used an ITO substrate reacted with (4-bromobenzyl)phosphonic acid in ethanol overnight. Once cleaned, the ITO slides were reacted with the bis(tri-tert-butylphosphine)palladium(0) in toluene and heated to 70 °C for 3 hours. After cleaning again, the slides were reacted with the monomer 2-bromo-5-chloromagnesio-3-methylthiophene at 40 °C overnight. With this technique, polymer films of up to 100 nm were formed. Using the palladium catalyst Locklin was able to double the grafting density of the palladium initiators compared to nickel initiators, reporting 1.1 x 10^{14} initiator molecules per cm^2 for palladium compared to 4.78 x 10^{13} initiator molecules per cm^2 for nickel. No grafting density or molecular weight for the surface-initiated polymer chains were reported, which could have helped determine whether this change in initiator concentration makes a difference with polymer chain density. Although the grafting density of the polymer brushes was not reported, ultraviolet–visible (UV-vis) spectrometry with p-polarized light showed that the polymer films possess a perpendicular orientation to the substrate, which is predicted to be important for electrical properties. In addition, from the UV-vis results Locklin hypothesized that

the surface immobilized polymers had a sufficient grafting density to form a polymer brush structure.

One of the primary challenges of preparing polythiophene brushes is getting the surface ready for the surface-initiated polymerization. In 2014, Locklin et al. found a new approach to simplify the process of substrate preparation and increase the grafting density, while still being able to use a nickel catalyst.[112] This was achieved by first reacting a bromobenzene monolayer with an arene diazonium salt on a gold surface. At this point the normal approach would be to attach a nickel complex then do a ligand exchange in order to allow the polymerization to proceed in a controlled manor. Instead of this, Locklin et al. attached a Ni(II) complex of $Ni(dppp)Cl_2$ and electrochemically reduced it to the Ni(0) species used for the polymerization. After reduction a typical nickel catalyzed thiophene polymerization reaction, as previously reported by Locklin et al., took place using the monomer 2-bromo-5-chloromagnesio-3-methylthiophene.[86] Films up to 25 nm were reported using this new initiator system while maintaining a rms roughness of 5 nm. Using this new approach, the grafting density of the initiator was increased 6-fold compared to other solution generated initiator complexes, 1.29×10^{14} initiator molecules per cm^2 for the electrochemically reduced system compared to 4.78×10^{13} initiator molecules per cm^2 for typical solution generated nickel catalyst initiators. Although the initiator grafting density was found, no grafting density or molecular weight for the surface-initiated polymer chains were reported, which could have helped determine whether this change in initiator concentration makes a difference with polymer chain density.

Tailoring the side chains of polythiophenes opens the system up to the use of new solvents and functional groups, which can adapt the brushes for specific applications. In 2015 Kiriy et al. incorporated a bromohexane side chain on the polythiophene brush without an adverse effects on

the polymerization.[114] This polymerization process mimicked the previously discussed polymer brush synthesis except that the new functionalized monomer, 2-bromo-5-chloromagnesio-3-bromo- hexylthiophene, was used.[109] With this bromine functional group, a two-step transformation of the bromine into an ionizable amine group was performed. The brushes produced a 10% weight loss in TGA, which was similar to previous work without the bromine side chain and correlated to a 25 nm thick film around the silica particle substrate. The introduced amine group was shown to possess different optical properties, as determined from emission spectra, that were subject to changes in the surrounding chemical environment and could make this system useful for application as sensors. One of the main advances of this work is that it introduced a new process to vary the functionality of surface-immobilized polythiophenes.

Another important advancement in polythiophene brushes was being able to reinitiate the polymers to either increase the thickness of the polymer film or to make more advanced architectures, such as block copolymers. This was first demonstrated by Locklin et al. in 2015 when, after cleaning a prepared poly(3-methylthiophene) brush and reacting the end group aryl bromide with a nickel complex, reinitiation and further polymerization was shown to occur.[113] To achieve this, ITO slides were modified with aryl bromides, the bis(cyclooctadiene)nickel(0)/2,2'-bipyridine ($Ni(COD)_2$/bipy) initiator system then attached, and the previously discussed ligand exchange process with dppp performed. The ITO slide was then introduced to the monomer, 2-bromo-5-chloromagnesio-3-methylthiophene, to start the polymerization and produced the surface-immobilized polymer film. The slides were subsequently cleaned extensively with THF and DCM before being reacted again with the $Ni(COD)_2$/bipy system. After this, the above process to provide the initiation site was again performed before new monomer was added to allow the surface to be polymerized again. After repolymerization the

brushes were again thoroughly cleaned. This method showed that re-initiation occurred for the polythiophene brushes, but the rms roughness of the brush also drastically increased from 4 - 5 nm after the first polymerization to 50 nm after the second. This was hypothesized to be due to uneven re-initiation resulting in chains of different length on the surface. UV-Vis spectroscopy was also used to show that the polymer molecular weight did increase after the second polymerization, as opposed to reaction with new grafting sites on the surface. This technique represents a valuable first proof of concept for chain extension of polythiophene brushes that has the potential to lead to a variety of different polymer brushes structures.

4.4.2 Polyfluorene

Polyfluorene is another exciting conjugated polymer that Yokozawa was able to convert from step-growth to a living chain-growth Suzuki polycondensation in solution, and also has many of the same potential applications that polythiophenes possess.[81] Kiriy et al. used the work of Yokozawa as a basis and was able to synthesize a polyfluorene brush via the 'grafting from' technique with thicknesses up to 100 nm. This was achieved by reacting either a silane-based aryl bromide initiator or by using 10 nm thick poly(4-bromostyrene) coatings on the surface of either a silica wafer or a glass slide (**Figure 24**). Once cleaned, the aryl bromides were reacted with $Pd(P(tBu)_3)_2$ in toluene

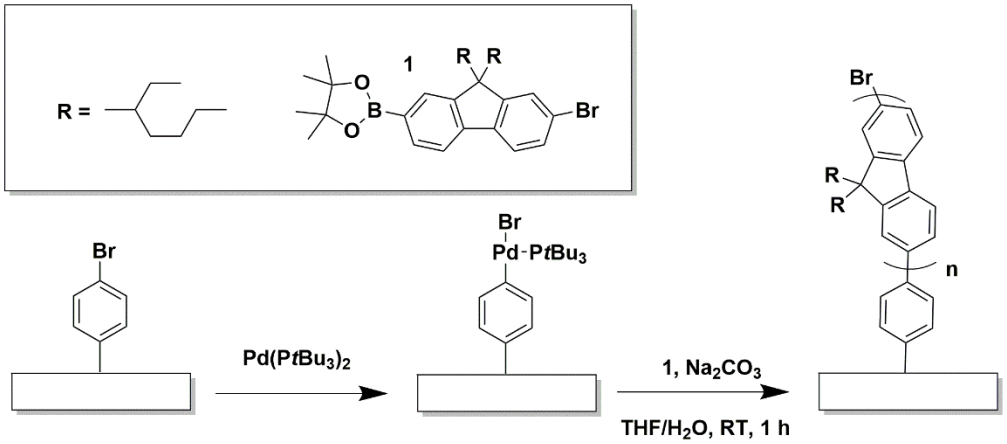

Figure 24. Reaction scheme shows 'grafting from' polymerization of polyfluorene performed by Kiriy et al starting with initiation, activation using Pd catalyst, and brush formation. [81]

at 70 °C. The substrate was then cleaned and placed in a reactor with the monomer 7-bromo-9,9-bis(2-ethyl-hexyl)-9H-fluoren-2-ylboric acid ester in THF at RT for 1 - 3 hours. Using this process, no polymerization in solution was found so the monomer solution was able to be used for multiple polymerizations. No grafting density or molecular weight properties were reported for the surface-initiated polymer chains. Using AFM, it was found that the surface of a 40 nm brush was relatively uniform, with a rms roughness of 1.1 nm. Patterned films were also prepared using a type of colloidal lithography and were analyzed with AFM to show controlled patterns.

4.4.3 Polyphenylene

The first example of polyphenylene brushes prepared using the 'grafting from' technique was performed in conjunction with Locklin's first polymerization of polythiophene.[86] This was achieved using the same synthesis procedure used to synthesize polythiophene except switching the monomer with 4-iodophenyl-magnesium chloride. First, a thiol initiator with an aryl bromide was attached to a gold substrate. The nickel complex was then attached and a ligand exchange performed to form the final $Ni(COD)(PPh_3)_2$ complex. Similar to other Kumada catalyst CGC reactions, free polymer was formed in solution, which is believed to be as a result of a chain transfer processes. While this work showed proof of concept, no grafting density or molecular weight data was reported for these new polymer films. The films were found to grow as thick as 42 nm but showed a globular morphology similar to the polythiophene brushes grown in the same study, although no rms roughness was reported for the polyphenylene brushes.

4.4.4 Poly(phenylene ethynylene)

More recently, the synthesis of poly(phenylene ethynylene) (PPE) was converted to a living CGC process by Bielawski et al.[78] In the initial solution polymerization, the monomer, 1,4-bis(2-ethylhexyloxy)-2-ethynyl-5-iodobenzene, was limited to a conversion of 58% using conditions similar to Sonogashira-coupling. Because of this low conversion, Stille-type conditions were used. This was performed using a stannylated monomer with a tributylstannane function group, in place of the ethyne proton in the original monomer, in order to increase the conversion. When the new monomer, ((2,5-bis(2-ethylhexyloxy)-4-iodophenyl)ethynyl)-tributylstannane, was reacted with a PhPd(P(t-Bu)$_3$)Br catalyst in solution, a conversion of 99% was achieved within 3 hours and resulted in a polymer with a M_n of 14,400 g/mol and a PDI of 1.47. This polymerization was performed with both copper iodide (20 mol %) and PPh_3 (20 mol %) to ensure higher molecular weights were produced. Following the initial solution polymerization studies Bielawski et al. then turned towards using this polymerization to synthesize surface-initiated PPE on Stöber silica particles. 200 nm silica particles were used with a silane-based initiator featuring an aryl bromide. The modified particles were then reacted at 70 °C with the Pd catalyst in toluene. Once cleaned, the initiator-modified silica particles were reacted with the monomer at 50 °C in the presence of both copper iodide and PPh_3 in THF (**Figure 25**). A grafting

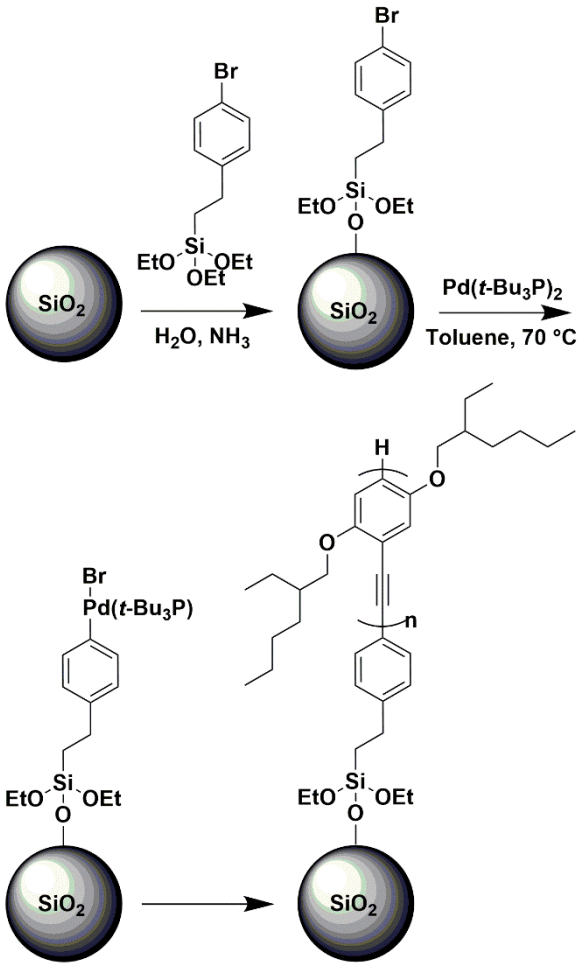

Figure 25. Reaction scheme shows the first example of synthesizing PPE using 'grafting-from' on silica nanoparticles performed by Bielawski et al. [78]

density of the initiator was calculated to be 0.46 organosilane molecules/nm^2, however, calculations of the polymer grafting density were not reported. A maximum weight loss of 14.1% was measured by TGA for the polymer-modified particles. HF was then used to cleave the polymer from the particles and a M_n of 24,500 g/mol was found using GPC. A re-initiation experiment was also performed and, using GPC, it was found that the molecular weight almost doubled, 11,300 g/mol compared to 21,900 g/mol, as measured before and after the second polymerization, respectively. This work represented the first example of the use of CGC for the solution synthesis of PPE as well as the first example of surface-immobilized PPE films. While no polymer grafting density was reported in this work, given the TGA and molecular weight characterization and, using the geometric surface area of 200 nm particles and 1.9 g/cm^3 density of silica particles, a grafting density of approximately 0.16 chains/nm^2 can be calculated, putting these surface-immobilized polymers in the brush regime.

4.4.5 Polyisocyanate

Polyisocyanates are widely considered to be rigid-rod or semiflexible polymers due to the amide linkage and the consequential helical shape the polymer chain forms.[160] Polyisocyanates have been used in a large range of applications including foams, insulating materials, plastics, composites, films, sealants, coatings, inks and adhesives since being developed in 1937 by Otto Bayer.[161] In 2017 Vatansever and Hamblen developed a surface-initiated polymerization using a titanium (IV) catalyst to grow poly(n-hexyl isocyanate) directly from silica nanoparticles using an insertion mechanism to prevent any side reactions.[83] To make the initiator hydroxyl-terminated nanoparticles two different pathways were utilized. Both initiation pathways started with silica nanoparticles and modified the surface with a primary alcohol. In order to activate the initiator hydroxyl-terminated nanoparticles with titanium, the particles were suspended in hexanes

at 0 °C and titanium tetrachloride was added dropwise. This was followed by letting the reaction warm to RT and reacting for 12 hours. The particles were then washed five times with hexanes to remove unreacted titanium. Finally, n-hexyl isocyanate was added to the particles in toluene. The polymerization was subsequently carried out for two hours followed by adding an end capping agent, acetyl chloride, to terminate the polymerization (**Figure 26**). The polymer-modified nanoparticles were then isolated by dissolving them in a THF/methanol mixture and precipitated in methanol. In order to isolate the polymer for characterization, the polymer-modified nanoparticles were added to a chloroform and acetone mixture containing HCl. The polymer was collected by dissolving in a THF/methanol mixture and precipitated in methanol to give the final cleaved polymer. A maximum molecular weight of approximately 64,000 g/mol and a PDI of 1.3 was found for the degrafted polymers. Well-defined molecular weights were obtained by changing the concentration of initiator to monomer ratio showing good control over the polymerization. Using TGA, weight loss began at around 260 °C for the polymer, with an overall weight loss of 96%. In an effort to investigate surface coverage, a value of 1.16-1.5 mmol/g of surface silanol groups was calculated based off the known amount of surface OH groups. This silanol surface coverage was then compared with the weight loss found for the polymer brush and the 64,000 g/mol molecular weight of the

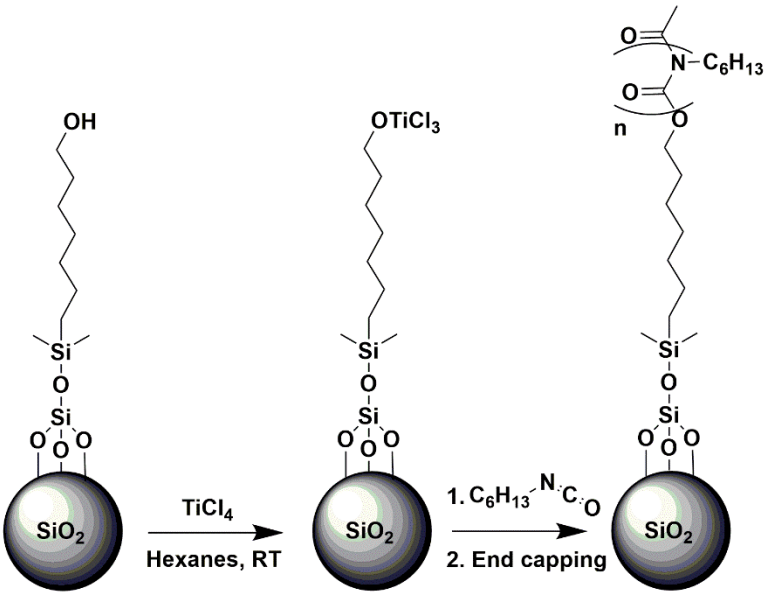

Figure 26. Reaction scheme shows surface-initiated polyisocyanate synthesis performed by Vatansever and Hamblen. [83]

degrafted chains. Assuming each surface silanol group became a polymer chain the weight loss percentage is in close agreement with the obtained molecular weight. This assumes, however, that each silanol group reacted with an initiator and that each initiator started a polymer chain.

4.4.6 Polyisocyanides

Polyisocyanides were first discovered to possess a helical conformation in 1974 by the Millich, Nolte, and Drenth groups.[162] This helical shape is of interest in applications such as electronic devices and bio-sensing devices due to the long range order that such polymers possess.[163] In 2008, Huck et al. demonstrated the first example of surface-initiated polymerization of polyisocynanides with the goal of optical and electronic applications.[84] Polymer brushes were grown on silica, gold, and quartz using an initiator with a primary amine. In order to attach the nickel catalyst to the surface, two approaches were utilized. The first method attached the amine monolayer to the surface first then reacted this layer with the nickel catalyst complex. This method was only able to grow brushes up to 19 nm thick, so a second method was utilized by attaching the nickel catalyst complex to the amine initiator first then reacting this complex to the surface. To prepare the polyisocyanide brushes, the activated substrates were reacted with different concentrations of L-isocyanoalanyl-L-alanine methyl ester monomer in DCM with reaction times ranging from 0.1 to 17 hours. The polymer-modified surfaces were then cleaned with chloroform and methanol and dried with nitrogen gas (**Figure 27**). Using AFM, a

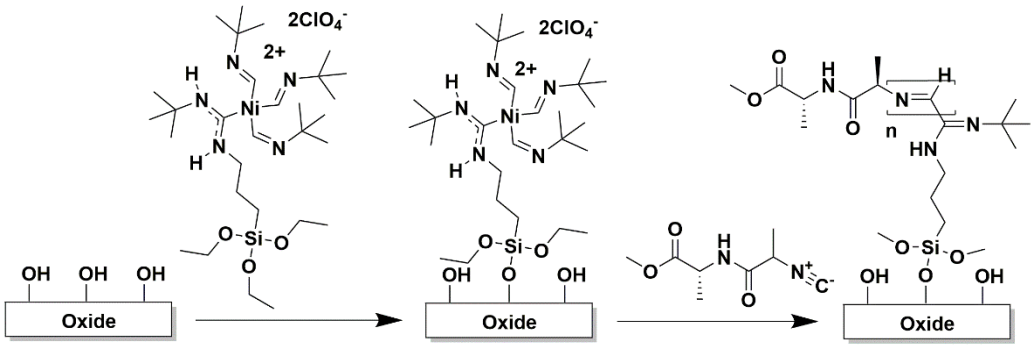

Figure 27. Reaction scheme shows surface-initiated polymerization of poly(isocyanide) synthesis on oxide surface performed by Huck et al. [84]

unique surface morphology was discovered, showing what was describe as 'feather-like' shapes (**Figure 28**). These shapes were hypothesized to be due to stiff bundles of the highly rigid polyisocyanide chains that were aligned. Brushes of up to 387 nm in thickness were synthesized but no molecular weight or grafting density data was reported. This was primarily because of the inherent difficulty in determining the molecular weight of the rigid polyisocynanide chains, due to low solubility on common solvents, and also because of the overall low amount of polymer produced on a flat substrate. Circular dichroism was used to determine if the brushes still had helical properties and indicated that the brushes did have a strong right-handed helical orientation. Lastly, FTIR spectroscopy was used to confirm that the brushes also possessed hydrogen bonding along the side chains, which is important in formation and stabilization of helical backbones and β-sheet-like arrangements.

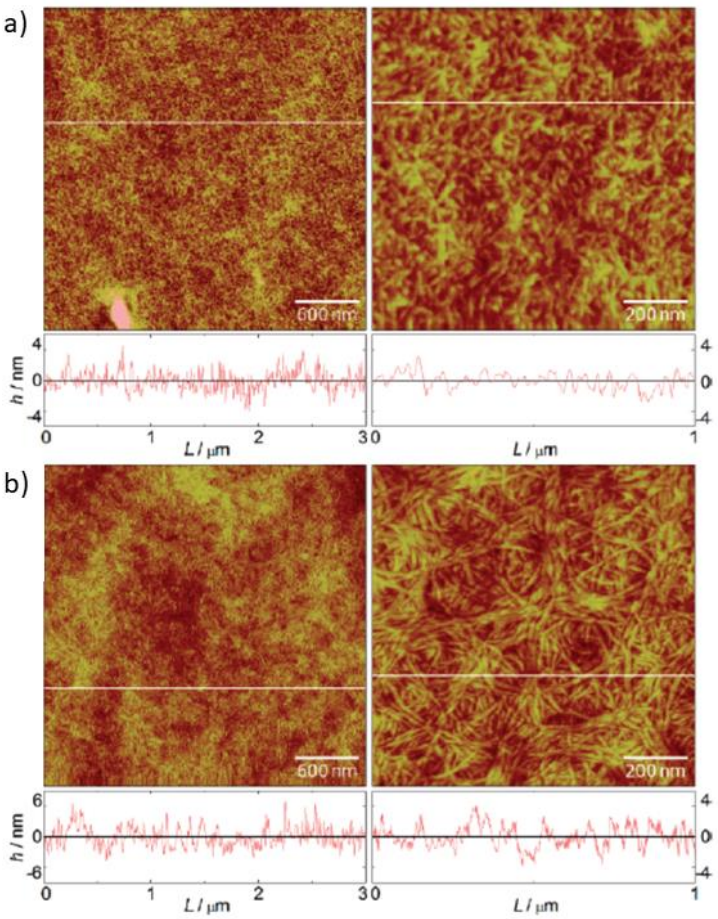

Figure 28. AFM topography of 56 and 387 nm thick poly(isocyanide) brushes a) and b) respectively. [84], Copyright 2008. Reproduced with permission from American Chemical Society.

Two years later, the Huck and Rowan groups further studied polyisocyanides to look into their conductive properties by adding a carbazole side group.[115] This was done using a similar polymerization scheme as the previous work but using the L-isocyanoalanine-2-(9H-carbazole-9-

yl)ethyl amide monomer instead. Similar to the previous study, the polymer formed was insoluble in common organic solvents so only limited characterization was performed and mostly on the electronic properties of the polymer films. With the new side group, polymer brushes were grown up to 150 nm and this polymer film had a higher water contact angle of 90° due to the increased hydrophobic character of the carbazole. Similar to the previous work, no grafting density or molecular weight characterization was reported due to the polymers being insoluble in common solvents. However, the authors stated that due to the "open" structure of the films, based on the films high rms roughness (6.3 nm roughness for a 73 thick film), a low grafting density was predicted. Solid state NMR spectroscopy was performed on the polymer and showed the characteristic peaks. Experiments varying the monomer concentration and reaction solvent were also attempted and showed that DCM as a solvent at higher monomer concentrations produced the thickest polymer films. AFM was performed on the polymer-modified surfaces but these systems did not show the 'feather-like' features that were seen in the previous study instead showing what the authors called 'moss-like' surfaces for the shorter 9 nm brushes and a 'fiber-like' appearance for the longer brushes. Electrical characterization of these polymer films showed a small dipole formation and they were successfully used with a LED, showing a large shift in the built-in voltage at zero bias. This work represented a significant progression in demonstrating the use of surface-immobilized polyisocyanides in new electronic applications.

4.5 Substituent Effect Polymerizations

4.5.1 Poly(phenylene oxide)

Poly(phenylene oxide)s (PPOs) have been used commercially for over five decades because of their good thermal and chemical resistance.[164] PPO and PPO-polymer mixtures are currently used in many applications including business machines, automotive parts, home

appliances, electrical parts, and personal care products.[165] Because of their properties, Kim et al. hypothesized that using PPO with SWCNs could help resolve some of the issues that plague solubility and processability of these structures.[85] In order to make the composite SWCN-PPO, an initiator was first attached to the surface of the SWCNs. This was achieved by reacting 4-fluoro-3-(trifluoromethyl)benzenediazonium tetra-fluoroborate to the SWCN walls using diazonium salt chemistry. Once formed, the initiator-modified SWCNs and potassium 4-fluoro-3-(trifluoromethyl)phenolate monomer were reacted in dimethyl sulfoxide (DMSO) at 130 °C for 6 days. This temperature was found to allow for the least amount of self-condensation of the monomer in solution. The final SWCN-PPO product was precipitated in a methanol/water solution then re-dissolved in dimethylacetamide and, again, precipitated in THF to remove organic impurities. Comparing the T_g, obtained from DSC, the grafted polymer showed a drastic increase of 75 °C, to a T_g of 120 °C, compared to free polymer, which has a T_g of 45 °C. It was hypothesized that this could be due to a higher level of ordering and reduced free polymer chain ends for the surface-immobilized polymer. The initiator grafting density was also obtained using TGA and GPC, giving a value of 1 initiator for every 56-60 surface carbon atoms. Using the surface area of the carbon nanotubes, this corresponds to 1 initiator/nm^2. Due to degradation of the PPO and SWCN at nearly the same temperature, a grafting density of the polymer chains was not directly calculated via TGA. However, based off the observed weight gain from the initiated SWCN to the SWCN-PPO, a molecular weight of 3,200 g/mol was estimated by the authors for the grafted PPO. GPC was also used to characterize a homopolymer synthesized in solution under the same conditions as the polymer brush, producing a M_n of 4500 g/mol and a PDI of 1.28. The final SWCN-PPO product was tested in different solvents to see whether the modification procedure

enhanced the solubility of the SWCNs. The authors reported that after several months of being dissolved in various organic solvents no sedimentation was observed.

4.5.2 Aromatic Polyamide

Aromatic polyamides have long been known for their excellent chemical, thermal, and mechanical properties, which are derived from the rod-like structure of the polymer chains and the presence of hydrogen bonding between chains.[166] These properties have given rise to the use of aromatic polyamides in many applications including advanced fabrics, coatings, fillers, advanced composites in the aerospace and armament industry, asbestos substitutes, electrical insulation, bullet-proof body armor, industrial filters, and protective and sport clothing.[22] In 2015, our group reported the first surface-initiated aromatic polyamide brushes prepared using substituent effect CGC.[2] As discussed previously, in early 2000 Yokozawa demonstrated that it was possible to convert aromatic polyamides traditionally prepared via a step-growth polymerization to a more controlled CGC polymerization via the use of substituent effects.[44] Using this fundamental work, our group developed a silane based initiator that could be attached to various silica substrates, including Stöber silica and silica wafers. Once cleaned, the initiator-modified silica was placed in a solution of THF and monomer, methyl 4-(octylamino)benzoate, and the solution was then cooled to 0 °C. Lithium bistrimethylsilyl amide, a strong non-nucleophilic base, was then

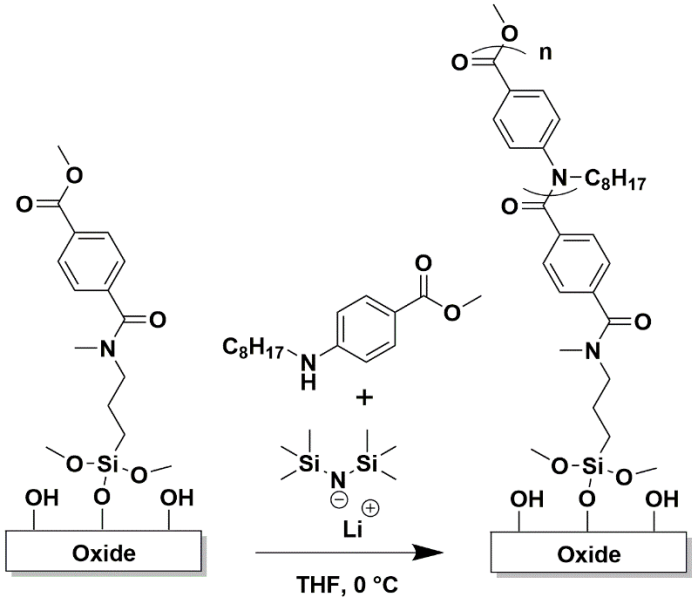

Figure 29. Reaction scheme shows the first surface-initiated aromatic polyamide brushes grown from silica surface performed by Prehn and Boyes. [2]

added to start the polymerization by deprotonation of the amine group on the monomer (**Figure 29)**. Polymer films up to 12 nm thick were produced from the silica wafers. Using HF to cleave the polymer from the Stöber silica, a M_n of 10,400 g/mol and a PDI of 1.4 were found using GPC. The Stöber silica also showed a weight loss of 3% using TGA, which was used with the molecular weight data to calculate a grafting density of 0.35 chains/nm^2 and demonstrate that a polymer brush structure was formed. The relatively thin polymer brushes produced in this system were attributed to the precipitation of lithium methoxide, a by-product of the CGC reaction, on the surface of the silica wafers. It was hypothesized that the thickness of the brushes could be improved by changing to a system that produces lithium phenoxide as a leaving group, as this has improved solubility in THF. Despite this, these new brushes represent a step forward in the development of new types of surface-immobilized polymer films for new applications and for improving upon existing technology such as reverse osmosis membranes and carbon dioxide capture devices.

4.6 Other Non-vinyl-based Polymerizations

4.6.1 Polyaniline

Polyaniline (PANI), similar to other conjugated polymers, has some very unique properties, such as excellent electrical, magnetic, and optical properties that have been used for batteries, electromagnetic shielding, gas sensors, electrochromic devices, and has potential for application in pesudocapacitors, electrochromics, bioengineering, bio/chemical sensors, solar

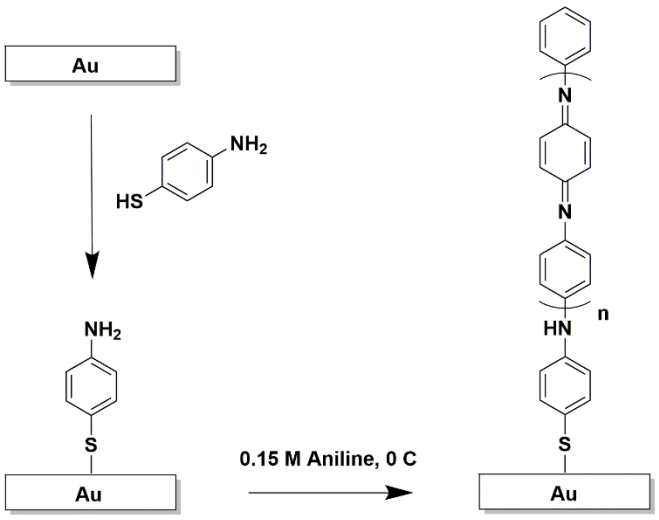

Figure 30. Reaction scheme shows PANI brush synthesis on a gold substrate. Synthesis was performed by Esachi et al. [79]

cells, electromagnetic interference (EMI) shielding, and OLEDs.[[167],[168],[169]] These applications stem from the high Young's modulus and durability of PANI, which results from conjugation along the backbone and the rigidity of the backbone. These properties translate to versatile redox behavior, excellent chemical and electrochemical stability, large capacitance, and electrochromic properties.[[79],[170]] For these reasons, Esashi et al. chose the synthesis of PANI brushes for application in data storage.[79] In data storage, the substrate material must have the capability of transmitting electrons, in addition to, mechanical properties capable of withstanding constant tapping on the surface. In this report, growth of the PANI polymer film was limited to 6 nm and was achieved using an oxidative polymerization of aniline. In order to make these films, a 10 nm layer of Cr and a 200 nm layer of Au were deposited via sputtering on a silicon wafer. The surface was then modified by placing the gold substrate in a methanol solution of 4-aminothiophenol for 24 hours. The initiator-modified gold substrate was then reacted with a solution of 0.15 M aniline, 1 M HCl, and 0.1 M $(NH_4)_2S_2O_8$ for 8 hours at 0 °C (**Figure 30**). Once completed, any physically absorbed polymer was removed by immersing the polymer film in NMP and sonicating for 24 hours. Using this PANI polymer film, the authors demonstrated that applying an electrical voltage allowed for reversible changing of the conductivity. This was hypothesized to be due to either oxidation-reduction or protonation–deprotonation of the PANI.

Further work with these polymer films demonstrated that with repeated polymerization of the same substrate, the thickness of the PANI brush could be increased up to 30 nm.[116] To further characterize the PANI brush surface, AFM was used to examine the topography, Young's modulus, friction, adhesion, and wear. The Young's modulus was found to be 3.8 GPa for the 30 nm brush, which is slightly above the 3.3 GPa value for poly(methyl methacrylate) (PMMA), which has been successfully used for thermomechanical recording.[116] However, the friction and adhesion were reported to be much higher when compared to GeSbTe and PMMA films, due to uneven surface coverage of the polymer brush (**Figure 31**). This was a disadvantage of this system due to the fact that in order for a data storage device to function properly a smooth surface is required. One of the proposed ways to improve the smoothness of the PANI film is by adding alkyl side chains to the PANI chain. This was hypothesized to produce more uniform coverage of the polymer film due to the side chains potentially weakening

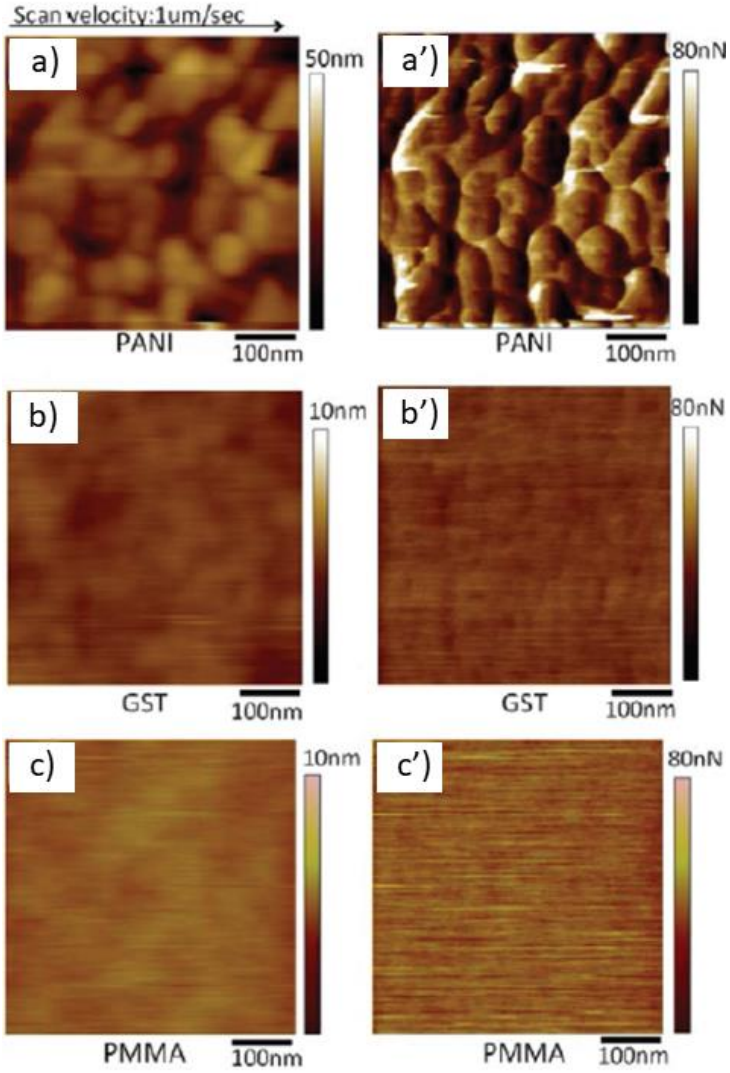

Figure 31. Images show AFM friction and topography plots of different surfaces. The left side images show topography while the right images show friction. a) and a') are the PANI brush. b) and b') are GeSbTe. c) and c') are poly methyl methacrylate films. [116], Adapted with permission. Open Access distributed under the terms of the Creative Commons Attribution License CC BY 4.0.

interactions between the surface-immobilized chains and, thus, preventing aggregation. Another proposed solution was to increase the grafting density of the brushes, which should result in a more uniform coverage.[171] However, as no grafting density or molecular weight data was reported for the PANI films, it is difficult to determine if the films were in the brush regime. Lastly, wear tests using the AFM to repeatedly scratch the surface showed very little wear compared to PMMA films under the same conditions. This demonstrated that these films should stand up to the repeated wear of a data storage tip tapping the surface.

In 2015 Gao et al. used PANI brushes for their potential in the biomedical field of electronics for sensing and imaging.[117] One long standing issue with PANI is poor resistance to dedoping, which in the field of biomedical imaging is especially problematic due to leaching of dopant ions, as well as effecting electrical and optical properties. In order to address these issues a PANI brush was synthesized on 70 nm magnetic nanoparticles (MNPs). This was done by first reacting the MNPs with dopamine to form a reactive core for the PANI to initiate from. To prepare for the polymerization, aniline was added to DI water while a separate solution of the oxidant, $(NH_4)_2S_2O_8$, was prepared in DI water, followed by the addition of HCl. Both solutions were placed at 4 °C. Meanwhile, a third solution of polydopamine covered MNPs were placed in DI water with the counter ion sodium dodecyl sulfate. The PANI solution and the oxidant solution were then added to the solution of MNPs and the reaction was carried out in darkness at RT for 24 hours. The particles were purified with repeated centrifugation and magnetic separation. No TGA or molecular weight characterization was reported and, thus, the grafting density of the PANI films was not calculated. TEM showed the thickness of the PANI layer to be approximately 15 nm. When compared to PANI covered MNPs prepared via the ‘grafting to’ technique, at a pH of 7 the grafted PANI particles showed a conductance over 2000 times better. This was reported to be due

to a polymer brush structure holding the oxidant much better than the more loosely covered traditional PANI particles. An additional discovery was that these particles possessed non-fouling properties and were shown to surpass the industry standard PEG, which has been used extensively for anti-fouling surfaces. Future application of PANI brushes potentially include batteries, electromagnetic shielding, gas sensors, electrochromic devices, electronic devices, bioimaging, sensing, coating, and smart textile.[79]

In 2019, Jiang et al. synthesized composite silica nanohybrid PANI particles with the application goal of using them as an anode material for lithium batteries.[118] To prepare these composite particles, 50 - 120 nm silica particles were modified with 3-aminopropyl triethoxysilane to act as an initiator for the polymerization. The amine-modified particles were then dispersed in ethanol using ultrasonication and aniline was subsequently added. The solution was cooled with ice and ammonium peroxydisulfate in an HCl solution was added dropwise to start the oxidative polymerization, which was carried out for 6 hours. The particles were then washed three times with ethanol to remove any physically absorbed polymer before being dried at 60 °C. XPS was used to confirm that the initiator layer was successfully grafted to the silica nanoparticles. FTIR spectroscopy was used to confirm the characteristic peaks for the initiator-modified particles, PANI particles, and the control system, PANI physically absorbed silica particles. TGA was used to show that a weight loss of 52% for the particles with PANI burnt off between 240 - 400 °C. SEM and TEM were used to image the particles and indicated a uniform polymer layer 2 - 5 nm thick. Although this layer is relatively thin, the layer appeared to be uniform, which the authors proposed to be an indication that the polymer films may have a high enough grafting density to produce a brush structure. No molecular weight characterization was performed, however, so a grafting density was not reported. The PANI-modified particles showed high levels of capacity,

2135 mA/g, and maintained 848 mA/g capacity after 100 cycles, while preserving the structural integrity and promoting the transport of both electrons and lithium ions.

4.6.2 Polypyrrole

In 2008 Wang and Ni showed that pyrrole could be initiated from the surface of TiO_2 films.[119] This was performed by first creating a layer of TiO_2 on an ITO slide. The slide was then placed in a quartz reactor with 0.1 M solution of pyrrole and UV-irradiated at 365 nm to polymerize the pyrrole. Raman spectroscopy demonstrated that with different reaction times the polypyrrole (PPy) peaks increased, indicating an increased thickness of the PPy film with reaction time. XPS was used to confirm that the PPy was attached to the TiO_2 film by showing the presence of the $-N^+$ species. From this, it was deduced that the PPy is oxidized due to π electrons from the conjugated pyrrole rings undergoing a charge-transfer mechanism with the TiO_2, which the authors hypothesized to mean a chemical bond was present. SEM and AFM images demonstrated a uniform coverage of the PPy film with a decrease in surface rms roughness, 13 nm, when compared to the TiO_2 film substrate, 25 nm. No grafting density or molecular weight data was reported for the films. However, linear scan voltammetry under dark and illumination showed increased photo response and improved film electrode properties compared to electrodeposited PPy films, which is important for their potential applications in photovoltaic cells and light emitting diodes.

Initiating the polymerization of pyrrole from a silica surface was first demonstrated in 2010 by Choi et al.[82] In this communication, surface-initiated polymerization of pyrrole was performed on mesoporous silica. This was hypothesized to be a result of a reactive nitrosyl ion (NO^+) surface species, which initiates the polymerization from the silica surface. It should be noted that a typical initiation process was not used and instead the initiation was hypothesized to function by using sodium nitrite to deprotonate surface silanol groups, which then allowed for the formation

of the nitrosyl ion and kept the polymerization from the surface. After polymerization, the average pore size of the mesoporous silica decreased from 9.27 nm to 9.06 nm, suggesting that while the polymer layer formed was extremely thin, polymerization of pyrrole from the surface of the mesoporous silica was possible. As no molecular weight or grafting density data was reported and because of the small change in pore size, the PPy films formed were most likely composed of small oligomers.

In 2017 surface-initiated PPy films on a vanadium pentoxide (V_2O_5) particles were reported by Jung et al.[120] Similar to Choi at al., the PPy chains were initiated off of the surface using a oxidizing agent. In this case this species was believed to be surface generated VO_2^+. To synthesize the hybrid V_2O_5 PPy particles, a 0.1 M pyrrole solution in water with V_2O_5 particles was stirred for 12 hours. The resulting product was then filtered, washed with water, and dried. SEM analysis showed a morphology that was hypothesized to be 10 – 30 nm PPy clumps or 'spherical particles' on the V_2O_5 surface. This morphology was suggested to be due to the surface-initiated PPy chains clumping together. Although uniform coverage was hypothesized, the clumping suggests the grafting density was low.[19] No molecular weight or grafting density data was reported for these films to confirm this. FTIR spectroscopy showed the characteristic PPy peaks, indicating that the observed clumps were indeed PPy. Despite the clumping, the authors did not observe any polymerization in solution, implying that the PPy was only initiated from the surface of the V_2O_5 particles.

In 2020 Nadeem et al. used a surface-initiated radical polymerization to form hybrid PPy sepiolite particles.[172] To synthesize the hybrid polymers, sepiolite clay was first modified with the silane initiator, vinyltriethoxysilane. The polymerization was then performed in a glass reactor tube with demineralized water and TWEEN-80 as a surfactant. The pyrrole monomer was slowly

added to the stirring solution, followed by the dropwise addition of the radical initiator, potassium persulphate. The system was then heated at 70 °C and the polymerization conducted for 8 hours. Following the polymerization, the system was filtered, and the product washed with demineralized water and acetone. Using FTIR spectroscopy, the characteristic PPy peaks were observed, which indicated successful modification of the clay. With TGA, over 50% weight loss was observed at 600 °C. However, as the surface-initiated PPy was not degrafted, no grafting density or molecular weight data for the polymer film was reported. Despite this, the method used in this report shows a potentially useful way to modify surfaces with pyrrole due to ease of synthesis and large amount of polymer produced.

4.6.3 Polycarbonate

Aliphatic polycarbonates are widely used in many applications including biodegradable and biocompatible materials, tissue implants, drug delivery, packaging films, medical sutures, and widely used with other polymers to improve mechanical properties.[173] In 2013, Lu et al. reported the first example of using aliphatic polycarbonates to help improve the properties of carbon nanotubes by surface-initiated immortal polymerization.[121] The polymerization was carried out on carboxylic acid functionalized multiwalled carbon nanotubes (MWCNs-COOH) using a binary catalyst system composed of a cobalt cyclohexenediimine complex and bis(triphenylphosphine)iminium chloride. To start the reaction, the complex, propylene oxide, and

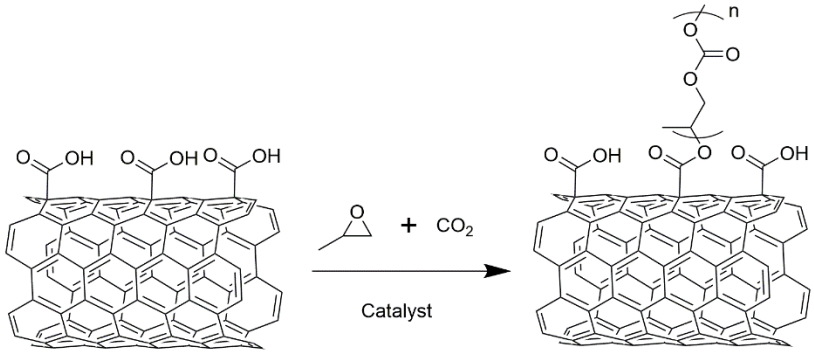

Figure 32. Reaction scheme shows surface-initiated polycarbonate brush using immortal polymerization mechanism on MWCN performed by Lu et al. [121]

MWCNs-COOH were added to an autoclave purged with nitrogen (**Figure 32**). The autoclave was mixed and charged with a CO_2 atmosphere, and the reaction carried out until the mixture turned into the solid phase. The composite material was then dissolved and filtered, followed by drying the product overnight. The chemical attachment and formation of the polymer were confirmed using FTIR and NMR spectroscopy, while SEM and TEM showed a thickness of up to 3 nm for the polymer on the MWNTs. The authors demonstrated that the polymer coating enhanced solution stability of the MWNTs as indicated by the fact that no sedimentation was observed of the product in DCM, THF, chloroform, acetone, dimethylformamide, or DMSO after sitting for 14 months. Although TGA was performed, no grafting density for the polymer-modified MWNTs was reported. The molecular weight of free polycarbonate, formed in solution during the polymerization, was shown to have a M_n ranging from 19,100 to 93,700 g/mol with PDI's ranging from 1.08 to 1.19. Characterization of the mechanical properties, including tensile strength, Young's modulus, flexural stress, and flexural modulus, all showed improvements when 3 wt.% polycarbonate MWNTs were mixed with a polycarbonate matrix compared to unmodified polycarbonate. While the tensile strength, Young's modulus, and flexural stress doubled in value, the flexural modulus increased by almost five times. This represents an exciting example of yet another new semi-flexible surface-initiated brush, which, in the future, could be adapted to flat surfaces or larger nanoparticles to allow for more detailed characterization.

In 2014, Carlmark et al. used a different reaction scheme to make surface-initiated polycarbonate from cellulose surfaces.[122] Instead of using an immortal polymerization like Lu et al., a ring opening mechanism was utilized. Unlike many surface-initiated polymerizations, in this case, no initiator needed to be added to the surface as cellulose has a high concentration of alcohols on the surface that can be used to initiate the polymerization. To make the polycarbonate

films, two different catalyst were utilized but all other reaction conditions remained the same. In addition, a sacrificial solution initiator was also used to allow for an approximation of the molecular weight of the surface-initiated polymers, as degrafting the surface-attached polymers from cellulose is difficult. A typical reaction was performed by adding filter paper, the cellulose substrate, to a purged vial then adding the monomer, trimethylene carbonate, followed by additional argon purging. DCM and the sacrificial initiator, benzylic alcohol, were then added followed by a catalyst solution of either 1,8-diazabicyclo[5.4.0]undec-7-ene (DBU) or 1,5,7-triazabicyclo [4.4.0]dec-5-ene (TBD). The solution was mixed at RT for 1 minute before being placed at 40 °C for the desired reaction time, which ranged from 1 minute to 24 hours. Due to the lack of a carbonyl IR peak in cellulose, the polycarbonate carbonyl IR peak was used to measure the amount of polycarbonate grafted to the surface. Using this technique, it was shown that changing the concentration of sacrificial initiator modified the film thickness, with a lower concentration of initiator producing a thicker film. Because cellulose and grafted polycarbonate degradations overlap in TGA, an exact percent of grown polycarbonate was not determined. As a result, no grafting density or molecular weight data was reported for the surface-initiated polymer. Using the polymer formed in solution from the sacrificial initiator, the molecular weight of the polycarbonate ranged from 7,200 to 61,000 g/mol with the PDIs varying from 1.36 to 2.06. The PDI values were relatively high in some case but this was hypothesized to be due to residual water on the cellulose that can also initiated chains, in addition to the potential for chain scission of the propagating brushes. Although no grafting density measurements were reported, SEM showed uniform coverage of the polymer film with increased smoothness compared to the unmodified cellulose paper, which the authors suggest indicates a relatively high grafting density and uniform coverage. Contact angle measurements showed a water contact angle of 100°, which was higher

than the unmodified polycarbonate films. This was hypothesized to be due to the relatively rough underlying cellulose substrate.

5. Conclusion and Future Perspective

Polymer brushes have fascinated scientist over the last three decades with the promise of unique film properties due to the closely packed polymer chains on a surface and their unique conformations.[18] Until more recently, vinyl-based monomers have been the primary focus for the preparation of polymer brushes. However, the discovery of techniques that are capable of converting traditional step-growth polymers into chain-growth polymers, primarily using CGC and ring opening polymerization techniques, have provided new pathways for the synthesis of polymer brushes using the 'grafting from' approach. These non-vinyl-based polymer brushes have come a long way in the past two decades and have gone from theory to the experimental realization of brushes, which include polynorbornenes, polypeptides, polyesters, polyoxazoline, polyaniline, polythiophenes, polyfluorenes, polyphenylenes, polyphenyleneethynlene, polypyrrole, polyisocyanate, poly(isocyanides), and polyamides.[[2],[21],[75],[76],[77],[78],[79],[80],[81],[82],[83],[84],[86]] The reported potential applications of these brushes have ranged from OPVs, OLEDs, tribological coatings, membranes for water purification and desalination, membranes for fuel cells, high performance coatings, and biosensing, and are only a glimpse of what is possible using these new films.[[2],[3]]

Although these polymer brushes are reported to have much promise in future applications, there is still much room for advancement in this area of research. One of the critical areas that needs to be addressed with non-vinyl-based polymer brushes is solubility. Many of these polymers, especially those containing aromatic rings or conjugation on the backbone, are plagued by low solubility, which inhibits how thick the brushes can be grown and the molecular weights that can

be achieved. In addition to this, low solubility can also inhibit characterization of the polymers using conventional analytical techniques. One attempt to solve this issue has been to add solubilizing side chains to the monomers used for brush synthesis, which has shown solubility improvements.[[2],[78],[81],[83],[154]] While these side chains help solubilize the propagating chains during the polymerization, which helps increase the obtainable molecular weight, they can have the negative side effect of altering the physical properties, such as lowering of the Young's modulus and durability.[[174],[175]] Utilizing techniques, such as post polymerization removal of the solubilizing chains, could solve the problem of low solubility without decreasing the desired physical properties and could greatly increase the application and future directions of these films.

Another hurdle to overcome in improving the understanding and development of non-vinyl-based brushes is to improve the characterization of the brushes, in particularly with respect to grafting density, and what defines a polymer chain being in the brush regime. This topic has been studied extensively with brushes based on vinyl monomers but has received limited attention for the new emerging non-vinyl-based brushes.[[17],[24],[19]] Indeed, the importance of developing a structural definition for polymer brush formation and being able to distinguish between 'true' polymer brushes and simply grafted polymer films was highlight by Brittain and Minko in 2007.[29] In this paper, the authors conclude that reporting the Σ value, or at the very least the grafting density, for grafted polymer films is critical in defining or using the term polymer brush. As can be easily seen in the above review, many of the studies do not include either the polymer film Σ value or grafting density, while others may include the initiator grafting density but fail to report the polymer chain grafting density, which is paramount because these two grafting densities do not have a direct correlation in most cases.[176] In order to obtain a better understanding of how Σ or grafting density influence the properties of non-vinyl-based brushes, it is vital that

research in this area starts to report these values. However, this is intimately tied to two other factors. The first, as discussed above, is polymer solubility, which is typically required to accurately determine polymer molecular weight. The molecular weight is required to calculate grafting density, which in turn, is required for the calculation of Σ. The other factor is the need for further theoretical studies investigating the values of Σ or grafting density required for polymer brush formation with semi-flexible or rigid rod polymers. While these values have been defined and experimentally demonstrated for random coil polymers prepared from vinyl-based monomers, intuitively, they will be significantly different for polymers that adopt other conformations. As such, target values or ranges to confirm the adoption of a brush conformation need to be set. This will allow for consistency in the use of the term polymer brush and also provide affirmation that a polymer brush structure is required or responsible for improvements observed in film properties. Finally, characterization techniques, such as neutron scattering, could also help provide experimental information into how these polymer brushes structured and whether or not these films are in the brush regime.

Developing a better understanding of the various mechanical properties obtained from these semi-flexible or rigid rod polymer brushes compared to their other conformational counter parts is important for many of the proposed future applications. Many different properties have been predicted for semi-flexible polymers by entering the brush regime compared to a physically absorbed films, mushroom structures, and flexible brushes. These properties, such as improved lubricity, optoelectronic properties, and high strength films, are based off the polymers forming the highly ordered brush regime making understanding and characterizing this step very important as highlighted above. Measuring these properties is important and in many cases for these non-vinyl-based films has not been performed. Characterizing mechanical properties, such as Young's

modulus, friction, adhesion, and wear, has been limited for most of the reported systems. AFM has been widely adopted to characterize polymer films but has been mostly limited to topography despite its many functions. Fundamental studies using AFMs force measurement capabilities with non-vinyl-based polymer brushes is important in aiding future studies to measure the potential beneficial properties of semi-flexible and rigid rod polymer brushes. Alternatively, the recently developed surface wrinkling technique has been used to determine polymer brush film properties, such as Young's modulus. However, this technique has had limited use with non-vinyl-based polymer brushes and has potential to aid in mechanical characterization. Characterizing optical and electrical properties has been reported much more frequently. This is typically performed using UV-vis spectroscopy, fluorescent spectroscopy and various electrical characterization techniques and is one area where most of the reviewed polymer films interested in such properties have reported improved brush properties compared to physically absorbed polymers.

Despite these hurdles, there is tremendous promise in the future of non-vinyl-based polymer brushes, where surface modification using polymer films has the potential to dramatically change surface properties and provide access to new technologies. Research over the past 30 years has moved from theoretical studies to experimental realization to meet the scientific communities expanding need for new polymers for surface modification. The outstanding work of people in this field has been directly responsible for refining and discovering new polymerization processes, developing new characterization techniques, and identifying new polymers that can be used to form polymer brushes. Notwithstanding this, there are still many types of polymers that are traditionally synthesized using a step-growth process that could produce novel polymer brushes if converted into a chain-growth polymerization, such as polyureas, polyurethanes, aromatic polyesters, polysiloxanes, aromatic polycarbonates, and polysulfides, to name a few. While some

of these polymers can be prepared via ROP, expansion to include aromatic systems and the synthesis of well-defined rigid rod polymers for surface modification is yet to be realized.

Acknowledgements

SGB and CJR gratefully acknowledges the support of this work by the National Science Foundation under grant CHE MSN #1807863.

CRediT Author Statement

Caleb J. Reese: Conceptualization, Investigation, Writing – original draft. Stephen G. Boyes: Writing – review & editing, Funding acquisition, Supervision.

References

[1] Yokozawa T, Ohta Y. Transformation of step-growth polymerization into living chain-growth polymerization. Chem Rev 2016;116:1950–68. https://doi.org/10.1021/acs.chemrev.5b00393.

[2] Prehn FC, Boyes SG. Surface-initiated chain growth polyaramid brushes. Macromolecules 2015;48:4269–80. https://doi.org/10.1021/acs.macromol.5b00957.

[3] Okamoto K, Luscombe CK. Controlled polymerizations for the synthesis of semiconducting conjugated polymers. Polym Chem 2011;2:2424–34. https://doi.org/10.1039/c1py00171j.

[4] Hiemenz PC, Rajagopalan R. Principles of colloid surface chemistry third edition. 1997.

[5] Stamm M. Polymer surfaces and interfaces. Berlin, Heidelberg: Springer Berlin Heidelberg; 2008. https://doi.org/10.1007/978-3-540-73865-7.

[6] Hu G, Hoppe S, Feng L, Fonteix C. Nano-scale phenomena and applications in polymer

processing. Chem Eng Sci 2007;62:3528–37. https://doi.org/10.1016/j.ces.2007.02.052.

[7] Yoon H, Choi M, Lee KJ, Jang J. Versatile strategies for fabricating polymer nanomaterials with controlled size and morphology. Macromol Res 2008;16:85–102. https://doi.org/10.1007/BF03218836.

[8] Prencipe G, Tabakman SM, Welsher K, Liu Z, Goodwin AP, Zhang L, et al. PEG branched polymer for functionalization of nanomaterials with ultralong blood circulation. J Am Chem Soc 2009;131:4783–7. https://doi.org/10.1021/ja809086q.

[9] Li C, Bai H, Shi G. Conducting polymer nanomaterials: electrosynthesis and applications. Chem Soc Rev 2009;38:2397–409. https://doi.org/10.1039/b816681c.

[10] Yoon H, Jang J. Conducting-polymer nanomaterials for high-performance sensor applications: Issues and challenges. Adv Funct Mater 2009;19:1567–76. https://doi.org/10.1002/adfm.200801141.

[11] Silvestre C, Duraccio D, Cimmino S. Food packaging based on polymer nanomaterials. Prog Polym Sci 2011;36:1766–82. https://doi.org/10.1016/j.progpolymsci.2011.02.003.

[12] Adali-Kaya Z, Tse Sum Bui B, Falcimaigne-Cordin A, Haupt K. Molecularly imprinted polymer nanomaterials and nanocomposites: atom-transfer radical polymerization with acidic monomers. Angew Chemie Int Ed 2015;54:5192–5. https://doi.org/10.1002/anie.201412494.

[13] Nemani SK, Annavarapu RK, Mohammadian B, Raiyan A, Heil J, Haque MA, et al. Surface Modification of Polymers: Methods and Applications. Adv Mater Interfaces 2018;5:1801247. https://doi.org/10.1002/admi.201801247.

[14] Feng C, Huang X. Polymer brushes: Efficient synthesis and applications. Acc Chem Res 2018;51:2314–23. https://doi.org/10.1021/acs.accounts.8b00307.

[15] Giussi JM, Cortez ML, Marmisollé WA, Azzaroni O. Practical use of polymer brushes in sustainable energy applications: interfacial nanoarchitectonics for high-efficiency devices. Chem Soc Rev 2019;48:814–49. https://doi.org/10.1039/C8CS00705E.

[16] Azzaroni O. Polymer brushes here, there, and everywhere: Recent advances in their practical applications and emerging opportunities in multiple research fields. J Polym Sci Part A Polym Chem 2012;50:3225–58. https://doi.org/10.1002/pola.26119.

[17] Advincula RC, Brittain WJ, Caster KC, Rühe J, editors. Poltmer brushes synthesis, characterization, applications. Weinheim, FRG: Wiley-VCH Verlag GmbH & Co. KGaA; 2004. https://doi.org/10.1002/3527603824.

[18] Milner ST. Polymer brushes. Science (80-) 1991;251:905–14. https://doi.org/10.1126/science.251.4996.905.

[19] Chen WL, Cordero R, Tran H, Ober CK. 50th anniversary perspective: polymer brushes: novel surfaces for future materials. Macromolecules 2017;50:4089–113. https://doi.org/10.1021/acs.macromol.7b00450.

[20] Beers KL, Gaynor SG, Matyjaszewski K, Sheiko SS, Möller M. The synthesis of densely grafted copolymers by atom transfer radical polymerization. Macromolecules 1998;31:9413–5. https://doi.org/10.1021/ma981402i.

[21] Shen Y, Li Z, Klok H-A. Polypeptide brushes grown via surface-initiated ring-opening polymerization of α-amino acid N-carboxyanhydrides. Chinese J Polym Sci 2015;33:931–

46. https://doi.org/10.1007/s10118-015-1654-7.

[22] García JM, García FC, Serna F, de la Peña JL. High-performance aromatic polyamides. Prog Polym Sci 2010;35:623–86. https://doi.org/10.1016/j.progpolymsci.2009.09.002.

[23] Morse DC, Fredrickson GH. Semiflexible polymers near interfaces. Phys Rev Lett 1994;73:3235–8. https://doi.org/10.1103/PhysRevLett.73.3235.

[24] Kim M, Schmitt S, Choi J, Krutty J, Gopalan P. From self-assembled monolayers to coatings: Advances in the synthesis and nanobio applications of polymer brushes. Polymers (Basel) 2015;7:1346–78. https://doi.org/10.3390/polym7071346.

[25] Zoppe JO, Ataman NC, Mocny P, Wang J, Moraes J, Klok H-A. Surface-initiated controlled radical polymerization: state-of-the-art, opportunities, and challenges in surface and interface engineering with polymer brushes. Chem Rev 2017;117:1105–318. https://doi.org/10.1021/acs.chemrev.6b00314.

[26] Luzinov I, Julthongpiput D, Malz H, Pionteck J, Tsukruk V V. Polystyrene layers grafted to epoxy-modified silicon surfaces. Macromolecules 2000;33:1043–8. https://doi.org/10.1021/ma990926v.

[27] Yan J, Bockstaller MR, Matyjaszewski K. Brush-modified materials: Control of molecular architecture, assembly behavior, properties and applications. Prog Polym Sci 2020;100:101180/1-51. https://doi.org/10.1016/j.progpolymsci.2019.101180.

[28] Jordan R, editor. Surface-initiated polymerization II. vol. 198. Berlin/Heidelberg: Springer-Verlag; 2006. https://doi.org/10.1007/11586142.

[29] Brittain WJ, Minko S. A structural definition of polymer brushes. J Polym Sci Part A

Polym Chem 2007;45:3505–12. https://doi.org/10.1002/pola.22180.

[30] Milchev A, Binder K. Unconventional ordering behavior of semi-flexible polymers in dense brushes under compression. Soft Matter 2014;10:3783–97. https://doi.org/10.1039/c3sm53133c.

[31] Dumont ELP, Belmas H, Hess H. Observing the mushroom-to-brush transition for kinesin proteins. Langmuir 2013;29:15142–5. https://doi.org/10.1021/la4030712.

[32] Rogers ME, Long TE. Synthetic methods in step-growth polymers. Hoboken, NJ, USA: John Wiley & Sons, Inc.; 2003. https://doi.org/10.1002/0471220523.

[33] Chechik V, Crooks RM, Stirling CJM. Reactions and reactivity in self-assembled monolayers. Adv Mater 2000;12:1161–71. https://doi.org/10.1002/1521-4095(200008)12:16<1161::AID-ADMA1161>3.0.CO;2-C.

[34] Nicosia C, Huskens J. Reactive self-assembled monolayers: from surface functionalization to gradient formation. Mater Horiz 2014;1:32–45. https://doi.org/10.1039/C3MH00046J.

[35] Kondo T, Yamada R, Uosaki K. Self-assembled monolayer (SAM). Organ. Org. Ultrathin Film., Weinheim, Germany: Wiley-VCH Verlag GmbH & Co. KGaA; 2012, p. 7–42. https://doi.org/10.1002/9783527654666.ch2.

[36] Senaratne W, Andruzzi L, Ober CK. Self-assembled monolayers and polymer brushes in biotechnology: current applications and future perspectives. Biomacromolecules 2005;6:2427–48. https://doi.org/10.1021/bm050180a.

[37] Mittal V, editor. Polymer brushes substrates, technologies, and properties. CRC Press; 2012.

[38] Wakabayashi R, Sugiura Y, Shibue T, Kuroda K. Practical Conversion of Chlorosilanes into Alkoxysilanes without Generating HCl ** 2011;50:10708–11. https://doi.org/10.1002/anie.201104948.

[39] Barbey R, Lavanant L, Paripovic D, Schüwer N, Sugnaux C, Tugulu S, et al. Polymer brushes via surface-initiated controlled radical polymerization: Synthesis, characterization, properties, and applications. Chem Rev 2009;109:5437–527. https://doi.org/10.1021/cr900045a.

[40] Shircliff RA, Stradins P, Moutinho H, Fennell J, Ghirardi ML, Cowley SW, et al. Angle-resolved XPS analysis and characterization of monolayer and multilayer silane films for DNA coupling to silica. Langmuir 2013;29:4057–67. https://doi.org/10.1021/la304719y.

[41] Ayres N. Polymer brushes: Applications in biomaterials and nanotechnology. Polym Chem 2010;1:769–77. https://doi.org/10.1039/B9PY00246D.

[42] Ma S, Zhang X, Yu B, Zhou F. Brushing up functional materials. NPG Asia Mater 2019;11:1–39. https://doi.org/10.1038/s41427-019-0121-2.

[43] Yokozawa T, Shimura H. Condensative chain polymerization. II. Preferential esterification of propagating end group in Pd-catalyzed CO-insertion polycondensation of 4-bromophenol derivatives. J Polym Sci Part A Polym Chem 1999;37:2607–18. https://doi.org/10.1002/(SICI)1099-0518(19990715)37:14<2607::AID-POLA35>3.0.CO;2-H.

[44] Yokozawa T, Asai T, Sugi R, Ishigooka S, Hiraoka S. Chain-growth polycondensation for nonbiological polyamides of defined architecture. J Am Chem Soc 2000;122:8313–4. https://doi.org/10.1021/ja001871b.

[45] Yokozawa T, Suzuki Y, Hiraoka S. Aromatic polyethers with low polydispersities from chain-growth polycondensation. J Am Chem Soc 2001;123:9902–3. https://doi.org/10.1021/ja011499f.

[46] Yokoyama A, Miyakoshi R, Yokozawa T. Chain-growth polymerization for poly(3-hexylthiophene) with a defined molecular weight and a low polydispersity. Macromolecules 2004;37:1169–71. https://doi.org/10.1021/ma035396o.

[47] Sheina EE, Liu J, Iovu MC, Laird DW, McCullough RD. Chain growth mechanism for regioregular nickel-initiated cross-coupling polymerizations. Macromolecules 2004;37:3526–8. https://doi.org/10.1021/ma0357063.

[48] Iovu MC, Sheina EE, Gil RR, McCullough RD. Experimental evidence for the quasi-"living" nature of the Grignard metathesis method for the synthesis of regioregular poly(3-alkylthiophenes). Macromolecules 2005;38:8649–56. https://doi.org/10.1021/ma051122k.

[49] Yokoyama A, Yokozawa T. Converting step-growth to chain-growth condensation polymerization. Macromolecules 2007;40:4093–101. https://doi.org/10.1021/ma061357b.

[50] Yokozawa T, Ohta Y. Scope of controlled synthesis via chain-growth condensation polymerization: from aromatic polyamides to π-conjugated polymers. Chem Commun 2013;49:8281–310. https://doi.org/10.1039/c3cc43603a.

[51] Yokozawa T, Yokoyama A. Chain-growth polycondensation: The living polymerization process in polycondensation. Prog Polym Sci 2007;32:147–72. https://doi.org/10.1016/j.progpolymsci.2006.08.001.

[52] Yokoyama A, Masukawa T, Yamazaki Y, Yokozawa T. Successive chain-growth

condensation polymerization for the synthesis of well-defined diblock copolymers of aromatic polyamide and aromatic polyether. Macromol Rapid Commun 2009;30:24–8. https://doi.org/10.1002/marc.200800546.

[53] Kiriy A, Senkovskyy V, Sommer M. Kumada catalyst-transfer polycondensation: mechanism, opportunities, and challenges. Macromol Rapid Commun 2011;32:1503–17. https://doi.org/10.1002/marc.201100316.

[54] Yokozawa T, Yokoyama A. Chain-growth condensation polymerization for the synthesis of well-defined condensation polymers and π-conjugated polymers. Chem Rev 2009;109:5595–619. https://doi.org/10.1021/cr900041c.

[55] McCullough RD, Lowe RD. Enhanced electrical conductivity in regioselectively synthesized poly(3-alkylthiophenes). J Chem Soc Chem Commun 1992:70–2. https://doi.org/10.1039/c39920000070.

[56] McCullough RD, Lowe RD, Jayaraman M, Anderson DL. Design, synthesis, and control of conducting polymer architectures: structurally homogeneous poly(3-alkylthiophenes). J Org Chem 1993;58:904–12. https://doi.org/10.1021/jo00056a024.

[57] Loewe RS, Khersonsky SM, McCullough RD. A simple method to prepare head-to-tail coupled, regioregular poly(3-alkylthiophenes) using grignard metathesis. Adv Mater 1999;11:250–3. https://doi.org/10.1002/(SICI)1521-4095(199903)11:3<250::AID-ADMA250>3.0.CO;2-J.

[58] Loewe RS, Ewbank PC, Liu J, Zhai L, Mccullough RD. Regioregular, head-to-tail coupled poly (3-alkylthiophenes) made easy by the GRIM method: Investigation of the reaction and the origin of regioselectivity. Macromolecules 2001;34:4324–33.

https://doi.org/https://doi.org/10.1021/ma001677+.

[59] Gu Z, Tan Y, Tsuchiya K, Shimomura T, Ogino K. Synthesis and characterization of poly(3-hexylthiophene)-b-polystyrene for photovoltaic application. Polymers (Basel) 2011;3:558–70. https://doi.org/10.3390/polym3010558.

[60] Zenkina O V., Karton A, Freeman D, Shimon LJW, Martin JML, van der Boom ME. Directing aryl−I versus aryl−Br bond activation by nickel via a ring walking process. Inorg Chem 2008;47:5114–21. https://doi.org/10.1021/ic702289n.

[61] Lenz RW, Handlovits CE, Smith HA. Phenylene sulfide polymers. III. The synthesis of linear polyphenylene sulfide. J Polym Sci 1962;58:351–67. https://doi.org/10.1002/pol.1962.1205816620.

[62] Risse W, Heitz W, Freitag D, Bottenbruch L. Preparation and characterization of poly[oxy(2,6-dimethyl-1,4-phenylene)] with functional end groups. Die Makromol Chemie 1985;1853:1835–53. https://doi.org/https://doi.org/10.1002/macp.1985.021860912.

[63] Ridd JH, Yousaf TI. Polymerisation and related reactions involving nucleophilic aromatic substitution. Part 1. The rates of reaction of substituted 4-halogenobenzophenones with the potassium salts of substituted 4-hydroxybenzophenones. J Chem Soc Trans 2 1988:1729–34. https://doi.org/10.1039/p29880001729.

[64] Robello DR, Ulman A, Urankar EJ. Poly(p-phenylene sulfone). Macromolecules 1993;26:6718–21. https://doi.org/10.1021/ma00077a004.

[65] Matyjaszewski K, Greszta D, Hrkach JS, Kim HK. Sonochemical synthesis of

polysilylenes by reductive coupling of disubstituted dichlorosilanes with alkali metals. Macromolecules 1995;28:59–72. https://doi.org/10.1021/ma00105a007.

[66] Miyatake K, Hlil AR, Hay AS. High molecular weight aromatic polyformals free of macrocyclic oligomers. A condensative chain polymerization reaction. Macromolecules 2001;34:4288–90. https://doi.org/10.1021/ma002020r.

[67] Iwashita K, Yokoyama A, Yokozawa T. Synthesis of well-defined aromatic polyesters by chain-growth polycondensation under suppression of transesterification. J Polym Sci Part A Polym Chem 2005;43:4109–17. https://doi.org/10.1002/pola.20907.

[68] Prehn FC, Etz BD, Reese CJ, Vyas S, Boyes SG. Chain-growth polycondensation via the substituent effect: Investigation of the monomer structure on synthesis of poly(N-octyl-benzamide). J Polym Sci 2020;58:2389–406. https://doi.org/10.1002/pol.20200435.

[69] McGrath J. Ring-opening polymerization: Introduction, 1985, p. 1–22. https://doi.org/10.1021/bk-1985-0286.ch001.

[70] Dubois P. Handbook of ring-opening polymerization. Wiley; 2009. https://doi.org/10.1002/9783527628407.

[71] Nuyken O, Pask S. Ring-opening polymerization—An introductory review. Polymers (Basel) 2013;5:361–403. https://doi.org/10.3390/polym5020361.

[72] Leuchs H, Manasse W. Über die isomerie der carbäthoxyl-glycyl glycinester. Berichte Der Dtsch Chem Gesellschaft 1907;40:3235–49. https://doi.org/10.1002/cber.19070400387.

[73] Matyjaszewski K. Controlled and Living Polymerizations. n.d. https://doi.org/10.1002/9783527629091.

[74] Matyjaszewski K, Dong H, Jakubowski W, Pietrasik J, Kusumo A. Grafting from surfaces for “everyone”: ARGET ATRP in the presence of air. Langmuir 2007;23:4528–31. https://doi.org/10.1021/la063402e.

[75] Husemann M, Mecerreyes D, Hawker CJ, Hedrick JL, Shah R, Abbott NL. Surface-initiated polymerization for amplification of self-assembled monolayers patterned by microcontact printing. Angew Chemie Int Ed 1999;38:647–9. https://doi.org/10.1002/(SICI)1521-3773(19990301)38:5<647::AID-ANIE647>3.3.CO;2-S.

[76] Jordan R, Ulman A. Surface initiated living cationic polymerization of 2-oxazolines. J Am Chem Soc 1998;120:243–7. https://doi.org/10.1021/ja973392r.

[77] Kim NY, Jeon NL, Choi IS, Takami S, Harada Y, Finnie KR, et al. Surface-initiated ring-opening metathesis polymerization on Si/SiO2. Macromolecules 2000;33:2793–5. https://doi.org/10.1021/ma000046c.

[78] Kang S, Ono RJ, Bielawski CW. Controlled catalyst transfer polycondensation and surface-initiated polymerization of a p-phenyleneethynylene-based monomer. J Am Chem Soc 2013;135:4984–7. https://doi.org/10.1021/ja401740m.

[79] Yoshida S, Ono T, Oi S, Esashi M. Reversible electrical modification on conductive polymer for proximity probe data storage. Nanotechnology 2005;16:2516–20. https://doi.org/10.1088/0957-4484/16/11/009.

[80] Senkovskyy V, Khanduyeva N, Komber H, Oertel U, Stamm M, Kuckling D, et al. Conductive polymer brushes of regioregular head-to-tail poly(3-alkylthiophenes) via catalyst-transfer surface-initiated polycondensation. J Am Chem Soc 2007;129:6626–32.

https://doi.org/10.1021/ja0710306.

[81] Beryozkina T, Boyko K, Khanduyeva N, Senkovskyy V, Horecha M, Oertel U, et al. Grafting of polyfluorene by surface-initiated suzuki polycondensation. Angew Chemie Int Ed 2009;48:2695–8. https://doi.org/10.1002/anie.200806217.

[82] Jung Y, Spray RL, Kim JH, Kim JM, Choi K-S. Selective polymerization of polypyrrole in silica mesopores using an in situ generated oxidizing agent on a silica surface. Chem Commun 2010;46:6566–8. https://doi.org/10.1039/c0cc01746a.

[83] Vatansever F, Hamblin MR. Surface-initiated polymerization with poly(n-hexylisocyanate) to covalently functionalize silica nanoparticles. Macromol Res 2017;25:97–107. https://doi.org/10.1007/s13233-017-5009-9.

[84] Lim E, Tu G, Schwartz E, Cornelissen JJLM, Rowan AE, Nolte RJM, et al. Synthesis and characterization of surface-initiated helical polyisocyanopeptide brushes. Macromolecules 2008;41:1945–51. https://doi.org/10.1021/ma702531u.

[85] Ka D, Park J, Kim SD, Lee S, Kim SY. Grafting of trifluoromethylated poly(phenylene oxide)s on a single-walled carbon nanotube via surface-initiated chain-growth condensation polymerization. J Polym Sci Part A Polym Chem 2017;55:3180–4. https://doi.org/10.1002/pola.28708.

[86] Sontag SK, Marshall N, Locklin J. Formation of conjugated polymer brushes by surface-initiated catalyst-transfer polycondensation. Chem Commun 2009:3354–6. https://doi.org/10.1039/b907264k.

[87] Binder K, Milchev A. Polymer brushes on flat and curved surfaces: How computer

simulations can help to test theories and to interpret experiments. J Polym Sci Part B Polym Phys 2012;50:1515–55. https://doi.org/10.1002/polb.23168.

[88] Wijmans CM, Leermakers FAM, Fleer GJ. Chain stiffness and bond correlations in polymer brushes. J Chem Phys 1994;101:8214–23. https://doi.org/10.1063/1.468206.

[89] Egorov SA, Hsu H-P, Milchev A, Binder K. Semiflexible polymer brushes and the brush-mushroom crossover. Soft Matter 2015;11:2604–16. https://doi.org/10.1039/C4SM02862G.

[90] Amoskov VM, Birshtein TM, Pryamitsyn VA. Theory of liquid-crystalline (LC) polymer brushes: Interpenetrating brushes. Macromolecules 1998;31:3720–30. https://doi.org/10.1021/ma970985d.

[91] Zhao B, Brittain W. Polymer brushes: surface-immobilized macromolecules. Prog Polym Sci 2000;25:677–710. https://doi.org/10.1016/S0079-6700(00)00012-5.

[92] Chae HG, Kumar S. Rigid-rod polymeric fibers. J Appl Polym Sci 2006;100:791–802. https://doi.org/10.1002/app.22680.

[93] Juang A, Scherman OA, Grubbs RH, Lewis NS. Formation of covalently attached polymer overlayers on Si(111) surfaces using ring-opening metathesis polymerization methods. Langmuir 2001;17:1321–3. https://doi.org/10.1021/la0012945.

[94] Fursule IA, Abtahi A, Watkins CB, Graham KR, Berron BJ. In situ crosslinking of surface-initiated ring opening metathesis polymerization of polynorbornene for improved stability. J Colloid Interface Sci 2018;510:86–94. https://doi.org/10.1016/j.jcis.2017.09.050.

[95] Deng X, Prozorovska L, Jennings GK. Metal chelating polymer thin films by surface-initiated ROMP and modification. J Phys Chem C 2019;123:23511–9. https://doi.org/10.1021/acs.jpcc.9b06410.

[96] Menzel H, Witte P. Synthesis of polypeptide brushes. Polym. Brushes, Weinheim, FRG: Wiley-VCH Verlag GmbH & Co. KGaA; 2005, p. 87–103. https://doi.org/10.1002/3527603824.ch4.

[97] Wibowo SH, Sulistio A, Wong EHH, Blencowe A, Qiao GG. Polypeptide films via N-carboxyanhydride ring-opening polymerization (NCA-ROP): past, present and future. Chem Commun 2014;50:4971–88. https://doi.org/10.1039/c4cc00293h.

[98] González-Henríquez CM, Sarabia-Vallejos MA, Rodríguez-Hernández J. Strategies to fabricate polypeptide-based structures via ring-opening polymerization of n-carboxyanhydrides. Polymers (Basel) 2017;9:551/1-62. https://doi.org/10.3390/polym9110551.

[99] Yoon KR, Lee K-B, Chi YS, Yun WS, Joo S-W, Choi IS. Surface-initiated, enzymatic polymerization of biodegradable polyesters. Adv Mater 2003;15:2063–6. https://doi.org/10.1002/adma.200305562.

[100] Choi IS, Langer R. Surface-initiated polymerization of L-lactide: coating of solid substrates with a biodegradable polymer. Macromolecules 2001;34:5361–3. https://doi.org/10.1021/ma010148i.

[101] Tian J, Zhou H, Jiang R, Chen J, Mao L, Liu M, et al. Preparation and biological imaging of fluorescent hydroxyapatite nanoparticles with poly(2-ethyl-2-oxazoline) through surface-initiated cationic ring-opening polymerization. Mater Sci Eng C

2020;108:110424. https://doi.org/10.1016/j.msec.2019.110424.

[102] Bissadi G, Weberskirch R. Formation of polyoxazoline-silica nanoparticles via the surface-initiated cationic polymerization of 2-methyl-2-oxazoline. Polym Chem 2016;7:5157–68. https://doi.org/10.1039/C6PY01034B.

[103] Bissadi G, Weberskirch R. Efficient synthesis of polyoxazoline-silica hybrid nanoparticles by using the "grafting-onto" approach. Polym Chem 2016;7:1271–80. https://doi.org/10.1039/C5PY01775K.

[104] Qu L, Veca LM, Lin Y, Kitaygorodskiy A, Chen B, McCall AM, et al. Soluble nylon-functionalized carbon nanotubes from anionic ring-opening polymerization from nanotube surface. Macromolecules 2005;38:10328–31. https://doi.org/10.1021/ma051762n.

[105] Yang M, Gao Y, He JP, Li HM. Preparation of polyamide 6/silica nanocomposites from silica surface initiated ring-opening anionic polymerization. Express Polym Lett 2007;1:433–42. https://doi.org/10.3144/expresspolymlett.2007.61.

[106] Huang S, Toh CL, Yang L, Phua S, Zhou R, Dasari A, et al. Reinforcing nylon 6 via surface-initiated anionic ring-opening polymerization from stacked-cup carbon nanofibers. Compos Sci Technol 2014;93:30–7. https://doi.org/10.1016/j.compscitech.2013.12.015.

[107] Kubono A, Yuasa N, Shao H-L, Umemoto S, Okui N. In-situ study on alternating vapor deposition polymerization of alkyl polyamide with normal molecular orientation. Thin Solid Films 1996;289:107–11. https://doi.org/10.1016/S0040-6090(96)08913-4.

[108] Zhou H, Toney MF, Bent SF. Cross-linked ultrathin polyurea films via molecular layer deposition. Macromolecules 2013;46:5638–43. https://doi.org/10.1021/ma400998m.

[109] Senkovskyy V, Tkachov R, Beryozkina T, Komber H, Oertel U, Horecha M, et al. "Hairy" poly(3-hexylthiophene) particles prepared via surface-initiated Kumada catalyst-transfer polycondensation. J Am Chem Soc 2009;131:16445–53. https://doi.org/10.1021/ja904885w.

[110] Doubina N, Jenkins JL, Paniagua SA, Mazzio KA, MacDonald GA, Jen AKY, et al. Surface-initiated synthesis of poly(3-methylthiophene) from indium tin oxide and its electrochemical properties. Langmuir 2012;28:1900–8. https://doi.org/10.1021/la204117u.

[111] Huddleston NE, Sontag SK, Bilbrey JA, Sheppard GR, Locklin J. Palladium-mediated surface-initiated Kumada catalyst polycondensation: A facile route towards oriented conjugated polymers. Macromol Rapid Commun 2012;33:2115–20. https://doi.org/10.1002/marc.201200472.

[112] Roy A, Gao J, Bilbrey JA, Huddleston NE, Locklin J. Rapid electrochemical reduction of Ni(II) generates reactive monolayers for conjugated polymer brushes in one step. Langmuir 2014;30:10465–70. https://doi.org/10.1021/la502050n.

[113] Huddleston NE, Roy A, Bilbrey JA, Zhao Y, Locklin J. Functionalization of reactive end groups in surface-initiated kumada catalyst-transfer polycondensation. Macromol Symp 2015;351:27–36. https://doi.org/10.1002/masy.201300126.

[114] Chakravarthula SN, Xiao B, Imel ZE, Atkins DC, Georgiou P. Microparticle-supported conjugated polyelectrolyte brushes prepared by surface-initiated kumada catalyst transfer polycondensation for sensor applications. Proc Annu Conf Int Speech Commun Assoc INTERSPEECH 2015;2015-Janua:668–72. https://doi.org/10.1002/marc.201000411.

[115] Schwartz E, Lim E, Gowda CM, Liscio A, Fenwick O, Tu G, et al. Synthesis,

characterization, and surface initiated polymerization of carbazole functionalized isocyanides. Chem Mater 2010;22:2597–607. https://doi.org/10.1021/cm903664g.

[116] Yoshida S, Fujinami S, Esashi M. Investigation of mechanical and tribological properties of polyaniline brush by atomic force microscopy for scanning probe-based data storage. E-Journal Surf Sci Nanotechnol 2013;11:53–9. https://doi.org/10.1380/ejssnt.2013.53.

[117] Li J, Yoon SJ, Hsieh B-Y, Tai W, O'Donnell M, Gao X. Stably doped conducting polymer nanoshells by surface initiated polymerization. Nano Lett 2015;15:8217–22. https://doi.org/10.1021/acs.nanolett.5b03728.

[118] Huang R, Xie Y, Chang Q, Xiong J, Guan S, Yuan S, et al. PANI-encapsulated Si nanocomposites with a chemical bond linkage in the interface exhibiting higher electrochemical stability as anode materials for lithium-ion batteries. Nano 2019;14:1950078/1-14. https://doi.org/10.1142/S1793292019500784.

[119] Wang J, Ni X. Photoresponsive polypyrrole-TiO_2 nanoparticles film fabricated by a novel surface initiated polymerization. Solid State Commun 2008;146:239–44. https://doi.org/10.1016/j.ssc.2008.02.022.

[120] Yang HJ, Yang TH, Kang JH, Kim S, Jung Y. Novel surface-initiated polymerization of pyrrole on a vanadium pentoxide surface. J Nanosci Nanotechnol 2017;17:5574–7. https://doi.org/10.1166/jnn.2017.14150.

[121] Wang Y-M, Song X-Y, Shao S-H, Xu P-X, Ren W-M, Lu X-B. Functionalization of carbon nanotubes by surface-initiated immortal alternating polymerization of CO_2 and epoxides. Polym Chem 2013;4:629–36. https://doi.org/10.1039/C2PY20753B.

[122] Pendergraph SA, Klein G, Johansson MKG, Carlmark A. Mild and rapid surface initiated ring-opening polymerisation of trimethylene carbonate from cellulose. RSC Adv 2014;4:20737–43. https://doi.org/10.1039/c4ra01788a.

[123] Yoshimura T, Tatsuura S, Sotoyama W. Polymer films formed with monolayer growth steps by molecular layer deposition. Appl Phys Lett 1991;59:482–4. https://doi.org/10.1063/1.105415.

[124] George S, Dameron A, Du Y, Adamczyk NM, Davidson S. Molecular layer deposition of organic and hybrid organic-inorganic films. ECS Trans., vol. 11, ECS; 2007, p. 81–90. https://doi.org/10.1149/1.2779072.

[125] Adamczyk NM, Dameron AA, George SM. Molecular layer deposition of poly(p-phenylene terephthalamide) films using terephthaloyl chloride and p-phenylenediamine. Langmuir 2008;24:2081–9. https://doi.org/10.1021/la7025279.

[126] Sundberg P, Karppinen M. Organic and inorganic–organic thin film structures by molecular layer deposition: A review. Beilstein J Nanotechnol 2014;5:1104–36. https://doi.org/10.3762/bjnano.5.123.

[127] Kubono A, Okui N, Tanaka K, Umemoto S, Sakai T. Highly oriented polyamide thin films prepared by vapor deposition polymerization. Thin Solid Films 1991;199:385–93. https://doi.org/10.1016/0040-6090(91)90021-O.

[128] Yoshimura T, Tatsuura S, Sotoyama W, Matsuura A, Hayano T. Quantum wire and dot formation by chemical vapor deposition and molecular layer deposition of one-dimensional conjugated polymer. Appl Phys Lett 1992;60:268–70. https://doi.org/10.1063/1.106681.

[129] Lee JS, Lee Y-J, Tae EL, Park YS, Yoon KB. Synthesis of zeolite as ordered multicrystal arrays. Science (80-) 2003;301:818–21. https://doi.org/10.1126/science.1086441.

[130] Kim A, Filler MA, Kim S, Bent SF. Layer-by-layer growth on Ge(100) via spontaneous urea coupling reactions. J Am Chem Soc 2005;127:6123–32. https://doi.org/10.1021/ja042751x.

[131] Loscutoff PW, Lee H-B-R, Bent SF. Deposition of ultrathin polythiourea films by molecular layer deposition. Chem Mater 2010;22:5563–9. https://doi.org/10.1021/cm1016239.

[132] Ivanova T V., Maydannik PS, Cameron DC. Molecular layer deposition of polyethylene terephthalate thin films. J Vac Sci Technol A Vacuum, Surfaces, Film 2012;30:01A121/1-5. https://doi.org/10.1116/1.3662846.

[133] Du Y, George SM. Molecular layer deposition of nylon 6,6 films examined using in situ FTIR spectroscopy. J Phys Chem C 2007;111:8509–17. https://doi.org/10.1021/jp067041n.

[134] Mulpuri S V., Shin J, Shin B-G, Greiner A, Yoon DY. Synthesis and characterization of substituted polynorbornene derivatives. Polymer (Guildf) 2011;52:4377–86. https://doi.org/10.1016/j.polymer.2011.07.019.

[135] Moon JH, Swager TM. Poly(p-phenylene ethynylene) brushes. Macromolecules 2002;35:6086–9. https://doi.org/10.1021/ma025539r.

[136] Ye Q, Wang X, Li S, Zhou F. Surface-initiated ring-opening metathesis polymerization of pentadecafluorooctyl-5-norbornene-2-carboxylate from variable substrates modified with

sticky biomimic initiator. Macromolecules 2010;43:5554–60. https://doi.org/10.1021/ma100479x.

[137] Ye Q, He B, Zhang Y, Zhang J, Liu S, Zhou F. Grafting robust thick zwitterionic polymer brushes via subsurface-initiated ring-opening metathesis polymerization for antimicrobial and anti-biofouling. ACS Appl Mater Interfaces 2019;11:39171–8. https://doi.org/10.1021/acsami.9b11946.

[138] Lerum MFZ, Chen W. Acute degradation of surface-bound unsaturated polyolefins in common solvents under ambient conditions. Langmuir 2009;25:11250–4. https://doi.org/10.1021/la902340z.

[139] Escobar CA, Harl RR, Maxwell KE, Mahfuz NN, Rogers BR, Jennings GK. Amplification of surface-initiated ring-opening metathesis polymerization of 5-(perfluoro-n-alkyl)norbornenes by macroinitiation. Langmuir 2013;29:12560–71. https://doi.org/10.1021/la402173z.

[140] Witte P, Menzel H. Nickel-mediated surface grafting from polymerization of α-amino acid-N-carboxyanhydrides. Macromol Chem Phys 2004;205:1735–43. https://doi.org/10.1002/macp.200400100.

[141] Yoon KR, Chi YS, Lee K-B, Lee JK, Kim DJ, Koh Y-J, et al. Surface-initiated, ring-opening polymerization of p-dioxanone from gold and silicon oxide surfaces. J Mater Chem 2003;13:2910–4. https://doi.org/10.1039/b305903k.

[142] Kim Y-R, Paik H, Ober CK, Coates GW, Batt CA. Enzymatic surface-initiated polymerization: a novel approach for the in situ solid-phase synthesis of biocompatible polymer poly(3-hydroxybutyrate). Biomacromolecules 2004;5:889–94.

https://doi.org/10.1021/bm0344147.

[143] Grubbs JB, Arnold RM, Roy A, Brooks K, Bilbrey JA, Gao J, et al. Degradable polycaprolactone and polylactide homopolymer and block copolymer brushes prepared by surface-initiated polymerization with triazabicyclodecene and zirconium catalysts. Langmuir 2015;31:10183–9. https://doi.org/10.1021/acs.langmuir.5b02093.

[144] Glassner M, Vergaelen M, Hoogenboom R. Poly(2-oxazoline)s: A comprehensive overview of polymer structures and their physical properties. Polym Int 2018;67:32–45. https://doi.org/10.1002/pi.5457.

[145] Huang L, Yang S, Chen J, Tian J, Huang Q, Huang H, et al. A facile surface modification strategy for fabrication of fluorescent silica nanoparticles with the aggregation-induced emission dye through surface-initiated cationic ring opening polymerization. Mater Sci Eng C 2019;94:270–8. https://doi.org/10.1016/j.msec.2018.09.042.

[146] Yoshinaga K, Hidaka Y. Cationic graft-polymerization of 2-methyl-2-oxazoline on monodispersed polymer-coated ultrafine silica particles. Polym J 1994;26:1070–9. https://doi.org/10.1295/polymj.26.1070.

[147] Karagoz B, Gunes D, Bicak N. Preparation of crosslinked poly(2-bromoethyl methacrylate) microspheres and decoration of their surfaces with functional polymer brushes. Macromol Chem Phys 2010;211:1999–2007. https://doi.org/10.1002/macp.201000137.

[148] Lim J, Gupta B, George W. The potential for high performance fiber from nylon 6. Prog Polym Sci 1989;14:763–809. https://doi.org/10.1016/0079-6700(89)90009-9.

[149] Subbulakshmi MS, Kasturiya N, Hansraj, Bajaj P, Agarwal AK. Production of flame-retardant nylon 6 and 6.6. J Macromol Sci Part C Polym Rev 2000;40:85–104. https://doi.org/10.1081/MC-100100580.

[150] Unal H, Findik F, Mimaroglu A. Mechanical behavior of nylon composites containing talc and kaolin. J Appl Polym Sci 2003;88:1694–7. https://doi.org/10.1002/app.11927.

[151] Bousquet A, Awada H, Hiorns RC, Dagron-Lartigau C, Billon L. Conjugated-polymer grafting on inorganic and organic substrates: A new trend in organic electronic materials. Prog Polym Sci 2014;39:1847–77. https://doi.org/10.1016/j.progpolymsci.2014.03.003.

[152] Bobade RS. Polythiophene composites: a review of selected applications. J Polym Eng 2011;31:209–15. https://doi.org/10.1515/polyeng.2011.044.

[153] Mehmood U, Al-Ahmed A, Hussein IA. Review on recent advances in polythiophene based photovoltaic devices. Renew Sustain Energy Rev 2016;57:550–61. https://doi.org/10.1016/j.rser.2015.12.177.

[154] Marshall N, Sontag SK, Locklin J. Surface-initiated polymerization of conjugated polymers. Chem Commun 2011;47:5681–9. https://doi.org/10.1039/c1cc10483g.

[155] Alonzi M, Lanari D, Marrocchi A, Petrucci C, Vaccaro L. Synthesis of polymeric semiconductors by a surface-initiated approach. RSC Adv 2013;3:23909/1-15. https://doi.org/10.1039/c3ra43680b.

[156] Geng Y, Huang L, Wu S, Wang F. Kumada chain-growth polycondensation as a universal method for synthesis of well-defined conjugated polymers. Sci China Chem 2010;53:1620–33. https://doi.org/10.1007/s11426-010-4048-2.

[157] Bryan ZJ, McNeil AJ. Conjugated polymer synthesis via catalyst-transfer polycondensation (CTP): Mechanism, scope, and applications. Macromolecules 2013;46:8395–405. https://doi.org/10.1021/ma401314x.

[158] Wang S, Wang Z, Li J, Li L, Hu W. Surface-grafting polymers: From chemistry to organic electronics. Mater Chem Front 2020;4:692–714. https://doi.org/10.1039/c9qm00450e.

[159] Yokozawa T, Suzuki R, Nojima M, Ohta Y, Yokoyama A. Precision synthesis of poly(3-hexylthiophene) from catalyst-transfer suzuki−miyaura coupling polymerization. Macromol Rapid Commun 2011;32:801–6. https://doi.org/10.1002/marc.201100037.

[160] Satoh T, Ihara R, Kawato D, Nishikawa N, Suemasa D, Kondo Y, et al. Precise synthesis of clickable poly(n-hexyl isocyanate). Macromolecules 2012;45:3677–86. https://doi.org/10.1021/ma300555v.

[161] Golling FE, Pires R, Hecking A, Weikard J, Richter F, Danielmeier K, et al. Polyurethanes for coatings and adhesives – chemistry and applications. Polym Int 2019;68:848–55. https://doi.org/10.1002/pi.5665.

[162] Nolte RJM. Helical poly(isocyanides). Chem Soc Rev 1994;23:11–9. https://doi.org/10.1039/cs9942300011.

[163] Schwartz E, Koepf M, Kitto HJ, Nolte RJM, Rowan AE. Helical poly(isocyanides): past, present and future. Polym Chem 2011;2:33–47. https://doi.org/10.1039/C0PY00246A.

[164] Hay AS. Polymerization by oxidative coupling: Discovery and commercialization of PPO and Noryl resins. J Polym Sci Part A Polym Chem 1998;36:505–17. https://doi.org/10.1002/(SICI)1099-0518(199803)36:4<505::AID-POLA1>3.0.CO;2-O.

[165] Yeager G. Polyethers, aromatic. Encycl. Polym. Sci. Technol., vol. 11, Hoboken, NJ, USA: John Wiley & Sons, Inc.; 2004, p. 64–87. https://doi.org/10.1002/0471440264.pst268.

[166] Asadollahi M, Bastani D, Musavi SA. Enhancement of surface properties and performance of reverse osmosis membranes after surface modification: A review. Desalination 2017;420:330–83. https://doi.org/10.1016/j.desal.2017.05.027.

[167] Tan Y, Liu Y, Tang Z, Wang Z, Kong L, Kang L, et al. Concise N-doped carbon nanosheets/vanadium nitride nanoparticles materials via intercalative polymerization for supercapacitors. Sci Rep 2018;8:1–13. https://doi.org/10.1038/s41598-018-21082-w.

[168] Gu H, Zhang H, Lin J, Shao Q, Young DP, Sun L, et al. Large negative giant magnetoresistance at room temperature and electrical transport in cobalt ferrite-polyaniline nanocomposites. Polymer (Guildf) 2018;143:324–30. https://doi.org/10.1016/j.polymer.2018.04.008.

[169] Ghosh T, Basak U, Bairi P, Ghosh R, Pakhira M, Ball R, et al. Hierarchical nanocomposites by oligomer-initiated controlled polymerization of aniline on graphene oxide sheets for energy storage. ACS Appl Nano Mater 2020;3:1693–705. https://doi.org/10.1021/acsanm.9b02406.

[170] Kouidri FZ, Berenguer R, Benyoucef A, Morallon E. Tailoring the properties of polyanilines/SiC nanocomposites by engineering monomer and chain substituents. J Mol Struct 2019;1188:121–8. https://doi.org/10.1016/j.molstruc.2019.03.100.

[171] Devaux C, Chapel JP, Beyou E, Chaumont P. Controlled structure and density of “living” polystyrene brushes on flat silica surfaces. Eur Phys J E 2002;7:345–52.

https://doi.org/10.1140/epje/i2001-10098-2.

[172] Raza A, Tahir M, Nasir A, Yasin T, Nadeem M. Sepiolite grafted polypyrrole: Influence of degree of grafting on structural, thermal, and impedance properties of nanohybrid. J Appl Polym Sci 2020:1–11. https://doi.org/10.1002/app.49085.

[173] Thorat SD, Phillips PJ, Semenov V, Gakh A. Physical properties of aliphatic polycarbonates made from CO_2 and epoxides. J Appl Polym Sci 2003;89:1163–76. https://doi.org/10.1002/app.12355.

[174] Mei J, Bao Z. Side chain engineering in solution-processable conjugated polymers. Chem Mater 2014;26:604–15. https://doi.org/10.1021/cm4020805.

[175] Savagatrup S, Makaram AS, Burke DJ, Lipomi DJ. Mechanical properties of conjugated polymers and polymer-fullerene composites as a function of molecular structure. Adv Funct Mater 2014;24:1169–81. https://doi.org/10.1002/adfm.201302646.

[176] Lee W, Patra M, Linse P, Zauscher S. Scaling behavior of nanopatterned polymer brushes. Small 2007;3:63–6. https://doi.org/10.1002/smll.200600414.

Figure Captions

Figure 32. Illustration comparing of the ‘grafting from’ and ‘grafting to’ techniques for the preparation of polymer brushes. [24], Adapted with permission. Open Access distributed under the terms of the Creative Commons Attribution License CC BY 4.0.

Figure 33. Scheme depicting the different conformations polymers can adopt when attached to a surface.

Figure 34. Schematic of grafting density versus brush height in the transition from the mushroom regime to the brush regime.

Figure 35. Hydroxylated surface reactions with example silane initiators used for ‘grafting-from’ surface initiated polymerization. [[24],[37]]

Figure 36. Reaction schemes for commonly used radical surface-initiated polymer brush synthesis. (a) SI-ATRP, (b) SI-RAFT, (c) SI-NMP. [19]

Figure 37. Reaction scheme showing a proposed mechanism for nickel catalyst "ring-walking" across the aromatic backbone of polythiophene. [53]

Figure 38. Some of the first monomers used when CGC polymerization was observed. a) 4-halothiophenols b) 4-halo-2,6-dimethylphenols c) 4-fluoro-4′- hydroxybenzophenone d) sodium 4-fluorobenzenesulfinate e) methylphenyldichlorosilene f) dibromomethane with bisphenol A. [49]

Figure 39. Reaction scheme depicts CGC polyester formation comparing 3-acyl-2-benzothiazolone as a stable leaving group to the transesterification product as a less stable leaving group. [67]

Figure 40. Hypothesized mechanism for the synthesis of polyamides via CGC polymerization using substituent effects depicting inactive monomer, highly reactive initiator, and reactive propagation chain end. [54]

Figure 41. Scheme showing a general mechanism for ROP in which an initiator starts the reaction with a monomer which then kicks off the polymerization starting a reactive propagating chain end.

Figure 42. Illustration shows molecular simulation of flexible vs semi-flexible polymer brushes under pressure. a) flexible brush, b) flexible brush under compression, c) semiflexible brush, d) semiflexible brush under compression. [30], Copyright 2014. Reproduced with permission from Royal Society of Chemistry.

Figure 43. Schematic showing molecular layer deposition (MLD) method. In both the a) and b) schemes show bifunctional molecules reacting to the surface via a surface terminated reactive end group. [125], Copyright 2008. Reproduced with permission from American Chemical Society.

Figure 44. Reaction scheme shows the use of ROMP to grow polynorbornene brushes with different monomers that have successfully polymerized by Laibinis et al. starting with initiation of the surface and activation using a ruthenium catalyst. [77]

Figure 45. Reaction scheme shows the synthesis of a random polynorbornene brush with crosslinked PEG chain to help prevent solvent degradation performed by Berron et al. [94]

Figure 46. Reaction scheme shows initiation and propagation of SI-ROP utilizing a primary amine-initiated surface and an NCA monomer. [21]

Figure 47. Reaction pathways using SI-ROP organonickel catalyst mediated NCA polymerization using a) “block copolymerization approach”; and b) "alloc-amide approach". [21]

Figure 48. Reaction scheme shows the first example of SI polycaprolactone polymer brush synthesized by Abbot et al. starting from surface alcohol group to activation with catalyst then propagation by addition of caprolactone monomer. [75]

Figure 49. Proposed mechanism by Choi et al. for enzyme surface-initiated polymerization to form a polyester. [99]

Figure 50. Reaction scheme shows the first example of surface-initiated polymerization of polyoxazoline by Jordon and Ulman starting with a surface alcohol, activating the alcohol with triflate functional group, then propogating the chain with addition of monomer. [76]

Figure 51. Reaction scheme shows surface initiated polyoxazolines grown from silica nanoparticles including initiation step and polymerization steps as synthesized by Bissadi and Weberskirch. [102]

Figure 52. Reaction scheme shows surface-initiated nylon 6 from silica nanoparticles synthesized by Li et al. [105]

Figure 53. Reaction scheme of the first surface-initiated polythiophene brush synthesis demonstrated by Kiriy et al. [80]

Figure 54. Reaction scheme showing surface-initiated polythiophene surface initiation, initiator activation, switching nickel ligands for better reactivity, propagation, and termination. Synthesis performed by Luscombe et al. [110]

Figure 55. Reaction scheme shows 'Grafting from' polymerization of polyfluorene performed by Kiriy et al starting with initiation, activation using Pd catalyst, and propagation. [81]

Figure 56. Reaction scheme shows the first example of synthesizing PPE using 'grafting-from' on silica nanoparticles performed by Bielawski et al. demonstrating initiation, surface activation, and propagation. [78]

Figure 57. Reaction scheme shows surface-initiated polyisocyanate synthesis starting with initiator on silica, activation, propagation ,and termination performed by Vatansever and Hamblen. [83]

Figure 58. Reaction scheme shows surface-initiated polymerization of poly(isocyanide) synthesis on oxide surface, including initiation and propagation, performed by Huck et al. [84]

Figure 59. AFM topography of 56 and 387 nm thick poly(isocyanide) brushes a) and b) respectively. [84], Copyright 2008. Reproduced with permission from American Chemical Society.

Figure 60. Reaction scheme shows the first surface-initiated aromatic polyamide brushes grown from silica surface performed by Prehn and Boyes. [2]

Figure 61. Reaction scheme shows PANI brush synthesis on a gold substrate. Synthesis was performed by Esachi et al. [79]

Figure 62. Images show AFM friction and topography plots of different surfaces. The left side images show topography while the right images show friction. a) and a') are the PANI brush. b) and b') are GeSbTe. c) and c') are poly methyl methacrylate films. [116], Adapted with permission. Open Access distributed under the terms of the Creative Commons Attribution License CC BY 4.0.

Figure 32. Reaction scheme shows surface-initiated polycarbonate brush using immortal polymerization mechanism on MWCN performed by Lu et al. [121]